SYNTHESIS AND CHARACTERIZATION OF ION-IMPRINTED THERMOSENSITIVE POLYMERS FOR Fe^{3+} REMOVAL FROM HUMAN PLASMA

İNSAN PLAZMASINDAN Fe^{3+} UZAKLAŞTIRILMASI İÇİN İYON BASKILANMIŞ SICAKLIK DUYARLI POLİMERLERİN SENTEZİ VE KARAKTERİZASYONU

Seçil UTKU

A THESIS OF MASTER OF SCIENCE
Prepared In The Chemistry Department
According To The Regulations of
The Institute For Graduate Studies In Pure
And Applied Sciences of Hacettepe University

2007

İNSAN PLAZMASINDAN Fe^{3+} UZAKLAŞTIRILMASI İÇİN İYON BASKILANMIŞ SICAKLIK DUYARLI POLİMERLERİN SENTEZİ VE KARAKTERİZASYONU

Seçil UTKU

ÖZ

Sıcaklık duyarlı jeller, ilaç salım sistemleri, aktuatorlar, biyolojik bileşiklerin ve metallerin uzaklaştırılması uygulamalarında büyük bir ilgi uyandırmaktadır. Örnek bir jel olarak Poly(N-isopropylacrylamide) (poly(NIPA)), 32 °C civarında Düşük Kritik Çözünürlük Sıcaklığına (DKÇS) sahiptir. Su içerisinde düşük ve yüksek sıcaklıklarda sırasıyla hidrofilik ve hidrofobik özellik göstermektedir. Metalleri adsorbe eden yeni sıcaklık duyarlı jel adsorbentlerde poly(NIPA)'nın iskelet olarak kullanıldığı bilinmektedir. Özgün bir metalin kalıp olarak moleküler baskılama tekniği ile poly(NIPA) yapısına ağır metallerle etkileşen şelatlayıcı gruplar dahil edilebilmektedir. Metallerin biyolojik süreçlerde önemli roller oynadığı ve bazılarının temel zorunluluk olarak belirtilmesine rağmen, metal iyon seviyesi belirli sınır değerini aştığında zehir etkisi gösterebilmektedir. Demir zehirlenmesinin bazı belirtileri, örneğin kalp krizleri, şeker hastalıkları, eklem iltihabı, depresyon ve karaciğer yetmezliği, genetik bozukluklar veya kaza sonucu yutma gibi nedenlerle yüksek derişimlerde demirin absorpsiyonu ile ortaya çıkmaktadır. Bu çalışmanın amacı, iyon baskılanmış polimerler kullanılarak sulu çözeltilerden ve talasemi hastalarının plazmasından demir uzaklaştırılmasıdır.

Fe(III) baskılanmış katı fazın oluşturulması amacıyla Fe^{3+} iyonlarına yüksek seçicilik gösteren N-metakroil-(L)-sistein (MAC) kompleks oluşturucu monomer olarak kullanılmıştır. Poly(NIPA) sıcaklık duyarlı iskelet polimer kalıp olarak kullanılmıştır. Fe^{3+} iyonları ile etkileşen şelatlayıcı grup [N-methacryloyl-(L)-cysteine (MAC)], poly(NIPA)'ya moleküler baskılama tekniği ile dahil edilmiştir. Fe^{3+} iyonlarının uzaklaştırılmasından sonra, Fe^{3+} baskılanmış polimerik partiküller sulu çözeltilerden ve talasemi hastasının plazmasından Fe^{3+} uzaklaştırılması için kullanılmıştır. Başlangıç Fe^{3+} derişimi ortam pH'ının adsorpsiyon hızı ve adsorpsiyon miktarı üzerine etkisi poly(NIPA-MAC) ve Fe^{3+} baskılanmış poly(NIPA-MAC) partiküllerin her ikisi içinde incelenmiştir. Seçicilik çalışmalarında

ise Fe^{3+} iyonuna karşı Ni^{2+} ve Cd^{2+} metla iyonları karışımı kullanılmıştır. Aynı zamanda Fe^{3+} baskılanmış poly(NIPA-MAC) partiküllerin sulu çözeltilerde tekrar kullanımı da çalışılmıştır.

Anahtar Sözcükler : Sıcaklık Duyarlı Polimerler, İyon baskılama, Talasemi, Affinite bağlanması.

Danışman : Prof. Dr. Adil DENİZLİ, Hacettepe Üniversitesi, Kimya Bölümü, Beytepe, ANKARA

SYNTHESIS AND CHARACTERIZATION OF ION-IMPRINTED THERMOSENSITIVE POLYMERS FOR Fe^{3+} REMOVAL FROM HUMAN PLASMA

Seçil UTKU

ABSTRACT

Thermosensitive gels have attracted a great deal of attention for the applications to drug delivery systems, actuators, separation and removal of biological compounds and metals. Poly(*N*-isopropylacrylamide) (poly(NIPA)), a representative gel, has a lower critical solution temperature (LCST) in the vicinity of 32 °C i.e. showing hydrophilicity and hydrophobicity in water at lower and higher temperatures, respectively. Novel adsorbents using thermosensitive gels for trapping metals were reported where poly(NIPA) was used as a thermosensitive backbone polymer. A chelating group, which interacts with heavy metals, was introduced into poly(NIPA) with a molecular imprinting technique using a specific metal as the template. Although it is emphasized that metals play important roles in biological processes and some of them are classified as essential, the toxic symptoms will manifest when a metal ion level exceeds a certain threshold level. Many symptoms of iron toxicity, for example heart attacks, diabetes, arthritis, depression and liver failure, are arised from the absorption of iron in unacceptably high concentrations because of a genetic failure or by accidental ingestion. The aim of this study is to prepare ion-imprinted polymers for the removal of iron from aqueous solutions and solutions thalassemia patient`s plasma.

N-methacryloyl-(L)-cysteine (MAC) was selected as the metal complexing monomer, with the goal preparing a solid-phase which has a high selectivity for Fe^{3+} ions. Poly(NIPA) was used as a thermosensitive backbone polymer matrix. A chelating group [N-methacryloyl-(L)-cysteine (MAC)] which interacts with Fe^{3+} ions, was introduced into poly(NIPA) with a molecular imprinting technique. After removal of the Fe^{3+} ions, Fe^{3+}-imprinted particles were used for the removal of

Fe^{3+} ions from aqueous solutions and thalassemia patient's plasma. The effect of the initial Fe^{3+} concentration and pH of the medium on the adsorption rate and adsorption capacity were studied both on the poly(NIPA-MAC) and Fe^{3+}-imprinted poly(NIPA-MAC) particles. Selectivity studies of Fe^{3+} versus other interfering metal ions mixture which are Ni^{2+} and Cd^{2+} were also studied. Repeated use of the Fe^{3+}-imprinted poly(NIPA-MAC) particles from aqueous solutions is also discussed. Adsorption of Fe^{3+} ions from thalassemia patient's plasma both on the poly(NIPA-MAC) and Fe^{3+}-imprinted poly(NIPA-MAC) particles were studied in batch-wise.

ACKNOWLEDGEMENT

TABLE OF CONTENTS

LIST OF FIGURES

1. INTRODUCTION

Considerable researches have been focused on polymeric materials those change their structure and functions responding to external physical, chemical, and electrical stimuli (light, temperature, pH, substance concentration, solvent composition, and electric fields, etc.). These materials termed 'intelligent materials', sense one or more external stimuli (sensor) as signals, judge the magnitude of these signals (processor), and change their structure and functions in direct response (effecter). The response of the intelligent materials toward above described stimuli induce several kinds of changes such as phase, shape, surface energies, permeation rates, reaction rates, and molecule recognition. Introduction of stimuli-responsive polymeric materials as switching sequences into both artificial materials and bioactive compounds (peptides, proteins, nucleic acids, and others) permit modulation of their structure induced by corresponding external stimuli. 'On–off' switching of their respective functions, thus, can be achieved at molecular level (Okana et al., 1993a; Okana et al., 1993b; Okana et al., 1994; Okana et al., 1998; Hoffman et al.,1995). Intelligent materials embodying these concepts might contribute to establish fundamental principles for fabrication of novel systems.

Thermosensitive gels have attracted a great deal of attention for the applications to drug delivery systems, actuators and so on. Poly(*N*-isopropylacrylamide) (poly(NIPA)), a representative gel, has a lower critical solution temperature (LCST) in the vicinity of 32 °C (Hirotsu et al., 1987; Ito et al., 1989), i.e. showing hydrophilicity and hydrophobicity in water at lower and higher temperatures, respectively. Novel adsorbents using thermosensitive gels for trapping heavy metals were reported several papers (Kanazawa et al., 1994a; Kanazawa et al., 1994b; Tokuyama et al., 2005a; Tokuyama et al., 2005b), where poly(NIPA) was used as a thermosensitive backbone polymer. A chelating group, which interacts with heavy metals, was introduced into poly(NIPA) with a molecular imprinting technique (Wulff et al., 1998) using a specific metal as the template. The molecular imprinted adsorbents reconstruct multi-point adsorption sites at a specific temperature and disrupt them through swelling deformation at a lower temperature. The adsorbents, therefore, are suitable for the temperature swing

1

adsorption (TSA), i.e. the control of adsorption and desorption of a specific heavy metal with the change in temperature. TSA using the adsorbents described here provides an energy-saving and environmentally friendly process for the separation of both undesirable and valuable metals ions in aquatic environments, industrial effluents and biological samples.

Molecular recogition-based separation techniques have received much attention in various fields because of their high selectivity for target molecules (Garcia et al., 1998; Wulff et al., 1995). Molecular imprinting has been recognized as a promising technique for the preparation of such systems. Three steps are involved in ion-imprinting process: (i) Complexation of metal ion (template) to polymerizable ligand, (ii) Copolymerization of this complex, (iii) Removal of metal ion after copolymerization. After removal of target ion, the prepared matrix is put into a solution containing metal ions from which the imprinted ion should thus be preferentially extracted. In ion-imprinting process, the selectivity of an adsorbent is based on the specificity of the ligand, on the coordination geometry and coordination number of the ions, on their charges and sizes (Garcia et al., 1998; Wulff et al., 1995).

Numerous studies describing such methodology were carried out in order to adsorb metal ions (Nishide and Tsuchida, 1976; Kabanov, 1979; Tsukagoshi, 1993; Dai, 1999, 2000) but not so many studies concerning metal removal from human plasma using ion-imprinting materials were reported in the literature (Andaç et al., 2004; Andaç et al., 2007).

Thalassemia is the world's most common hereditary disease, and is a paradigm of monogenic genetic diseases (Weatherall and Clegg, 1996). Because of increased population mobility, the disease is found today throughout the world, even in places far from the tropical areas in which it arose. Therapy of thalassemia has in the past been confined to transfusion and chelation (Rund and Rachmilewitz, 1995). Recently, novel modes of therapy have been developed for thalassemia, based on the pathophysiology and molecular pathology of the disease, both of which have been extensively studied. The therapeutic modalities currently in use for the supportive treatment of thalassemia, both those that are standard therapy and those that are in clinical trials are such as; transfusion,

chelation (intravenous and oral), antioxidants and various inducers of fetal hemoglobin (hydroxyurea, erythropoietin, butyrates, hemin) (Rund and Rachmilewitz, 2000). Most of the newer therapies are suitable primarily for thalassemia intermedia patients. In addition, the treatment modalities currently in use for the curative treatment of thalassemia major will be discussed, including bone marrow transplantation in its various forms. Experimental therapeutic methods, such as intrauterine bone marrow transplantation and gene therapy, are included. Physicians caring for thalassemia patients have an increasing variety of treatment options available. Future clinical studies will determine the place of newer agents and modalities in improving the quality of life as well as the life expectancy of thalassemia patients (Rund and Rachmilewitz, 2000).

In this thesis, we prepared ion-imprinted polymeric particles, which were used for the selective removal of Fe^{3+} ions from thalassemia patient`s plasma. We synthesized N-methacryloyl-(L)-cysteine (MAC) as the metal complexing monomer, with the goal preparing a solid-phase which has a high selectivity for Fe^{3+} ions. Poly(NIPA) was used as a thermosensitive backbone polymer matrix. A chelating group [N-methacryloyl-(L)-cysteine (MAC)] which interacts with Fe^{3+} ions, was introduced into poly(NIPA) with a molecular imprinting technique. After removal of Fe^{3+} ions, Fe^{3+}-imprinted polymeric particles were used for the separation of Fe^{3+} ions from aqueous solutions and thalassemia patient's plasma. The effect of the initial Fe^{3+} concentration and pH of the medium on the adsorption rate and adsorption capacity were studied both on the poly(NIPA-MAC) and Fe^{3+}-imprinted poly(NIPA-MAC) gels. Selectivity studies of Fe^{3+} versus other interfering metal ions mixture which are Ni^{2+} and Cd^{2+} are reported here. Repeated use of the Fe^{3+}-imprinted poly(NIPA-MAC) particles from aqueous solutions is also discussed. Adsorption of Fe^{3+} ions from thalassemia patient's plasma both on the poly(NIPA-MAC) and Fe^{3+}-imprinted poly(NIPA-MAC) particles were studied in batch-wise.

2. GENERAL INFORNATION

2.1. Smart Polymers

Polymers such as proteins, polysaccharides and nucleic acids are present as basic components in living organic systems. Synthetic polymers, which are designed to mimic these biopolymers, have been developed into variety of functional forms to meet the industrial and scientific applications. The synthetic polymers can be classified into different categories based on their chemical properties. Out of these, some special types of polymers have emerged as a very useful class of polymers and have their own special chemical properties and applications in various areas. These polymers are coined with different names, based on their physical or chemical properties like, "stimuli-responsive polymers" (Jeong et al., 2002) or "smart polymers (SP)" (Hoffman, 2000) and (Galaev et al., 2000) or "intelligent polymers" (Kikuchi et al., 2002) or "environmental-sensitive" polymers (Qui et al., 2001). The characteristic feature that actually makes them "smart" is their ability to respond to very slight changes in the surrounding environment. The uniqueness of these materials lies not only in the fast macroscopic changes occurring in their structure but also these transitions being reversible. The responses are manifested as changes in one or more of the following—shape, surface characteristics, solubility, formation of an intricate molecular assembly, a sol-to-gel transition and others. The environmental trigger behind these transitions can be either change in temperature (Okano et al., 1993a) or pH shift (Twaittes et al., 2004), increase in ionic strength (Twaittes et al., 2004), presence of certain metabolic chemicals (Lomadze et al., 2005), addition of an oppositely charged polymer (Kabanov et al., 1994) and polycation–polyanion complex formation (Leclercq et al., 2003). More recently, changes in electric (Filipcsei et al., 2000) and magnetic field (Zrinyl et al., 2000), light or radiation forces (Juodkazis et al., 2000) have also been reported as stimuli for these polymers. The physical stimuli, such as temperature, electric or magnetic fields, and mechanical stress, will affect the level of various energy sources and alter molecular interactions at critical onset points (Figure 2.1). They undergo fast, reversible changes in microstructure from a hydrophilic to a hydrophobic state (Galaev et al., 1996). These changes are apparent at the macroscopic level as

precipitate formation from a solution or order-of-magnitude changes in the size and water content of stimuli-responsive hydrogels (Taylor et al., 1975). An appropriate proportion of hydrophobicity and hydrophilicity in the molecular structure of the polymer is believed to be required for the phase transition to occur.
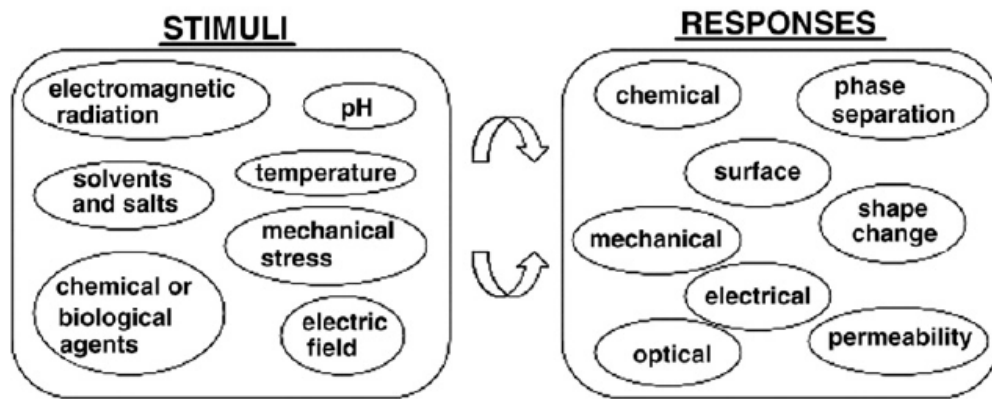
Figure 2.1.   Potential stimuli and responses of synthetic polymers.

Temperature-sensitive polymers exhibit lower critical solution temperature (LCST) behavior where phase separation is induced by surpassing a certain temperature threshold. Polymers of this type undergo a thermally induced, reversible phase transition; they are soluble in a solvent (water) at low temperatures but become insoluble as the temperature rises above the LCST (Yan et al., 2000). The LCST corresponds to the region in the phase diagram at which the enthalpy contribution of water hydrogen-bonded to the polymer chain becomes less than the entropic gain of the system as a whole and thus is largely dependent on the hydrogen-bonding capabilities of the constituent monomer units. In principle, the LCST of a given polymer can be "tuned" as desired by variation in hydrophilic or hydrophobic co-monomer content. Thermosensitive polymers can be classified into different groups depending on the mechanism and chemistry of the groups. These are (a) poly(*N*-alkyl substituted acrylamides) e.g. poly(*N*-isopropylacrylamide) with LCST of 32 °C (Heskins et al., 1968) and (b) poly (*N*-vinylalkylamides) e.g. poly(*N*-vinylcaprolactam) with a LCST of about 32–35 °C according to molecular mass of polymer (Suva et al., 1997). There are other types of temperature-responsive polymers such as poly(ethylene oxide)$_{106}$-poly(propylene oxide)$_{70}$-poly (ethylene oxide)$_{106}$ co-polymer (Wanka et al., 1994), which has the trade name Pluronic$^{®}$ F127 and poly lactic acid-co–polyethyleneglycol–polylactic acid (PLLA)/PEG/PLLA

triblock co-polymers (Na et al., 2006). Another interesting class of temperature-responsive polymers have recently emerged which involves elastin like polymers (ELPs) (Herrero-Vanella et al., 2005). The specific LCST of all these different polymeric systems show potential applications in bioengineering and biotechnology.

On the other hand in a typical pH-sensitive polymer, protonation/deprotonation events occur and impart the charge over the molecule (generally on carboxyl or amino groups), therefore it depends strongly on the pH. The pH-induced phase transition of pH-sensitive polymer tends to be very sharp and usually switches within 0.2–0.3 unit of pH. Co-polymers of methylmethacrylate and methacrylic acid undergo sharp conformational transition and collapse at low pH around 5, while co-polymers of methylmethacrylate with dimethylaminoethyl methacrylate are soluble at low pH but collapse and aggregate under slightly alkaline conditions. Other types of responsive polymers involve electric field (Filipcsei et al., 2000) and magnetic field (Zrinyl et al., 2000) the gels of which can shrink/swell in response to external electric or magnetic field stimuli. Polythiophene or sulphonated-polystyrene-based conducting polymers have shown bending in response to external field. The magnetic field-responsive gel which can be obtained by dispersing magnetic colloidal particle in poly (*N*-isopropylacrylamide-co-poly vinylalcohol) hydrogel matrix and get aggregated in external non-uniform magnetic field (Zrinyl et al., 2000).

These responses of polymer systems show usefulness in bio-related applications such as drug delivery (Qui et al., 2001; Chilkoti et al., 2002), bioseparation (Galaev et al., 2000), chromatography (Kikuchi et al., 2002), (Kobayashi et al., 2002) and (Anastase-Ravion et al., 2001) and cell culture (Kushida et al., 2005). Some systems have been developed to combine two or more stimuli-responsive mechanisms into one polymer system. For instance, temperature-sensitive polymers may also respond to pH changes (Pinkrah et al., 2003), (Peng et al., 2001) and (Bignotti et al., 2000). Two or more signals could be simultaneously applied in order to induce response in so called dual-responsive polymer systems (Kurisawa et al., 1998). Recently, biochemical stimuli have been considered as

another strategy, which involves the responses to antigen (Miyata et al., 1999), enzyme (Ulijn et al., 2006) and biochemical agents (Kang et al., 2003).

SP can be categorized into three classes according to their physical forms (Figure 2.2). They are (i) *linear free chains in solution*, where polymer undergoes a reversible collapse after an external stimulus is applied, (ii) *covalently cross-linked gels and reversible or physical gels*, which can be either microscopic or macroscopic
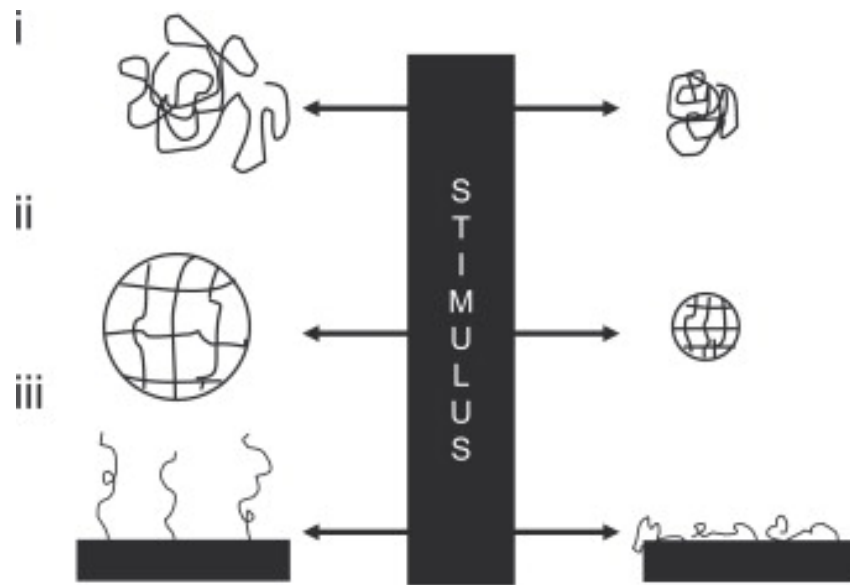
Figure 2.2.   Classification of the polymers by their physical form: (i) linear free chains in solution where polymer undergoes a reversible collapse after an external stimulus is applied; (ii) covalently cross-linked reversible gels where swelling or shrinking of the gels can be triggered by environmental change; and (iii) chain adsorbed or surface-grafted form, where the polymer reversibly swells or collapses on surface, once an external parameter is changed.

networks and for which swelling behavior is environmentally triggered and (iii) *chain adsorbed or surface-grafted form*, where the polymer reversibly swells or collapses on a surface, converting the interface from hydrophilic to hydrophobic and vice versa, once a specific external parameter is modified. SPs in all the three forms—in solution, as hydrogels and on surfaces can be conjugated with

biomolecules, thereby widening their potential scope of use in many interesting ways. Biological molecules that may be conjugated with SPs include proteins and oligopeptides, sugars and polysaccharides, single- and double-stranded oligonucleotides and DNA plasmids, simple lipids and phospholipids, and other recognition ligands and synthetic drug molecules. The polymer–biomolecule hybrid system is capable of responding to biological, physical and chemical stimuli. Hoffman and colleagues have pioneered the work in combining SPs with a wide variety of biomolecules (Stayton et al., 1998; Monji et al., 1997; Lackey et al., 1999; Fong et al., 1999). The SPs can be conjugated randomly or site-specifically to protein biomolecules (Gil and Hudson, 2004).

2.2. Temperature responsive polymers

Temperature is the most widely used stimulus in environmentally responsive polymer systems. The change of temperature is not only relatively easy to control, but also easily applicable both in vitro and in vivo. For example, temperature-responsive dishes can be utilized as a cell sheet manipulation techniques in vitro (Ebara et al., 2003; Nakajima et al., 2001; Yamato et al., 2000; Nandkumar et al., 2002; Uchida et al., 2000) and temperature-responsive hydrogels or micelles containing drug can be applied in vivo (Chilkoti et al., 2002; Weidner et al., 2001; Jeong et al., 2002; Meyer et al., 2001). One of the unique properties of temperature-responsive polymers is the presence of a critical solution temperature. Critical solution temperature is the temperature at which the phase of polymer and solution (or the other polymer) is discontinuously changed according to their composition (Figure 2.3). If the polymer solution (mostly water) has one phase below a specific temperature, which depends on the polymer concentration, and are phase-separated above this temperature, these polymers generally have a lower critical solution temperature (LCST), the lowest temperature of the phase separation curve on concentration–temperature diagram. Otherwise, it is called a higher critical solution temperature (HCST) or upper critical solution temperature (UCST). However, most applications are related to LCST-based polymer systems (Fujishge et al., 1989). For example, poly(*N*-isopropylacrylamide) (PNIPAAm) has a LCST, at which it undergoes a reversible volume phase transition caused by the coil-to-globule transition (Dautzengberg et al., 2000). Intramolecular collapse

occurs before intermolecular aggregation through LCST and the collapse of individual polymer chains increases the scattering of light in solution (cloud point). Phase separation between the collapsed polymer molecules and the expelled water follows this cloud point (Schild et al., 1992).

Besides the relationship between polymer and water molecules, there is another important characteristic of a temperature-responsive polymer. This is the intermolecular interaction in water medium, which might create hydrogel shrinkage, micelle aggregation or the physical cross-links.
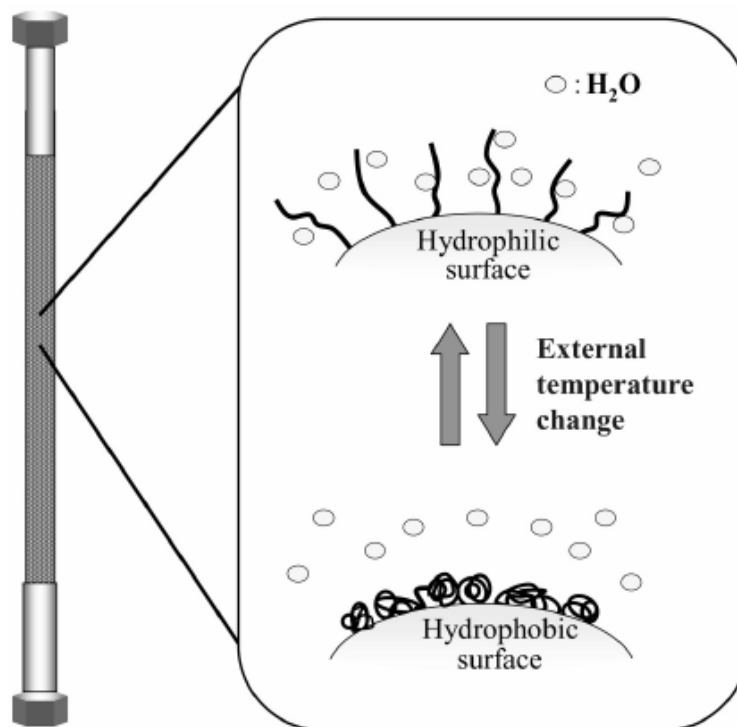
Figure 2.3.   Schematic illustration of thermally responsible stationary phases.

Generally, two types of intermolecular forces can be considered; hydrogen bonding and hydrophobic interactions. One example of an intermolecular association based on hydrogen bonding is a random coil-to-helix transition, at which by lowering the temperature, two or three biopolymer chains (e.g. gelatin) form a helix conformation that generates physical junctions to make a gel network (Guenet et al., 1992). Another example is the hydrogen bonding association/dissociation between different pendant groups, which can be controlled by temperature. Through this mechanism, reversible swelling/de-

swelling of hydrogels around a critical temperature was reported in random copolymer or interpenetrating polymer networks (IPNs) composed of polyacids (proton donor at low pH) and polyacrylamide (proton accepter) (Soutar et al., 1996; Garay et al., 1997). On the other hand, intermolecular association can be controlled by the balance of hydrophobic interactions and temperature. For example, triblock PEO–PPO–PEO copolymers (Pluronics, or Poloxamers) form a micelle structure above a critical micelle temperature (cmt) on the basis of hydrophobic effects of the PPO blocks (hydrophobic junction domain) that aggregate to form a core (Brown et al., 1992).

2.3. pH responsive polymers

A pH-responsive conformation with solubility changes is common behavior in biopolymers. The pH-responsive polymers consist of ionizable pendants that can accept and donate protons in response to the environmental change in pH. As the environmental pH changes, the degree of ionization in a polymer bearing weakly ionizable groups is dramatically altered at a specific pH that is called pK_a. This rapid change in net charge of pendant groups causes an alternation of the hydrodynamic volume of the polymer chains. The transition from collapsed state to expanded state is explained by the osmotic pressure exerted by mobile counterions neutralizing the network charges (Tonge et al., 2001). The polymers containing ionizable groups in their backbone form polyelectrolytes in the aqueous system. There are two types of pH-responsive polyelectrolytes; weak polyacids and weak polybases. The representative acidic pendant group of weak polyacids is the carboxylic group. Weak polyacids such as poly(acrylic acid) (PAAc) accept protons at low pH and release protons at neutral and high pH (Philippova et al., 1997). On the other hand, polybases like poly(4-vinylpyridine) is protonated at high pH and positively ionized at neutral and low pH (Pinkrah et al., 2003). Therefore, the proper selection between polyacids and polybases should be considered for the desired application. Even though a cross-linked homopolymer system of weak polyelecrolytes might show pH-responsive behavior, most pH-responsive polymer systems are designed by combining functional domains to control the pH-responsive properties. Hydrophobically modified pH-responsive polymers have a sensitive balance between charged repulsion and hydrophobic interactions. When

ionizable groups are protonated and electrostatic repulsion forces disappear within the polymer network, hydrophobic properties dominate, introducing hydrophobic effects that cause aggregation of the polymer chains from the aqueous environment (Philippova et al., 1997). Also the other collapse mechanism of pH-responsive polymer systems is based on the hydrogen bonding between the hydrogen in the protonated group and an electron-donating atom (e.g. oxygen or nitrogen) in the other functional groups, when the ionizable pendants groups are uncharged (Aoki et al., 1994; Yusa et al., 2002) (Figure 2.4).
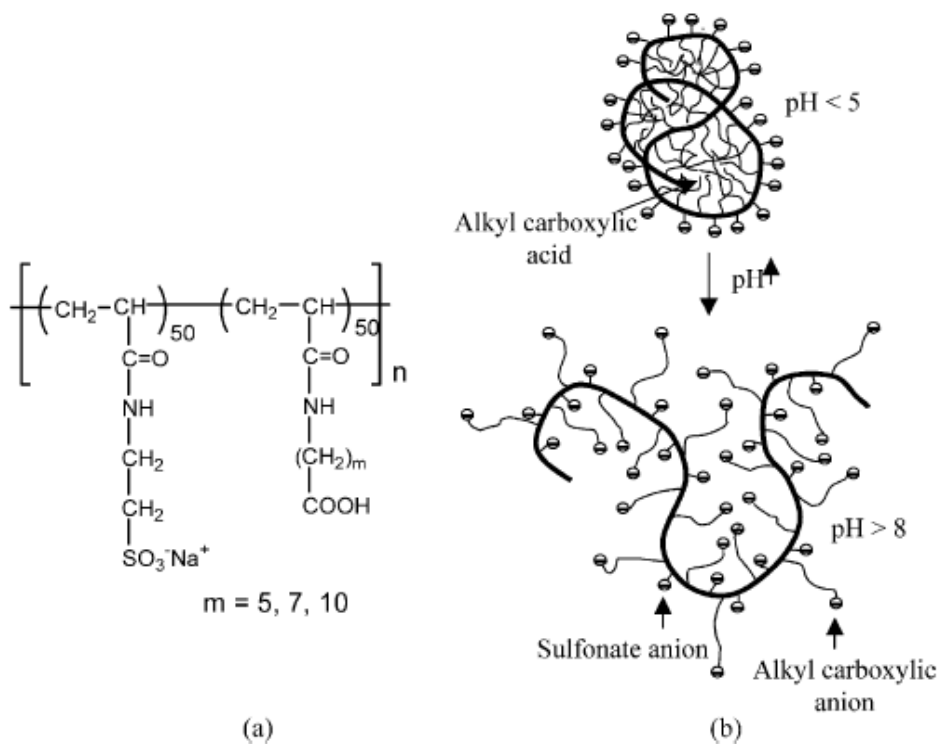
Figure 2.4.   (a) Copolymer of sodium 2-(acrylamido)-2-methylpropanesulfonate) (NaAMPS) with a series of monomers bearing long chain alkyl carboxyl pendents. (b) Schematic illustration of pH responsive unimer micelle (Yusa et al., 2002).

2.4. *N*-isopropylacrylamide and Copolymers

Important recent advances in PNIPAAm-based systems have focused on mechanistic understanding of phase transition, fine control of the structure–property relationship and novel biomedical applications. PNIPAAm is soluble

below 32°C and precipitates above 32°C in water (Schild et al., 1992). The phase transition temperature is referred to as lower critical solution temperature (LCST). Below the LCST, favorable interactions via hydrogen bonding between amide groups in polymer and water molecules lead to dissolution of polymer chains. Above the LCST, the hydrogen bonds are broken and water molecules are expelled from the polymer, resulting in precipitation of the polymer (Kujawa et al., 2001) The coil-to-globule transition of PNIPAAm was clearly seen in a nanometer scale using atomic force microscopy (AFM) (Zareie et al., 2000). In a recent study using laser scanning confocal microscopy (LSCM), the internal structure of PNIPAAm gel was shown to be composed of a continous two-domain structure with dense and sparse regions in the polymer network (Hirokawa et al., 1999).

By controlling the polymer composition and topology, the coil-to-globule transition could be kinetically and thermodynamically controlled. Copolymerization of NIPAAm with hydrophobic butylmethacrylate decreases the LCST of aqueous copolymer solution and copolymerization with hydrophilic comonomers, such as acrylic acid or hydroxy ethyl methacrylate, results in an increase in LCST (Kujawa, 2001). Depending on the content of hydrophilic moieties of poly(NIPAAm–co–acrylic acid) (in which –co– denotes block copolylmers) and poly(NIPAAm)–b–poly(ethylene glycol) (in which –b– denotes block copolymers) (PNIPAAm–b–PEG), at 37°C polymers exhibit sol-to-gel transition rather than precipitation (Ahn et al., 2001; Topp et al., 1997). Aoyagi *et al.* described an interesting example of molecular design of LCST polymers (Aoyagi et al., 2000). When 5 mole% of 2-carboxyisopropylacrylamide (CIPAAm) was copolymerized with NIPAAm, the copolymer showed little or no change in LCST, whereas 5 mole% of acrylic acid resulted in LCST increases of ~10°C, as measured in phosphate buffered saline (PBS) at pH 7.4. When both carboxylic acid groups and thermosensitivity are needed, this molecular design concept is very useful.

Polymer systems with more than one transition can be obtained by controlling polymer architecture. For example, hydrogels containing different LCST oligomer grafts showed dual swelling transitions with increasing temperature. The first transition resulted from oligoNIPAAm at 32°C, and the second transition occurred at 36°C owing to the presence of oligo(*N*-vinylcaprolactam) (Inoue et al., 1997).

Theoretical Information

Control of deswelling kinetics was also achieved by using graft copolymer structure. The comb-type grafted hydrogels of cross-linked P(NIPAAm) grafted with oligoNIPAAm (Yoshida et al., 1995) and poly(NIPAAm–g–PEG) (in which –g– denotes graft copolymers) (Kaneko et al., 1998) exhibited fast response to temperature changes. The authors suggested that grafted short chains of oligoNIPAAm in the former case contributed to fast dehydration, whereas in the latter case the hydrophilic PEG chains provided a water channel for a fast deswelling mechanism.

Recent studies of NIPAAm copolymers focused on biological applications such as separations, enzyme immobilization, gene delivery and cell culture (Bulmuş et al., 2001; Lee et al., 1998; Kim et al., 1999; Shimizu et al., 2001; Vernon et al., 1999; Oya et al., 1999). Hoffman *et al.* reviewed progress in smart bioconjugates that use stimuli-responsive properties of PNIPAAm (Hoffman, 2000). In a related application, the PNIPAAm polymers were investigated for on–off control of avidin–biotin binding (Bulmus et al., 2000). Below the transition temperature of 32°C, NIPAAm copolymers are in a fully extended conformation in water because of favorable polymer–water interactions. The PNIPAAm with fully extended conformation interferes with the biotin-binding site on the avidin, whereas above the transition temperature, the polymers are collapsed and cannot interfere with the binding sites. In related research aimed at the design of new bioseparation methods, PNIPAAms were conjugated to trypsin and chymotrypsin (Bulmus et al., 2000; Lee et al., 1998). As a result of this conjugation, specific enzyme activity–temperature profiles were demonstrated. Although the enzyme activity decreased to <50% of the native enzyme activity, the ease of separation by increasing temperature was advantageous.

Cell manipulation techniques using temperature-responsive culture surfaces grafted with PNIPAAm were also investigated (Shimizu et al., 2001). A decrease in culture temperature below the LCST resulted in the release of cardiac myocyte sheets from the cell culture dishes without enzymatic treatment. In another cell culture-related application, PNIPAAm–acrylic acid copolymers were used as a three-dimensional cell culture matrix useful for preservation of the phenotype of articular chondrocytes (Ahn et al., 2001). The chondrocytes cultured in a

monolayer lost their phenotype, whereas those cultured in the PNIPAAm-acrylic acid gel kept the phenotype and rounded-shape of the cells. PNIPAAm–acrylic acid copolymers were also used for entrapping islets of Langerhans for a refillable biohybrid artificial pancreas (Vernon et al., 1999).

A smart polymer that can recognize specific molecules was designed based on NIPAAm, *N,N*-trimethyaminopropylmethacrylamide and bisacrylamide (Oya et al., 1999). The smart gel was used to recognize pyranine-3 with three sulfonate groups and pyranine-4 containing 4 sulfonate groups. The 3- and 4-point multiple ionic interactions between polymers with positive charges and pyranine with negative charges were recognized differently. In the shrunken state, at 55°C, the gel adsorbed all of the pyranine molecules, whereas in the swollen state, at 25°C, the gel released them. The affinity study revealed that the binding site consists of three-point contacts in the case of pyranine-3 and four-point contacts for pyranine-4, indicating multipoint ionic interactions of molecular recognition. The gel demonstrated different affinity profiles for two pyranines as a function of temperature, indicating a promising method for affinity separations using stimuli-sensitive polymers.

Metal-seeded PNIPAAm copolymers are another interesting area of research. A metal can be incorporated into a gel by using copolymerizable metal ligands, followed by metal complex formation. PNIPAAm gels seeded with ferromagnetic materials demonstrated magnetic-field-sensitive swelling–deswelling transition. The transition resulted from the heat released by magnets in a magnetic field, followed by the collapse of temperature-sensitive PNIPAAm copolymer (Dagani et al., 1997). Yoshida *et al.* synthesized a gel with swelling–deswelling transition controlled by redox reaction using PNIPAAm seeded with tris (2,2′-bipyridyl) ruthenium (II) (Yoshida et al., 1999). The gel exhibited dynamic oscillating contraction and shrinking as ruthenium changed from +2 to +3 oxidation states periodically in the Belousov–Zhabotinsky reaction. At +3 oxidation state, the polymers increased water absorption by osmotic and electrostatic forces. The increased hydrophilicity raised the transition temperature and the gels swelled. At +2 oxidation state, the gel reverted to shrunken state. Therefore, the copolymer undergoes swelling–deswelling transition at a constant temperature.

The PNIPAAM copolymers have been studied for many applications that take advantage of their thermosensitive properties in water. Kinetics and thermodynamics of the phase transition might be controlled by well-designed molecular parameters. Biomedical applications of PNIPAAm copolymers in drug delivery, cell culture, molecular recognition, enzyme kinetics control and as magnetic valves have all been suggested.

In the search for degradable polymers with a LCST in water at 37°C, polyphospazenes with PEG and amino acid ester groups as side chains were investigated. Because of their biodegradability, these polymers might be considered as degradable counterparts of PNIPAAm (Song et al., 1999; Lee et al., 1999). Degradable poly(ethylene glycol)–poly(lactic acid-co-glycolic acid) (PEG–PLGA) copolymers, which are discussed below, also demonstrate PNIPAAm-like precipitation at polymer concentrations below the critical gel concentration (CGC) of ~15 wt% (Jeong et al., 1999a; Jeong et al., 1999b; Jeong, 2000)

2.5. Molecular Imprinting

Over the past decade, the introduction of specific binding domains within synthetic polymers by template-directed cross-linking of functional monomers (molecular imprinting or molecular templating) has attracted considerable attention (Yan et al., 2005). Molecular imprinting involves arranging polymerizable functional monomers around a template followed by polymerization and template removal (Figure 2.5). Arrangement is typically achieved by non-covalent interactions (e.g., H-bonds, ion pairing) or reversible covalent interactions. A properly designed molecularly imprinted polymer (MIP) can then bind the template or structurally similar analytes (Yan et al., 2005).

The advantages of MIP-based materials include: (i) binding affinities comparable to a biological recognition element (nM dissociation constants have been reported), (ii) robustness and stability under a wide range of chemical and physical conditions, and (iii) an ability to easily design recognition sites for analytes that lack suitable biorecognition elements (Yan et al., 2005). MIPs have been developed for a large variety of molecules and macromolecules including amino acids, mycotoxins, nucleotide bases, pesticides, pharmaceuticals, proteins, and

vitamins (Table 2.1; Zhang et al., 2005; Zhu et al., 2006; Urraca et al., 2006a; Urraca et al., 2006b; Tao et al., 2006; Sun et al., 2004; Piletaskaya et al., 2005; Matsunaga et al., 2006; Maiter et al., 2004; Huang et al., 2004; Homer et al., 2004; Hall et al., 2006; Graham et al., 2002; Benito-Pena et al., 2006; Ersöz et al., 2005; Odabaşı, et al., 2007; Özcan et al., 2006).
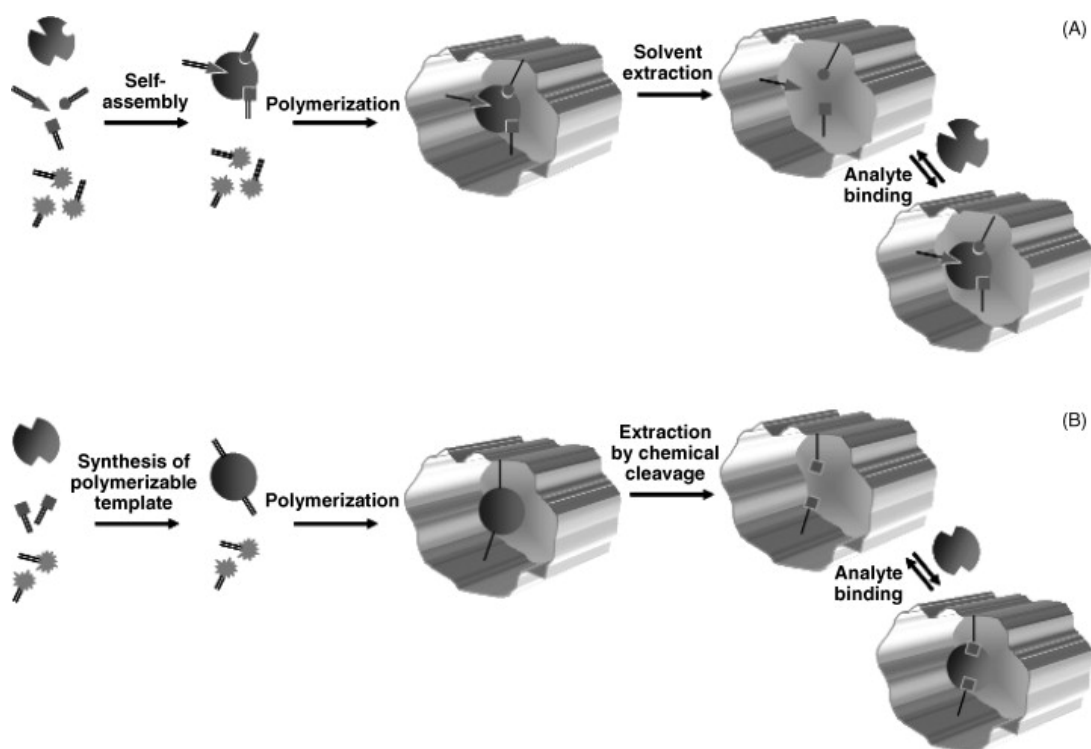
Figure 2.5.   Schematic representation of the two most common MIP fabrication strategies. (A) Non-covalent imprinting. (B) Covalent imprinting.

2.5.1. Molecularly imprinted materials

2.5.1.1.The basic strategy

Molecular imprinting involves arranging polymerizable functional monomers around a template (pseudo-target analyte or the actual target analyte) followed by polymerization and template removal. The basic concept is illustrated in Figure 2.5. Ensuring that the functional groups of the template molecule are interacting with complementary functionality of polymer-forming components is of major importance in this technique (Whitcombe et al., 2001). Arrangement is generally

achieved by: (i) non-covalent interactions (i.e., hydrogen bonds, ion pair interactions, hydrophobic interactions, Van der Waals forces, dipole–dipole bonds) or (ii) reversible covalent interactions. Mosbach (Ekberg et al., 1989; Mosbach et al., 1994) established the most common strategy (Figure 2.5a) which is based on non-covalent interactions between specific functional groups on the polymerizable monomers and the template to position the monomers in a particular orientation with respect to the template molecule prior to polymerization. Various polymerizable functional monomers commonly used for non-covalent molecular imprinting are illustrated in Figure 2.6a (Yan et al., 2005). A cross-linking monomer is generally used to form a three-dimensional rigid structure around the template molecule and produce stable binding cavities. Figure 2.6b (Yan et al., 2005) illustrates several of the more common cross-linker monomers that have been used.

Following polymerization and template removal, the functional groups within the templated polymeric matrix can subsequently recognize and bind the target analyte using the same non-covalent interactions. Arrangement using non-covalent interactions requires the template and target analyte to form a sufficient number of non-covalent intermolecular interactions to produce the binding pocket during polymerization. Therefore, non-covalent imprinting is not particularly successful for template or target molecules that do not possess appropriate functional groups (i.e., strong non-covalent interactions between the functional monomers and template are a key requirement) (Graham et al., 2002). Despite this limitation, non-covalent imprinting is very flexible in terms of the functional monomers and possible target molecules (Yan et al., 2005).

Reversible covalent interactions can be used to overcome the limitations of non-covalent imprinting (Figure 2.5b). Wulff et al. (Wulff et al., 1977) introduced a covalent molecular imprinting method that exploits reversible covalent bonds between binding site monomers and a template molecule. During imprinting, the strong (covalent) interactions aid in controlling the functional groups within/inside the templated binding cavity. The covalent bonds are then cleaved to release the template molecule, but they are later renewed or derivatized so the template site selectively binds the target molecule and/or transduces its presence upon binding.

Theoretical Information

Table 2.1.   Design and application examples of molecularly imprinted polymers.

Analyte class	Target analyte(s)	Template	Application	Polymer material(s)
Pharmaceuticals	Penicilin G	Penicilin G potassium salt	Binding assay	Methacrylic acid 2-Hydroxyethyl methacrylate Methacrylamide
	Penicilin G	Penicilin G procaine salt	Solid-phase extraction	1-(4-Vinylphenyl)-3-[3,5-bis(tri-fluromethyl)phenyl]urea Methacrylamide
	Methadone	Methadone	Chromatography	Methacrylic acid Hydroxyethyl methacrylate Itaconic acid
	Morphine	Morphine	Chromatography	Methacrylic acid Hydroxyethyl methacrylate
Mycotoxins	Ochratoxin A	2-[(1-Hydroxy-naphthalene-2-carbonyl)-amino]-phenyl-propionic acid	Solid-phase extraction	*tert*-Buyl methacrylic acid Tertiary amine methacrylic acid
	Zearalenone, α-Zearalenone	Cyclododecanyl-2,4-dihydroxybenzoate	Solid-phase extraction	1-Allylpiperazine
Amino acids	L-Histidine	L-Histidine	Sensor	Phenyltrimethoxysilane Methyltrimethoxysilane
	L-proline N-*tert*-Butoxycarbonyl-L-tryptophan N-*tert*-Butoxycarbonyl-L-tyramine	L-proline N-*tert*-Butoxycarbonyl-L-tryptophan N-*tert*-Butoxycarbonyl-L-tyramine	Sensor Chromatography Chromatography	Methacrylic acid Acrylamide Acrylamide
Nucleotide bases	Cytosine,thymine, guanine,adenine	9-Ethyladenine	Chromatography	Methacrylic acid
Pesticides	Monocrotophos	Monocrotophos	Solid-phase extraction	Acrylamide Methacrylic acid Acrylic acid
	1,1-Bis(4-chlorophenyl)-2,2,2-trichloro-ethane (DDT)	4,4'-Ethylidenebisphenol	Sensor	Bis(trimethoxysilylethyl)benzene
Proteins	Lysozyme Trypsin Cytochrome C Chymotrypsin	Lysozyme	Binding assay	Acrylic acid Methylene bis(acrylamide) 2-Methacryloylethyl Phosphoryl-choline
	Ovalbumin	Ovalbumin	Sensor	Tetraethoxysilane 3-Aminoproplytriethoxysilane n-Octyltrimethoxysilane Bis(2-hydroxy-ethy)aminopropyl-Triethoxysilane
	Lysozyme	N-methacryloyl-(L)-histidinemethylester (MAH)	Chromatography	Hydroxyethyl methacrylate
	Cytochrome C	N-methacryloyl(L)-histidine-copper(II)	Biochromatography	ethylene glycol dimethacrylate
Vitamins	Follic acid	N-Z-L-glutamic acid	Binding	2-Amino-6-methylpyridine 9-(3/4-Vinylbenzyl)adenine Methacrylamide 2-Methacrylamidopyridine 1-(4-Vinylphenyl)-3-(3-nitro-phenyl)uea
M.saccharide	Glucose	N-methacryloyl(L)-histidine-copper(II)	Biochromatography	N-methacryloyl(L)-histidine
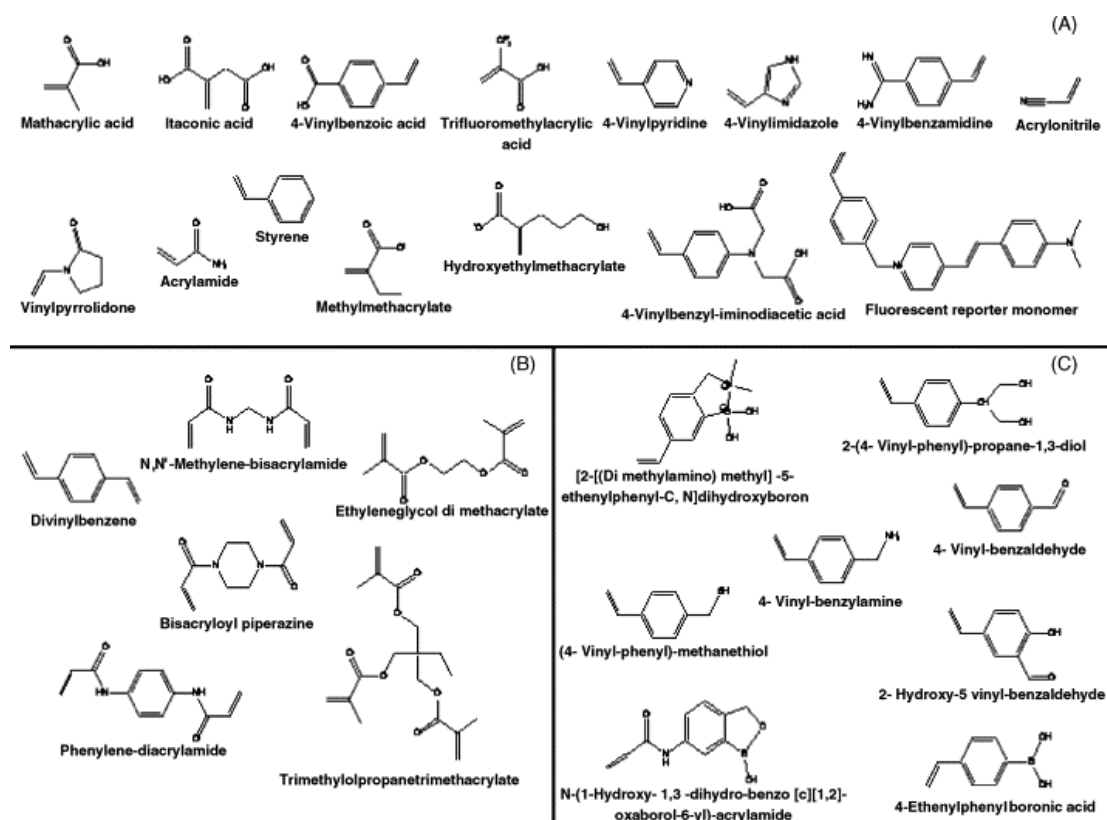
Figure 2.6.   (A) Examples of organic polymerizable functional monomers that can be used alone or in combination in non-covalent molecular imprinting. (B) Examples of cross-linking monomers that can be used for the synthesis of molecularly imprinted polymers. (C) Examples of organic polymerizable functional monomers that can be used in covalent molecular imprinting.

This type of imprinting creates strong interactions as a result of the restoration of the covalent bond between the matrix and the target; however, it is limited by the rather small number of useful reversible covalent interactions that can be used (Graham et al., 2002). Binding site monomers having a boronic acid, diol, aldehyde, or amine functional group have been successfully used for covalent molecular imprinting applications (Figure 2.6c) (Yan et al., 2005). Cross-linking monomers (Figure 2.6b) are also utilized in this approach to help stabilize and define the molecularly templated sites within the final material.

In both types of molecular imprinting (Figure 2.5), once the template is removed, three-dimensional cavities are generated within the final material that is

complementary to the template molecule in size, shape, and functionality. Essentially, one creates a molecular "memory" within the imprinted polymer matrix (Yan et al., 2005).

To overcome the drawbacks associated with covalent and non-covalent approaches to molecular imprinting, Whitcombe et al. (Whitcombe et al., 1995) described an alternative approach that exploits the positive aspects of covalent and non-covalent imprinting. In the sacrificial spacer (SS) approach, first developed for cholesterol binding, the authors used cholesteryl (4-vinyl)phenylcarbonate ester as a functional monomer, which operated as the covalently bound template monomer but was easily cleaved hydrolytically with the loss of CO_2. This combination resulted in the formation of a non-covalent recognition site within the final material bearing a phenolic residue capable of interacting with the template (i.e., cholesterol) through hydrogen bonding. Whitcombe and coworkers (Kirsch et al., 2004) has also reported on imprinting of small aromatic heterocycles in which MIPs were prepared by using two different sacrificial spacer methodologies (phenyldimethylsilylmethacrylate template) and were evaluated by comparison with pyridine-imprinted polymers prepared by the non-covalent molecular imprinting method. The non-covalently imprinted polymers showed no size selectivity for the smaller pyridine template. In contrast, the polymers prepared using the SS method exhibited more selective binding, particularly at analyte concentrations below 1.0 mM.

2.5.1.2. Material types

Choice of polymerizable functional building blocks is an important step in preparing molecularly imprinted materials. In general, these components are reactive monomers that are capable of forming stable network polymers or gels that maintain a "memory" for the template or template analog (Yan et al., 2005).

2.5.1.3. Organic materials

Figure 2.6 illustrates examples of typical organic monomers that are widely used to form MIPs. Polystyrenes/polyacrylates and inorganic polysiloxanes represent two major classes of precursors that have been successfully used for molecular

imprinting. The attractiveness of vinyl and acrylic polymers arises from the assortment of functional monomers available. These monomers can be positively or negatively charged, hydrogen bonding, hydrophobic, metal coordinating, etc. (Yan et al., 2005). Methacrylic acid (MAA) is the most widely used functional monomer because it can form hydrogen bonds with a wide variety of functional groups on a template/target analyte. In addition, one can induce analyte/template binding and/or removal under mild conditions (Kandimalla et al., 2004).

MIPs are often formed by solution polymerization and then mechanically ground to give smaller particles with micrometer diameters. Dispersion polymerization can also be used to fabricate MIPs. This approach obviates mechanical grinding and yields aggregates of spherical particles (Sellegren et al., 1994) or uniformly sized microspheres (Ye et al., 1999). Another means for preparing molecularly imprinted materials/supports involves forming imprinted membranes. These can be prepared as thin cross-linked imprinted polymer films (Krotz et al., 1996; Piletsky et al., 1995), by precipitation from solutions of linear polymers in the presence of the analyte (Wang et al., 1996), or by casting an imprinted polymer in the pores of an inert support membrane (Hong et al., 1998; Dzgoev et al., 1999).

2.5.1.4. Inorganic materials

The sol–gel technique (Brinker et al., 1989; Hench et al., 1992; Gupta et al., 2007) allows one to entrap active species within a readily tunable material (Avnir et al., 1995; Avnir et al., 1992a; Avnir et al., 1992b; Avnir et al., 1994; Brennan et al., 1999; Blum et al., 1999; Dave et al., 1994; Jin et al., 2002; Lan et al., 1999; Lev et al., 1995; Carturan et al., 2004; Chodavarapu et al., 2005). Figure 2.7 illustrates the individual steps for the formation of a class I xerogel prepared from tetraalkoxysilane precursors (Figure 2.7a) or a class II xerogel prepared from an organically modified silane (ORMOSIL) and tetraalkoxysilanes (Figure 2.7b). The individual steps associated with the sol–gel process are hydrolysis, condensation, and polycondensation. In the first step, metal or semi-metal alkoxide hydrolysis yields a hydroxylated product (silanol in this case) and the corresponding alcohol. This process is generally acid or base catalyzed and its rate is pH dependent. In the second step, condensation between (i) an alkoxide group and a silanol produces a siloxane and alcohol, or (ii) two silanols produce a siloxane and water.

These constituents continue to hydrolyze and condense, eventually forming a colloidal suspension of reactive nanoscale particles called a "sol".
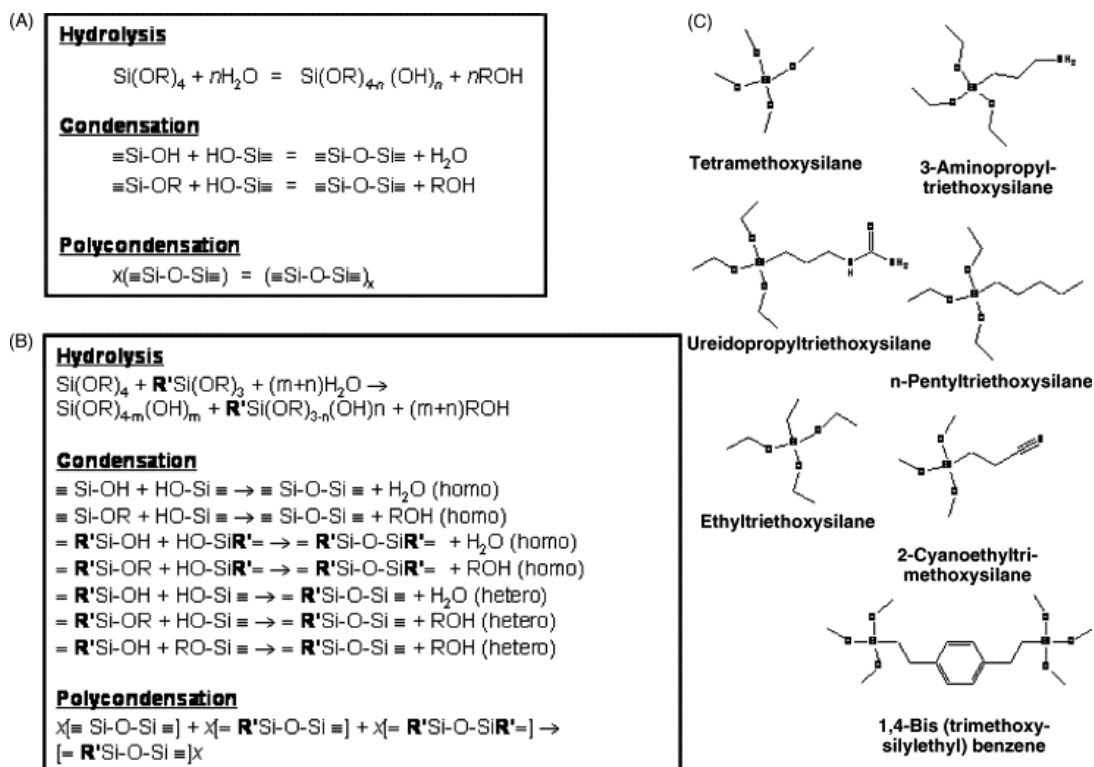
Figure 2.7.   Sol–gel processing. (A) For a tetraalkoxysilane. (B) For the co-hydrolysis and co-condensation of a tetraalkoxysilane and an alkyl-trialkoxysilane to form a class II ORMOSIL. (C) Representative compilation of silane-based alkoxide precursors that can be used alone or in combination to form xerogels.

The sol can be cast into thin films, fibers, or monoliths while it is still in the solution phase. In the third and final step, polycondensation between the sol particles occurs, resulting in a nano-porous, glass-like, three-dimensional network that is optically transparent. During this step, aging and drying of the sol–gel composite occurs; this process is accompanied by the loss of solvent (alcohol, water), which increases the strength and decreases the sol–gel-processed material's porosity. The method used to dry the gel can have a dramatic influence on the final material properties. When drying is performed under ambient conditions, the resulting composite is called a xerogel. An aerogel is formed when the sol is processed

under supercritical conditions. Xerogels have lower surface areas, smaller pore sizes, and higher densities in comparison to aerogels. Figure 2.7c shows several representative examples of silicon-based trialkyoxysilanes that one can use to form hybrid class II xerogels. Several commercial sources exist (Sigma–Aldrich, Gelest) and they offer an even wider variety of precursors including ones based on Ti, Ce, V, Zr, and Hf as well as Si.

Sol–gel-derived xerogels are attractive materials because their physicochemical properties can be tuned by choice of precursor(s) and the processing protocol (Brinker et al., 1989; Hench et al., 1992; Gupta et al., 2007) As examples, xerogel hosts may be prepared with: (i) a wide range of surface areas, mean pore dimensions, and pore size distributions, (ii) good thermal stability well beyond most dopant molecules, (iii) exceptional photostability, (iv) adjustable electrical conductivities, and (v) a reasonably broad optical window that allows the use of modern spectroscopic tools to study dopants within the xerogel.

2.5.2. Applications for Molecular Imprinted Polymers

In recent times, four main areas of application application for molecularly imprinted polymers have been pursued: (1) Affinity Separation, (2) Antibody Binding Mimics, (3) Enzyme Mimics and (4) Bio-Mimetic Sensors. These four areas continue to be the focus of most research efforts.

2.5.2.1. Affinity separation

Affinity separation is the single biggest application for imprinted polymers at present (Mosbach et al., 1998). In this context, their use as stationary phases in high performance liquid chromatography (HPLC) continues to be an important research avenue, in spite of its well-documented (current) limitations: low capacity and heterogeneous binding sites. In the research laboratory, HPLC using an imprinted stationary phase remains one of the most convenient methods for assessing the efficiency of a new imprinting protocol. Besides liquid chromatography, it is very noticeable that imprinted polymers as selective solid-phase extraction (SPE) media are very much in vogue. It may well be that this is the area in which we will see the first commercial application of these materials.

Other key lines of research in the affinity separation area include membranes and capillary electrophoresis (CE).

2.5.2.2. Antibody binding mimics

The demonstration that the strength and the selectivity of binding between an imprinted polymer and an analyte could be comparable, and in some cases even better than that between an antibody and an antigen generated enormous interest (Vlatakis et al., 1993). In an application sense, these antibody binding mimics ('plastic antibodies') offer a rapid and inexpensive route into stable and robust molecular recognition matrices (Haupt et al., 1998). They promise a real (non-immunogenic) alternative in applications that use antibodies in their insoluble form, e.g. immunoaffinity chromatography (c.f. affinity separation above), immunosensors (cf. Bio-mimetic sensors below) and immunoassays. Some recent immunoassay-related studies have focussed on developing new assay formats that do not rely upon radioligands, e.g. fluorescence and electro chemical assays.

2.5.2.3. Enzyme mimics

A dream for many working in the area of molecular imprinting has been to develop catalytically active imprinted polymers ('plastic enzymes') that are capable of mimicking Nature's enzymes. This task is, of course, an enormous undertaking, and the results reported to date tend to reflect this fact. Several different organic reactions have been successfully catalysed with molecularly imprinted polymers, including aldol condensations, ester hydrolyses, Diels–Alder reactions and β-eliminations. While molecularly imprinted polymers may not yet be able to compete with enzymes in terms of catalytic rate enhancements, they offer properties that are quite distinct from those of enzymes, e.g. their ready compatibility with organic solvents and their high temperature stability. Thus they are more useful as a complement to enzymes rather than as a replacement, at least for now.

2.5.2.4. Bio-mimetic sensors

For some time now, there have been several concerted attempts to make in-roads into the biosensor market with imprinted polymers. The idea is, of course, to

replace 'delicate' molecular recognition entities based on biomolecules with imprinted polymers (Kriz et al., 1997). Although the biosensor field is a very competitive area, one would expect molecularly imprinted polymers to challenge very strongly in this area given their many and varied attractive properties. Several potential applications have been demonstrated on a laboratory scale, but nothing, as yet, has found its way into the marketplace. Perhaps this is not so surprising bearing in mind the relatively tender age of this approach (Mosbach et al., 1999).

2.6. Thalassemia

Thalassemia is the world's most common monogenic disease (Weathrall et al., 1996), and due to migration, it is no longer confined to the tropical areas in which it arose. Since thalassemia is present in nearly all parts of the modern world, more interest has developed in the treatment of this group of diseases. Therapeutic modalities for the supportive or curative treatment of thalassemia have been expanded, offered a wide variety of therapeutic options, some currently in use, and others for future application. Concurrently, as the lifespan of affected patients has been extended by improvements in supportive care, the age distribution of the patient population has dramatically altered (Pignatti et al., 1998). Furthermore, in many countries, the use of DNA-based prenatal diagnosis has substantially reduced the number of births of affected individuals, and has accentuated the trend of increasing age of thalassemia patients. Approaching the new millennium, clinicians who care for thalassemia patients thus have at their disposal new treatment options, but they also face the challenges of an older, more complex patient population.

2.6.1. Therapeutic decisions in Thalassemia: the spectrum of the disease

Thalassemia has a very wide clinical range of severity, from transfusion dependency beginning in infancy, to a mild condition requiring little if any medical intervention. Thalassemia major (TM) is the severe form of the disease, presenting with transfusion-dependent anemia, generally in the first year of life. Thalassemia intermedia (TI) are the less severe form of the disease, and are highly variable.

The hallmark which can be used to differentiate TI from TM is the lack of transfusion dependency. However, despite this difference, many of the problematic clinical manifestations facing thalassemia patients overlap and occur in both TI as well as TM patients. For example, although all TM patients require chelation, some TI patients, even those who are untransfused, may hyperabsorb iron and also require chelation. Furthermore, some patients undergo an evolution of their clinical picture as they grow through childhood, into adolescence and adulthood. A patient may begin life with a relatively high hemoglobin and little disability, and later, require blood transfusion and associated chelation therapy and suffer many of the disabling manifestations of the disease.

To clarify the overall treatment approach, it can be said that, of the supportive modalites listed below, transfusion and chelation are used predominantly for TM patients. These individuals require transfusion to sustain life, and thus are iron loaded from an early age due to transfusional iron deposition. TI patients can also require transfusion, but infrequently. A subset of TI patients may require chelation due to iron hyperabsorption. On the other hand, the supportive treatment modalities aimed at increasing fetal hemoglobin production (hydroxyurea, erythropoietin, etc.) are almost exclusively applicable to therapy of TI patients. These modalities require a certain level of baseline effective erythropoiesis in order to be beneficial, and therefore they are not generally beneficial in TM. Finally, the curative modalities we review (such as bone marrow transplantation) are predominantly appropriate for treating TM patients, since most curative modalities are not only costly but are associated with some risk of mortality and morbidity. The mild to moderate degree of disability suffered by most patients with TI generally does not warrant the use of these costly and risky types of treatment. A small subset of the most severely affected TI patients can be considered candidates for curative treatment such as BMT. Lastly, in most cases, the use of the novel experimental modes of curative therapy (such as gene therapy) will be most appropriate for consideration for the treatment of TM.

2.6.2. Treatment of β-thalassemia

The therapeutic options for the thalassemias are expanding with each passing year. Supportive Treatments including; transfusion therapy, chelation therapy are

most commanly used treatments for Thalassemia. The overall outlook for thalassemia patients include a greatly increased life expectancy, which brings with it new manifestations of the disease, and the many associated challenges which arise when dealing with the older thalassemia patients. However, it is gratifying to be able to utilize some of the newer currently available therapeutic tools as Bone marrow transplantation (BMT) and Gene Therapy. Current standards of care should include all of the supportive as well as the curative methodologies, and should be available to patients in all geographic regions of the world.

2.6.2.1. Supportive treatment

2.6.2.1.1. Transfusion therapy

The mainstay of supportive care for the anemic patient with β-thalassemia is blood transfusion. The three principles guiding transfusional support of the thalassemia patient in the 1990s, which will be guidelines for the future as well, are: (a) to transfuse to the minimum hemoglobin needed to assure growth and good quality of life, thus minimizing iron overload; (b) to assure that blood is free of blood-borne viral agents (insofar as is possible); (c) to use leukocyte filters for their many beneficial effects, including reduction of the incidence of transfusion reactions, minimizing immunosuppression and reducing the transmission of certain infectious agents.

The level of pretransfusion hemoglobin has, in the past, been a subject of major controversy. Levels as high as Hb of 12.0 was advocated in some centers. It is now generally accepted that a lower pretransfusion hemoglobin level, somewhere between 9 and 10 gm/dl, is sufficient to suppress erythropoiesis and allow for normal growth and development (Cazzola et al., 1995; Piomelli et al., 1995). It is generally felt that maintaining a higher baseline hemoglobin level does little to improve the patient's clinical condition, at a price of much increased iron overload. The precise definition of the 'ideal' baseline varies from center to center, some aiming at Hb of 9–9.5, and others at a Hb of 9.5–10.0 (Piomelli et al., 1995). Determination of the serum transferrin receptor has been used to document adequate suppression of endogenous ineffective erythropoiesis at these levels of hemoglobin (Cazzola et al., 1995).

Frozen, washed blood was previously advocated as the ideal type of blood to administer to thalassemia patients as it was virtually leukocyte-free, and leukocytes are a frequent cause of transfusion reactions. Both leukocyte debris itself, as well as cytokines secreted by white blood cells, can cause transfusion reactions. However, it has also recently been recognized that frozen red blood cells are poor in 2–3 DPG and so, have reduced oxygen-carrying capacity. Furthermore, frozen RBC has reduced survival due to a large loss of cells in vitro and in vivo, ultimately increasing transfusion requirement (Piomelli et al., 1995). Aside from this, the use of frozen washed cells is extremely expensive. Therefore, their use has been largely abandoned, except for rare cases of patients with extensive alloimmunization requiring rare blood types. Instead, leukocyte-depletion is performed, which can achieve many of the same beneficial effects as can washing of the RBC. This can be done by bedside filtering of the blood with any of a number of commercially-available in-line filters. These filters are expensive, and therefore they are not routinely used in many of the developing nations where the incidence of thalassemia is high.

The preferred method of reducing transfusion reactions is to perform leukofiltration at the time of blood collection from the donor, or at the time of red cell storage as components. This nearly eliminates the secretion of cytokines into the unit of RBC, since only a negligible number of white blood cells remain in the unit of blood at the time of storage. Furthermore, WBC debris is virtually eliminated. This will hopefully become standard procedure for collecting blood in all countries and will improve the safety of transfusions for all who need them.

Many viral agents can be transmitted by transfusion, including hepatitis B, C, HIV, HTLV types I and II, and CMV. The viral complications of transfusion therapy for thalassemia continue to be problematic, and have recently been extensively reviewed (De Montalembert, et al., 1995).

2.6.2.1.2. Chelation therapy

There is no doubt that the judicious use of chelation has been one of the most effective therapeutic advances in prolonging life of thalassemia patients. This complex subject has recently been reviewed comprehensively (Hersko et al.,

1998). We will highlight some of the issues surrounding standard chelation therapy and the newer drugs for chelation.

2.6.2.1.3. Intravenous chelation

Parenteral chelation is a mainstay of therapy for transfusion dependent patients with thalassemia. The use of desferrioxamine has recently been extensively and cogently reviewed (Oliveri et al., 1997). In brief, this drug has been proven to be of great utility in the treatment of thalassemia, reversing organ toxicity and prolonging life expectancy when properly used. However, the drug is problematic in that it can be irritating when injected locally. In addition, most studies have found that in order to achieve sufficient iron removal, the patient must use desferrioxamine by continuous subcutaneous infusion for many hours per day, for at least 250 days of the year. This rigorous and often uncomfortable treatment regimen generally results in poor compliance particularly during adolescence and young adulthood. In a small number of patients, the treatment can not be easily administered because the drug causes local allergic reactions.

After many years of monitored use and observation of patients, it is now clear that desferrioxamine can be toxic when given in excessive doses. It can have neurological side effects (Oliveri et al., 1997), affecting sensorineural function (vision, hearing). Other adverse effects are seen in the skeletal system, expressed as decreased growth velocity. Therefore, parenteral chelation must be dealt with cautiously, and consideration given to the age at which chelation is initiated and the total dose given. Close monitoring for toxicity is imperative as chelation is instituted and becomes routine in each individual patient.

2.6.2.1.4. Oral chelation

Deferiprone, or L1, is the primary oral chelator currently used in therapeutic trials around the world. This drug was first introduced in 1985 (Kontoghiorghes et al., 1985), and after in vitro and animal studies proved it effective, it was initially used for myelodysplasia (Kontoghiorghes et al., 1987) and then later introduced for treatment of thalassemia (Kontoghiorghes et al., 1990).

Theoretical Information

Although the goal of chelation is the reduction of toxic tissue iron stores and thereby, the prevention of end organ disease due to iron overload, another potential beneficial mechanism may be the removal of iron from the RBC membrane. The pathophysiology of thalassemia results in part from RBC membrane damage, including oxidative damage mediated by abnormal free iron deposits on RBC membranes. Since L1 is able to penetrate the RBC membrane, it may be therapeutically useful by removing iron from its potentially toxic location on membranes of thalassemic RBC (Shalev et al., 1995).

The urgent need for an effective, affordable oral chelator can not be understated. Thalassemia is a disease of the Third World. In most countries in which the disease is prevalent, conditions (including both financial considerations and sanitary conditions) required for use of parenteral chelation are not present. The parenteral medication, desferrioxamine, is extremely costly, as is the sterile and disposable equipment necessary for adminstering the drug. On the other hand, L1 is substantially less costly to manufacture and its oral route of adminstration would make it potentially available to thousands of patients who would otherwise receive no chelation at all.

From its very inception, L1 has been a controversial drug. The long term administration of the drug was reviewed recently (Olivieri et al., 1996). The controversy around the drug initially centered on two aspects, the first being the efficacy of the drug at restoring negative iron balance, compared to the efficacy of desferrioxamine. Initial reports regarding the efficacy of the drug, when administered to patients for 1–15 months, suggested that it was not sufficient for achieving negative iron balance in transfused TM patients (Kontoghiorghes et al., 1990; Tondury et al., 1990). Later reports by these same investigators, which were based on slightly longer term studies (12–22 months), indicated that L1 could achieve significant reduction in ferritin levels in transfusion dependent thalassemia (Agarwal et al., 1992; Al-Rafaie et al., 1992; Olivieri et al., 1995). Another recent study again suggested L1 was inadequate therapy (Olivieri et al., 1998). This negative report of the efficacy of L1 as an oral chelator has come under much criticism.

Nevertheless, even if L1 is a less effective chelator, many have argued that L1 could be used for limited periods of time during which treatment with desferrioxamine may not be feasible. For example, L1 could be used to prevent a rise in ferritin to dangerous levels in newly noncompliant patients who had previously received adequate chelation (Olivieri et al., 1996). Indeed, even in developed countries where desferrioxamine is freely available, L1 may be of value for use during adolescence, when psychological turmoil may result in potentially life-threatening noncompliance. The judicious use of L1 may be preferable to no chelation at all.

The second concern regarding L1 which has been the subject of controversy has been the toxicity of the drug. Both neutropenia and agranulocytosis have been reported (Olivieri et al., 1995; Hoffbrand et al., 1989; Al-Rafaie et al., 1994), with one fatality reported in MDS. The myelotoxicity is reversible either spontaneously or in response to growth factors (granulocyte-colony stimulating factor). This myelotoxicity was the subject of much attention, particulaly since the use of the drug was planned predominantly in countries where facilities for careful monitoring of white blood counts may not exist. This focus on myelotoxicity tended to overshadow concern over the other adverse effects of the drug. For instance, the most common adverse effect of L1 involves the joints, with arthritis and arthralgias which could be persistent, requiring cessation of therapy (Olivieri et al., 1995; Al-Rafaie et al., 1995).

The controversy during the last year surrounding the toxicity of L1 is one of the most heated therapeutic debates ever to take place in the field of hematology. In particular, the implication has been made that L1 causes progression of hepatic fibrosis (Olivieri et al., 1998). Since this report was published, others have reported that L1 is an effective and safe chelator, and furthermore, that it does not cause progression of hepatic fibrosis (Piga et al., 1998). Future results from other centers should help resolve the actual risk-benefit ratio for the use of L1. In the meantime, caution is required when utilizing this drug, which should be reserved for selected patients who have substantive reasons that prevent treatment with the standard, well proven drug, desferrioxamine. However, on the basis of all information available to date, we do not believe that the use of L1 should not be precluded,

particularly in patients who can be monitored for possible toxic effects of the drug, and when no other alternative is available.

2.6.2.1.5. Chelation: combinations and new agents

For the purpose of iron trapping, it is possible that a combination of different types of chelators, such as L1 plus desferrioxamine, may chelate iron more successfully that a single drug (Grady et al., 1998; Wonke et al., 1998). This approach has only recently been explored, and combination therapy may prove to be important. It is logical that adminstration of lower doses of several chelators should have less toxicity than higher doses of a single drug. Furthermore, a 'cocktail' of chemically different drugs with different iron carrying capacities may work synergistically and therefore be more efficient than each drug admimistered alone (Grady et al., 1998; Wonke et al., 1998). For example, desferrioxamine, a hexadentate molecule, and L1, a bidentate chelator were used in combination in a recent study. Deferiprone was administered orally three times daily, in combination with 8 h of nightly subcutaneous desferrioxamine. A 24–129% increase in iron excretion using the combination was found, compared to desferrioxamine alone (Grady et al., 1998a). Administration of the 2 drugs simultaneously resulted in an even greater increment in iron excretion (Grady et al., 1998a). It is important to exploit all conventional agents (Table 2.2), alone and in combination, using innovative dosing, since few novel chelating drugs will be available for clinical use in the near future.

Although many hundreds of compounds have been tested, only rare drugs show potential for use as chelators, and even fewer are effective and nontoxic when given orally. One of the newer drugs is HBED, a polyanionic amine. This drug was initially reported as effective in oral form, though later reports were less encouraging. Recently, a report has appeared suggesting that the drug has therapeutic potential (Bergeron, 1998). Oral HBED has been used as an adjunct to either parenteral desferrioxamine or to oral L1 therapy (Grady et al., 1998a; Grady et al., 1998b). In addition, a recent report demonstrated that HBED, when administered subcutaneously to animals, was a more effective chelator than desferrioxamine, with no apparent toxicity. It is therefore possible that HBED alone could be administered subcutaneously, similarly to the method of administering

desferrioxamine, but on a reduced schedule (Bergeron et al., 1999). This could prove valuable for patients who develop allergic reactions to injection of desferrioxamine, or for those who are unwilling to administer a daily dose of a parenteral chelator.

Table 2.2. Iron Chelators.

Iron Chelators				
Name	**Formula**	**MW**	**Dent**	**Route**
DFO	4-[3,5-bis-(hydroxyphenyl)-1,2,4-triazol-1-4-]-benzoic acid	560	6	parenteral
HBED	N,N'-bis(o-hydoxybenzyl) ethylene daimine-N,N'-diacedic acid	388	6	oral/ parenteral
PIH	Pyridoxal is a nicotinoyl hydrazone	262	3	oral
DFT	4'hydoxy-(S)desazadeamethyl-desfemithiocin;(S)-4,5-dihydro-2-[2,4-dihydroxyphenyl]-4-thiazolecarboxylic acid	238	3	oral
DFP(L1)	1,2'-dimethyl-3-hydroxypyridin-4-one	139	2	oral
S-DFO	hydroxyethely-starch-bound(40SD02)	250.000	6	i.v.
ICL-670	4-[3,5-bis-(hydroxyphenyl)-1,2,4- triazol-1-4-]-benzoic acid	373	3	oral
GT 56-252	4,5-dihydro-2-[2,4-dihydroxyphenyl]-4-methylthiazole-4(S)-carboxylic acid	252	3	oral

3. EXPERIMENTAL

3.1. MATERIALS

N-isopropylacrylamide (NIPA), the crosslinker *N,N*-methylenebis(acrylamide) (MBAAm), the initiator ammonium persulfate (APS), the accelerator *N,N,N',N'*-tetramethylenediamine (TEMED) were obtained from Aldrich Chem. Co. (USA). NIPA monomer was purified by crystallization from toluene/n-hexane mixture before polymerization. Methacryloylchloride and L-cysteine were obtained from Fluka (Germay). All other chemicals were of reagent grade and were purchased from Merck AG (Darmstadt, Germany). All water used in the adsorption experiments was purified using a Barnstead (Dubuque, IA) ROpure LP® reverse osmosis unit with a high flow cellulose acetate membrane (Barnstead D2731) followed by a Barnstead D3804 NANOpure® organic/colloid removal and ion exchange packed-bed system. Resulting purified water (deionized water) has a specific conductivity of 18.2 µS.

3.2. PREPARATION OF POLYMERIC GELS

3.2.1. Synthesis of N-methacryloyl-L-cysteine

The following experimental procedure was applied for the synthesis of N-methacryloyl-L-cysteine (MAC) monomer: 5.0 g of cysteine and 0.2 g of $NaNO_2$ were dissolved in 30 mL of K_2CO_3 aqueous solution (5%, v/v). This solution was cooled to $0^°C$. 4.0 mL of methacryloyl chloride was poured slowly into this solution under nitrogen atmosphere and then this solution was stirred magnetically at room temperature for 2 h. At the end of this period, the pH of this solution was adjusted to 7.0 and then was extracted with ethylacetate. The aqueous phase was evaporated in a rotary evaporator. The residue (i.e., MAC) was crystallized in ethanol and ethylacetate.

3.2.2. Preparation of MAC-Fe^{3+} Complex

In order to prepare, MAC-Fe^{3+} complex, 0.404 g iron nitrate (Fe(NO$_3$)$_3$.9H$_2$O) (1.0 mmol) was dissolved in 15 ml H$_2$O. 0.38 g N-methacryloyl-L-cysteine (MAC) (2.0 mmol) was added slowly to this solution with continuous stirring at room

temperature. The solution was allowed to be stirred for 3 h. MAC-Fe^{+3} complex solution was used directly in the polymerization procedure.

3.2.3. Preparation of Fe^{3+}-imprinted poly(NIPA-MAC) Gel

The Fe^{3+} imprinted poly(NIPA-MAC) was prepared by free radical polymerization. *N*-isopropylacrylamide (NIPA) monomer was purified by crystallization from toluene/n-hexane mixture. *N,N*-methylenebis(acrylamide) (MBAAm) was used as a cross-linker agent. *N,N,N',N'*-tetramethylenediamine (TEMED) and ammonium persulfate (APS) were used as the accelerator and initiator, respectively. The polymerization was performed in H$_2$O at room temperature for 24 hours in poly(vinylchloride) plastic tubes. The preparation conditions are summarized in Table 3.1. The formed gel was washed extensively with deionized water and dried in lyophilizator.

Table 3.1. Preparation conditions of Fe^{3+} impinted poly(NIPA-MAC) gels.

Monomer:	NIPA	0.150 g
Chelating Monomer:	MAC-Fe^{3+} complex	1 mL
Cross-linker:	MBAAm	0.02 g
Accelerator:	TEMED	100 µL
Initiator:	APS	0.01 g

poly(NIPA) gels were prepared without chelating monomer and non-imprinted poly(NIPA-MAC) gels were synthesized using only MAC monomer.

3.2.4. Removal of the Template (Fe^{3+} ions)

In order to remove the template (Fe^{3+} ions), from lyophilized poly(NIPA-MAC) Fe^{3+} complex, the polymeric gel was ground to make particles. The particles of poly(NIPA-MAC)Fe^{3+} complex, were added into the 0.1 M HNO$_3$ acidic solution for 12 h at room temperature. The template free polymers were centrifuged and dried in lyophilizator.

3.3.   CHARACTERIZATION of Poly(NIPA-MAC) GELS

3.3.1. Determination of Swelling Ratio

The swelling kinetic of the poly(NIPA-MAC) gels was measured gravimetrically. The dried samples were placed in distilled water at 22°C and removed from water at regular time intervals. After the water on the surfaces of the gels was wiped off with moistened filter paper, the weights of the gels were recorded. The swelling ratio was defined as follows:

$$ SR = \frac{m_t - m_d}{m_d} \qquad (3.1) $$

where, m_d is the mass of dry gel, m_t is the mass of the swollen gels at time t.

3.3.2. Determination of Equilibrium Swelling Ratio

For the temperature-response studies, the poly(NIPA-MAC) gels were equilibrated in distilled water at temperatures ranging from 5 to 60°C. The poly(NIPA-MAC) gels were allowed to swell in distilled water for at least 24 h at each predetermined temperature, controlled up to ±0.1°C in a constant-temperature water bath (Julabo, F34, Germany). The gravimetric method was employed to study the poly(NIPA-MAC) gel swelling ratio for finding Low Critical Solubility Temperature (LCST). After immersion in distilled water at a predetermined temperature, the gels were removed from the water and blotted with wet filter paper for the removal of excess water on the gel surface; they were then weighed. After this weight measurement, the gels were re-equilibrated in distilled water at another predetermined temperature, and their swollen weight was determined. The average values of three measurements were taken for each gel, and the equilibrium swelling ratio was calculated as follows:

$$ ESR = \frac{m_s - m_d}{m_d} \qquad (3.2) $$

where *md* is the mass of dry gel, m_s is the mass of the swollen gel.

3.3.3. Elemental Analysis

To evaluate the degree of MAC incorporation the poly(NIPA-MAC) and the Fe^{3+}-imprinted poly(NIPA-MAC) gels were subjected to elemental analysis using a Leco Elemental Analyzer (Model CHNS-932).

3.3.4. FTIR Studies

FTIR spectra of MAC and poly(NIPA), and the Fe^{3+}-imprinted and template removed poly(NIPA-MAC) gels were obtained by using a FTIR spectrophotometer (FTIR 8000 Series, Shimadzu, Japan). The dry gels (about 0.1 g) was thoroughly mixed with KBr (0.1 g, IR Grade, Merck, Germany), and pressed into a pellet and the FTIR spectrum was then recorded.

3.3.5. Raman studies

Raman spectra of samples were recorded using Labram HR Raman spectrometer (Jobin Yvon, France) with a He-Ne Laser source emitting at 633 nm, 600-1200 grooves/mm holographic grating and a charge coupled device (CCD) detector. Raman spectra were obtained in 250 s integrations with an average of three scans. Spectra were recorded with reproducibility within 1 cm^{-1}, hole 400 μm, slit 150 μm and resolution 0.1 μm.

3.3.6. NMR Studies

The proton NMR spectrum of MAC monomer was taken in $CDCl_3$ on a JEOL GX-400-300 MHz instrument. The residual non-deuterated solvent (TMS) served as an internal reference. Chemical shifts were reported in ppm (δ) downfield relative to TMS.

3.4. BLOOD COMPATIBILITY STUDIES

3.4.1. Coagulation Time (CT)

Poly(NIPA) and Fe^{3+}-imprinted poly(NIPA-MAC) particles were incubated in 0.1 M phosphate buffer solution (pH: 7.4) for 24 h at room temperature and washed on a glass filter with 0.5 M NaCl solution and distilled water. Fresh frozen pooled human plasma (0.1 mL) was preheated to $37^{\circ}C$ for 2 min and then 10 mg of non-imprinted and imprinted poly(NIPA-MAC) particles were added into this medium and mixed immediately. The clotting time was measured by using fibrometer method (Doumas et al., 1971).

3.4.2. Activated Partial Thromboplastin Time (APTT)

Poly(NIPA) and Fe^{3+}-imprinted poly(NIPA-MAC) particles were incubated in 0.1 M phosphate buffer solution (pH: 7.4) for 24 h at room temperature and washed on a glass filter with 0.5 M NaCl solution and distilled water. Fresh frozen pooled human plasma (0.1 mL) was preheated to $37^{\circ}C$ for 2 min. The partial thromboplastin (0.3 mL, bioMerieux, Marcy-l'Etoile, France) was also preheated to $37^{\circ}C$ for 2 min and was added to preheated human plasma. Then, 10 mg of non-imprinted and imprinted poly(NIPA-MAC) particles were added into this medium. Thirty seconds later, $CaCl_2$ (0.1 mL, 0.025 M) was added, then, the active partial thromboplastin time (APTT) was determined by using the fibrometer method (Lagergren and Olsson, 1974).

3.4.3. Prothrombin Time (PT)

In order to determine prothrombin time (PT), one-stage prothrombin method was used (Brash, 1991). The non-imprinted and the Fe^{3+}-imprinted poly(NIPA-MAC) particles were incubated in 0.1 M phosphate buffer solution (pH: 7.4) for 24 h at room temperature. Fresh frozen pooled human plasma (0.1 M) was preheated to $37^{\circ}C$ for 2 min. The thromboplastin (0.2 mL, bioMerieux, Marcy-l'Etoile, France) was also preheated to $37^{\circ}C$ for 2 min and was added to preheated human plasma.

Then, 10 mg of non-imprinted and imprinted poly(NIPA-MAC) particles were added into this medium. Thirty seconds later, $CaCl_2$ (0.1 mL, 0.025 M) was transferred into the medium. After these operations, the prothrombin time was measured by using fibrometer method (Doumas and Biggs, 1971).

3.4.4. Cell Adhesion Studies

Human blood (heparinized, 500 IU/kg) was contacted with the non-imprinted and the Fe^{3+}-imprinted poly(NIPA-MAC) particles at in-vitro system. It should be noted that prior to the blood contact, polymeric particles were washed with 0.1 M KCl in buffer until no further impurities (monitored by the absorbance at 280 nm) was detected in the washing solution. Polymeric gels were incubated with blood for 1 h. Blood samples were withdrawn at the beginning and at the end of the procedure, and the platelet and leukocyte count of samples were determined by microscopy.

3.5. ADSORPTION-DESORPTION STUDIES

3.5.1. Adsorption of Fe^{3+} from Aqueous Solution

Adsorption of Fe^{3+} ions both on the poly(NIPA-MAC) and Fe^{3+}-imprinted poly(NIPA-MAC) particles were studied from aqueous solutions in batch-wise. Nitrate salt was used as the source of Fe^{3+} ions. The effects of the initial Fe^{3+} concentration and pH of the medium on the adsorption rate and adsorption capacity were studied. By this purpose, 10 mL of aqueous solutions containing different amounts of Fe^{3+} ions (in the range of 5-300 ppm) were treated with 100 mg of the poly(NIPA-MAC) and Fe^{3+}-imprinted poly(NIPA-MAC) particles at room temperature and magnetically stirred at a speed of 400 rpm. Different pH ranges (2.0-6.0) were adjusted with 1 M HNO_3 and 1 M NaOH. After the desired treatment periods, the concentration of the Fe^{3+} ions in the aqueous phase was measured by using a Perkin-Elmer AAnalyst 800 atomic absorption spectrometer with deuterium background correction equipped with Perkin-Elmer hollow cathode iron lamp. The working current/wavelength was 30 mA per 248.3 nm with spectral bandwidth of 0.5 nm. The instruments response was periodically checked with known Fe^{3+} solution standards.

Experimental

The amount of Fe^{3+} adsorption per unit mass of the particles was evaluated by using the following expression:

$$Q = [(C_O-C) . V] / m \qquad (3.3)$$

Here, Q is the amount Fe^{3+} ions adsorbed onto unit mass of the particles (mg/g); C_O and C are the concentrations of the Fe^{3+} ions in the initial solution and in the aqueous phase after treatment for certain period of time, respectively (mg/L); V is the volume of the solution (L); and m is the mass of the particles used (g).

3.5.2. Adsorption of Fe^{3+}Ions From Human Plasma

Adsorption of Fe^{3+} ions from thalassemia patient's plasma on the Fe^{3+}-imprinted poly(NIPA-MAC) particles were studied in batch-wise. Fresh human plasma was used in all experiments and obtained from a thalassemic donor. HIV and Hepatitis tests were performed to donor blood samples. Blood samples were centrifuged at 500 g for 30 min at room temperature. Then, thalassemia patient's plasma was incubated with a 100 mg of the Fe^{3+}-imprinted poly(NIPA-MAC) particles at $20^{\circ}C$ for 3 h. The concentration of the Fe^{3+} ions in plasma, after the desired treatment periods was measured by using a atomic absorption spectrophotometer (Analyst 800/Perkin Elmer, USA). Deuterium background correction was used and the spectral slit width was 0.5 nm. A hollow cathode Fe^{3+} lamp was used. The instrument response was periodically checked with known Fe^{3+} solution standards. The experiments were performed in replicates of three and the samples were analyzed in replicates of three as well. For each set of data present, standard statistical methods were used to determine the mean values and standard deviations. Confidence intervals of 95% were calculated for each set of samples in order to determine the margin of error.

3.5.3. Selectivity Experiments

In order to show Fe^{3+} (Iron; ionic radius: 64 pm) specificity of the Fe^{3+}-imprinted poly(NIPA-MAC) particles, competitive adsorptions (i.e., Nickel Ni^{2+}; ionic radius: 69 pm and Cadmium, Cd^{2+}; ionic radius: 97 pm) were also studied. 100 mg/L iron, copper and nickel ions used in aqueous solutions. The Fe^{3+}-imprinted poly(NIPA-

MAC) particles were treated with this competitive ions. After adsorption equilibrium, the concentration of Ni^{2+} and Cd^{2+} ions in the remaining solution was measured by AAS.

Distribution and selectivity coefficients of Ni^{2+} and Cd^{2+} with respect to Fe^{3+} were calculated as explained by the following Equation (3.4)

$$K_d = [(C_i - C_f)/C_f] \times V/m \tag{3.4}$$

Here, K_d represents the distribution coefficient; C_i and C_f are initial and final concentrations of metal ions, respectively. V is the volume of the solution (mL) and m is the mass of beads used (g).

The selectivity coefficient for the binding of a metal ion in the presence of competitor species (Eq. 3.5) can be obtained from equilibrium binding data according to (Eq. 3.6).

$$M_1(\text{solution}) + M_2(\text{sorbent}) <=> M_2(\text{solution}) + M_1(\text{sorbent}) \tag{3.5}$$
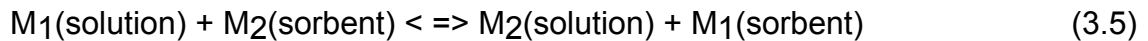
$$K = ([M_2]\text{solution} [M_2]\text{sorbent}) / ([M_1]\text{solution} [M_2]\text{sorbent}) \tag{3.6}$$

$$= K_d (Cd^{2+}) / (K_d(X^{2+}))$$

where k is the selectivity coefficient and X^{2+} represents Ni^{2+} and Cd^{2+} ions. A comparison of the k values of the imprinted beads with those metal ions allows an estimation of the effect of imprinting on selectivity.

A relative selectivity coefficient k' (eq. 3.7) can be defined as

$$K' = k_{\text{imprinted}}/k_{\text{control}} \tag{3.7}$$

3.6. DESORPTION AND REPEATED USE

Desorption of Fe^{3+} ions were studied 0,1 M nitric acid (HNO_3) solution. The Fe^{3+}-imprinted poly(NIPA-MAC) particles were placed in this desorption medium and stirred continuously (at a stirring rate of 400 rpm) for 1 h at room temperature. The

final Fe^{3+} ions concentration in the desorption medium was measured by atomic adsorption spectrometer. The desorption ratio was calculated from the amount of Fe^{3+} ions adsorbed on the gels and the final Fe^{3+} ions concentration in the desorption medium by the following equation (3.8)

$$\text{Desorption Ratio} = \frac{\text{amount of } Fe^{3+} \text{ ions desorbed to the elution medium}}{\text{amount of } Fe^{3+} \text{ ions adsorbed on the gels}} \times 100 \qquad (3.8)$$

In order to test the reusability of the non imprinted and the Fe^{3+} imprinted poly(NIPA-MAC) particles, Fe^{3+} ions adsorption-desorption procedure was repeated five times by using the same polymeric sorbent. In order to regenerate and sterilize, after desorption; the gels were washed with 50 Mm NaOH solution.

4. RESULTS AND DISCUSSIONS

4.1. CHARACTERIZATION of Poly(NIPA-MAC) GELS

4.1.1. Determination of Swelling Ratio

The swelling kinetic curves of the poly(NIPA), non-imprinted poly(NIPA-MAC) and template removed Fe^{3+}-imprinted poly(NIPA-MAC) particles are shown in Figure 4.1. The data show that the swelling rate decreased with introducing MAC monomer into the poly(NIPA) structure. The poly(NIPA-MAC) has about 11.81 swelling ratio within 240 min, whereas the poly(NIPA) has about 12.56 within the same time frames. This can be concluded as; increase of intramolecular interactions (hydrogen bonds) between MAC and NIPA groups would lead to a reduction in the rate of water absorption. Template removed Fe^{3+}-imprinted poly(NIPA-MAC) has about 10.87 swelling ratio within 240 min, whereas non-imprinted poly(NIPA-MAC) has about 11.81 within the same time frames. The reduction of water adsorption in Fe^{3+}-imprinted poly(NIPA-MAC) gels can be concluded as; some Fe^{3+} ions remained in the complex form with the MAC residue of polymeric gels after using 0.1 M HNO_3, resulted blockage of MAC groups which were interacting with water molecules during swelling.
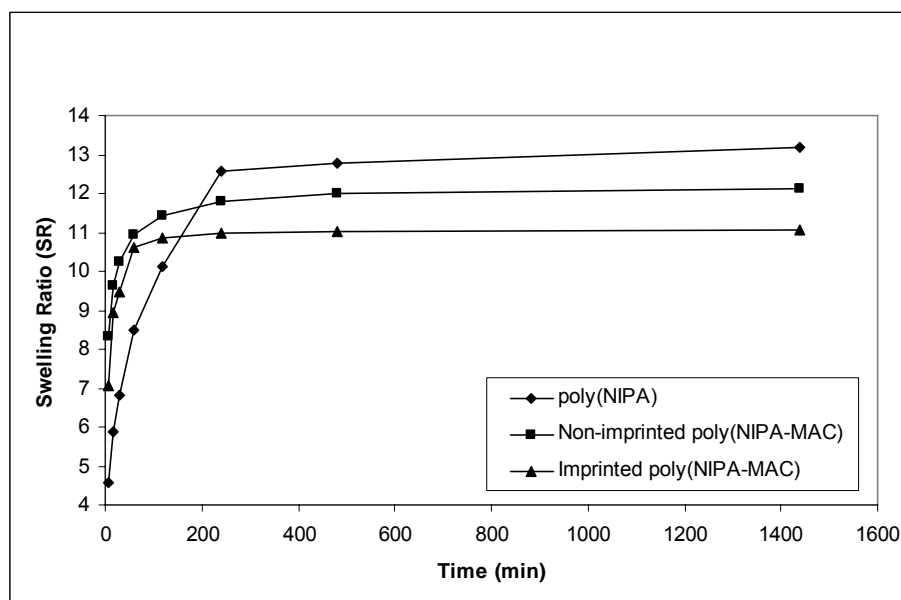
Figure 4.1. Swelling kinetics of poly(NIPA), non-imprinted and Fe^{3+} imprinted poly(NIPA-MAC) particles, T: 22°C, pH: 7.0.

4.1.2. Determination of Equilibrium Swelling Ratio

Figure 4.2 shows the temperature dependence of the equilibrium swelling ratio and LCST of the poly(NIPA), non-imprinted poly(NIPA-MAC) and template removed Fe^{3+}-imprinted poly(NIPA-MAC) particles when the temperature increased from 5 to 60°C. Usually, the volume phase transition temperature or LCST of these hydrogel is defined as the temperature at which the swelling ratio has decreased to a half of its value at the initial temperature or room temperature (Wu et al.1992). The hydrogel`s LCST is also regarded as the temperature at which phase-separation degree (changes of the swelling ratio vs. temperature changes around the transition temperature, $\Delta SR/\Delta T$) is greatest or the temperature at which the swelling ratio of hydrogel decreased most dramatically (Zhang et al., 1999; Zhang et al., 2000). The data show that all the poly(NIPA) particles showed a LCST temperature about 32°C which was matching with the literature (Schild, 1992). Introducing MAC residue into the polymer structure, the LCST temperature increased from 32°C to 34°C and 36°C, at non-imprinted poly(NIPA-MAC) and template removed Fe^{3+}-imprinted poly(NIPA-MAC) particles, respectively. As shown in Figure 4.1 increase of intramolecular interactions (hydrogen bonds) between MAC and NIPA groups lead to a reduction in the rate of water absorption and these strong interactions of two constituent monomers may shift the LCST temperatures to higher values than plain poly(NIPA) particles by inhibiting the shrinking of the particles. The highest LCST temperature (36°C) was observed at template removed Fe^{3+}-imprinted poly(NIPA-MAC) gels, which may be concluded as effect of remaining Fe^{3+} ions after removal of template on the inhibition of shrinking of the gels is higher than the non-imprinted particles by interaction of the Fe^{3+} ions with water molecules. Poly(NIPA), non-imprinted poly(NIPA-MAC) and template removed Fe^{3+}-imprinted poly(NIPA-MAC) particles exhibit a negative temperature sensitive, which is swelling at lower temperature and shrinking at higher temperature. Under equilibrium swelling conditions, all gels showed increasing swelling at lower temperatures, but they deswelled at high temperatures because of the aggregation of the network chains. When the external temperature was increased from 5 to 60°C, the volume or water content inside

gels decreased slowly during the shrinkage, and the water release rate is controlled mainly by collective diffusion of the hydrogel (Zhang et al., 2003).

In addition, as can be shown in Figure 4.2., there was no obvious effect of the MAC content on the equilibrium swelling ratio of the gels at temperatures above the LCST. This suggests that regardless of the amount of cross-linker, all the poly(NIPA) particles may collapse into similar collapsed structure at above LCST.
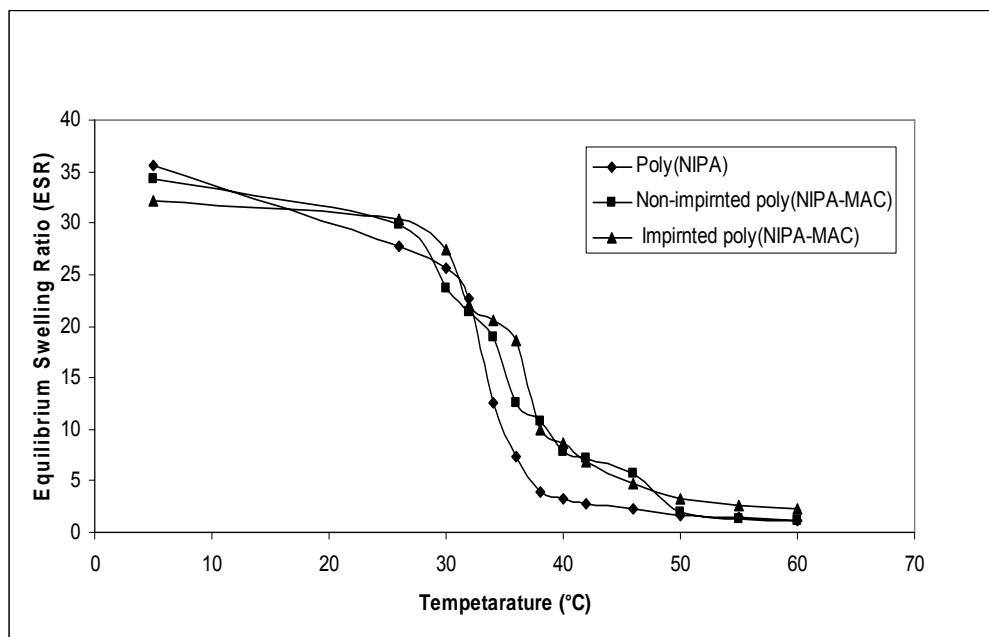
Figure 4.2.   Equilibrium swelling ratios of the poly(NIPA), non-imprinted poly(NIPA-MAC) and Fe^{3+} imprinted poly(NIPA-MAC) particles in water as a function of temperature.

Digital photograph of the template removed poly(NIPA-MAC) gel below (22°C) and above (38°C) its LCST temperature was shown in Figure 4.3. Template removed poly(NIPA-MAC) gels showed a quick response to temperature and shrinkage was very rapid in around 30 seconds.

4.1.3. Elemental Analysis

The incorporation of the MAC was found to be 814.70 µmol/g and 276.45 µmol/g polymer in non-imprinted and Fe^{3+}-imprinted poly(NIPA-MAC) particles by using sulfur stoichiometry. Note that NIPA and other polymerization ingredients do not contain sulfur. This sulfur amount determined by elemental

analysis comes from only incorporated MAC groups into the polymeric structure.

Figure 4.3.   Digital photograph of the template removed poly(NIPA-MAC) gels below (22°C) and above (38°C) at LCST temperature.

4.1.4. FTIR Studies

The molecular formula of synthesized MAC co-monomer and MAC-Fe^{3+} complex is shown in Figure 4.4. In order to confirm complex formation between Fe^{3+} and MAC monomer, FTIR spectroscopy was performed. FTIR spectrum of MAC has the characteristic stretching vibration carboxyl–carbonyl, amide I and amide II absorption bands at 1607 cm^{-1}, 1533 cm^{-1} and 1453 cm^{-1}, respectively (Figure 4.5). The S–H bending peak appears at 2625 cm^{-1} of MAC. For the characteristic determination of complex, due to linear coordinate covalent complex formation, the S-H bending peak at 2625 cm^{-1} slips to the down field at 2514 cm^{-1}, as a result of decreasing the electron density of sulfhydryl of MAC monomer.
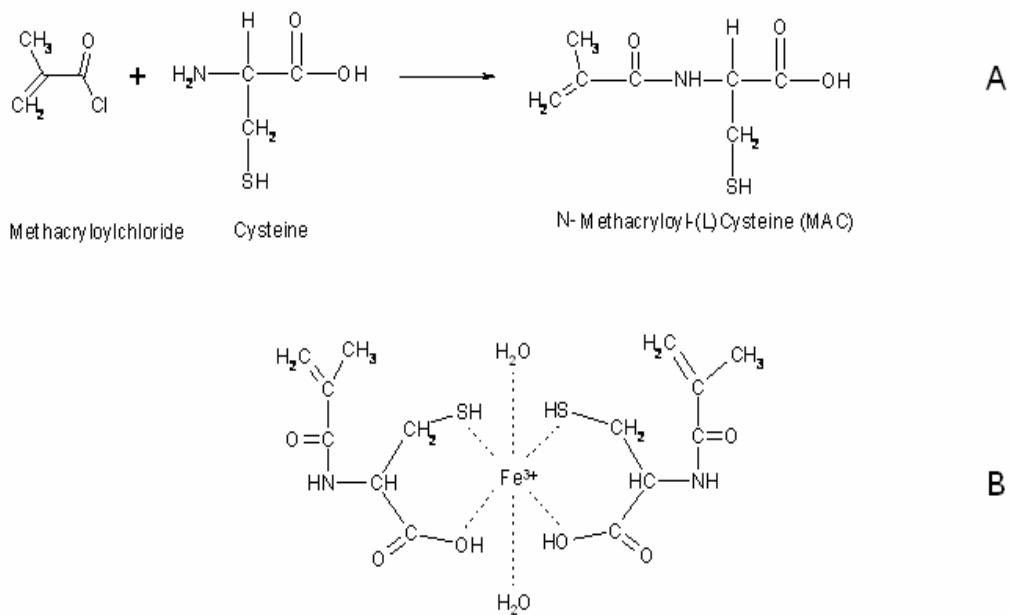
Figure 4.4.   The molecular formula of (A) MAC monomer; (B) MAC
Fe^{3+}complex.

Then, MAC–Fe^{3+} complex were polymerized with NIPA monomer by free radical polymerization (Figure 4.6). The FTIR spectrum of non-imprinted poly(NIPA-MAC) (Figure 4.7) and Fe^{3+}-imprinted poly(NIPA-MAC) (Figure 4.7)   particles showed a broad band in the range of 3600–3200 cm^{-1}, which belongs to N–H stretching vibration of the poly(NIPA). The typical amide I band (1648 cm^{-1}), consisting of C=O stretch of poly(NIPA) and amide II band (1541 cm^{-1}), including N–H vibration were evident in both spectrum.
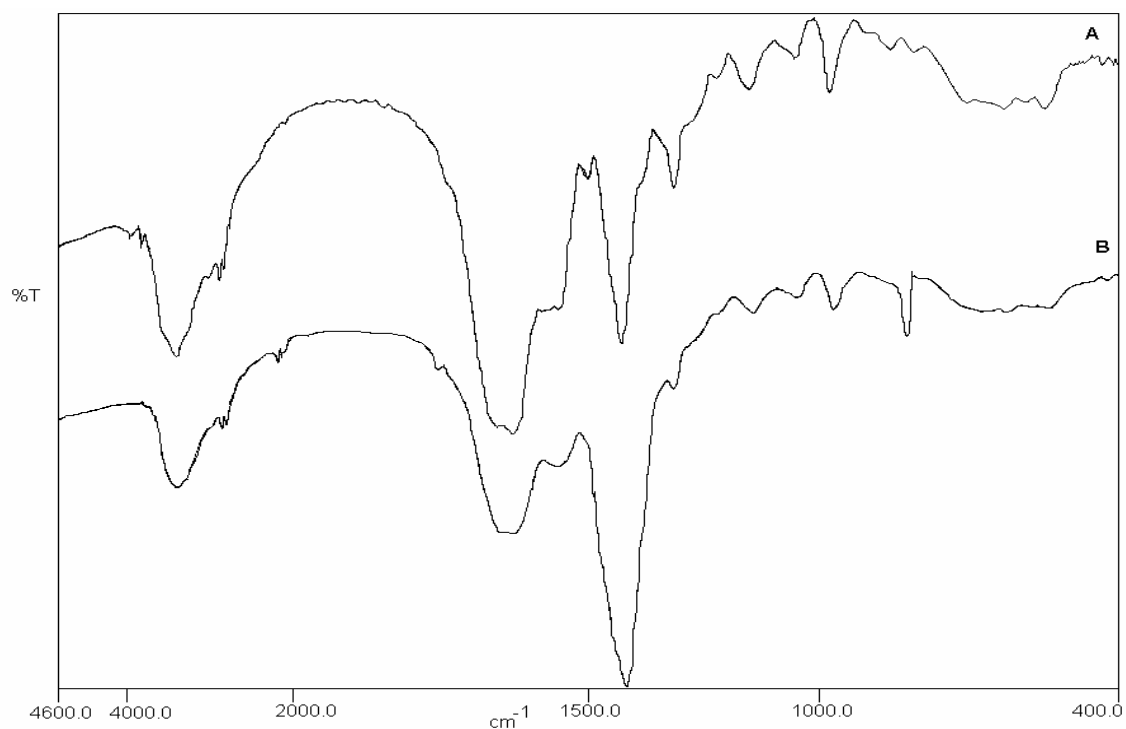
Figure 4.5.   FTIR spectra of MAC monomer and MAC- Fe^{3+} complex.
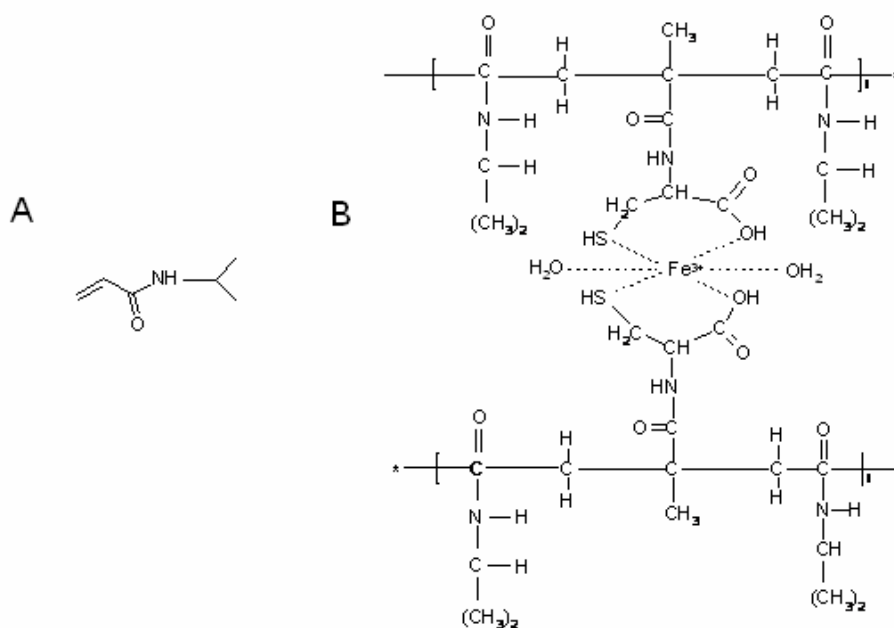
Figure 4.6.   Molecular formula of (A) NIPA monomer; (B) poly(NIPA-MAC)- Fe^{3+} complex.
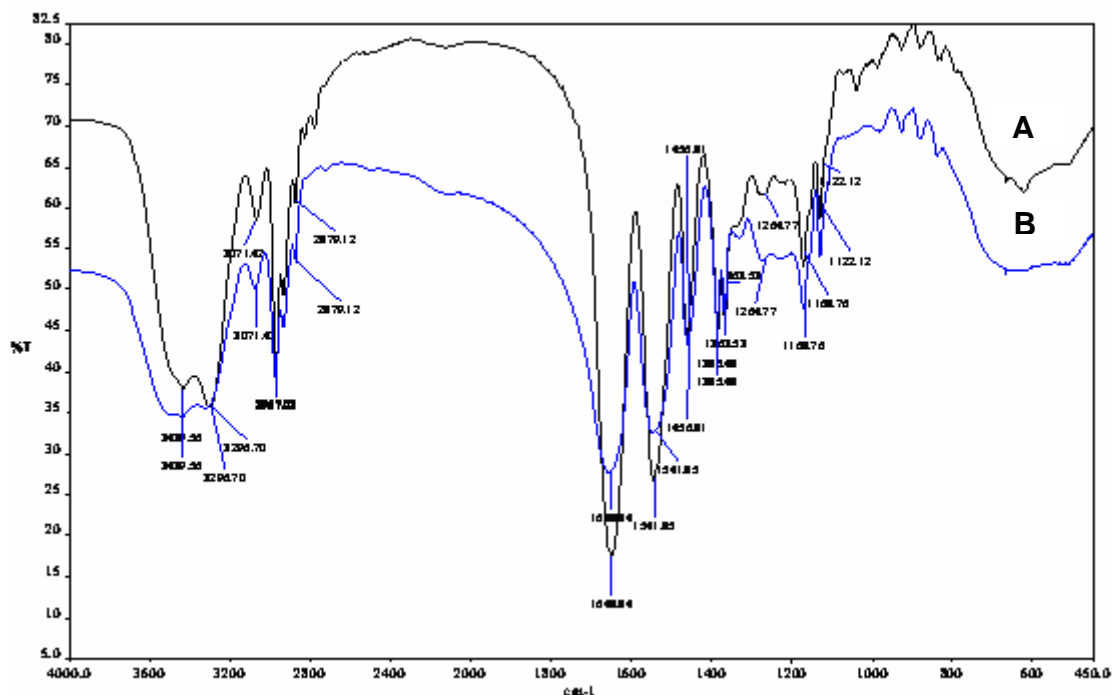
Figure 7.7.   FTIR spectra of (A) non-imprinted poly(NIPA-MAC)   and (B) poly(NIPA-MAC)-Fe^{3+} complex.

The C-S peak of MAC monomer in the structure of poly(NIPA-MAC) around 620 cm^{-1} was disappeared in the case where NIPA monomer was polymerized with MAC-Fe^{3+} complex because of decreasing the electron density in C-S interaction (Lezzi, et.al,1994).

4.1.5. Raman studies

Raman spectra in the range of 50-1000 cm^{-1} were performed to confirm the formation of the complex (Figure 4.8). The band observed at 692 cm^{-1} can be assigned to the n (C-S) stretching vibration (shifts to 670.2 cm^{-1} in complex monomer). The band at 513.4 cm^{-1} is from the bending mode of d (C-C-C) (shifts to 512.8 cm^{-1} in complex monomer). The formation of bands at 190.6 cm^{-1}, 541.2 cm^{-1}, 824.4 cm^{-1} are assigned to the complex formation with MAC-Fe^{3+}. The appearance of the n (C-S) stretching vibration bands at 630-750 cm^{-1} confirms the formation of MAC- Fe^{3+}complex (Yakhandra et.al, 1983).
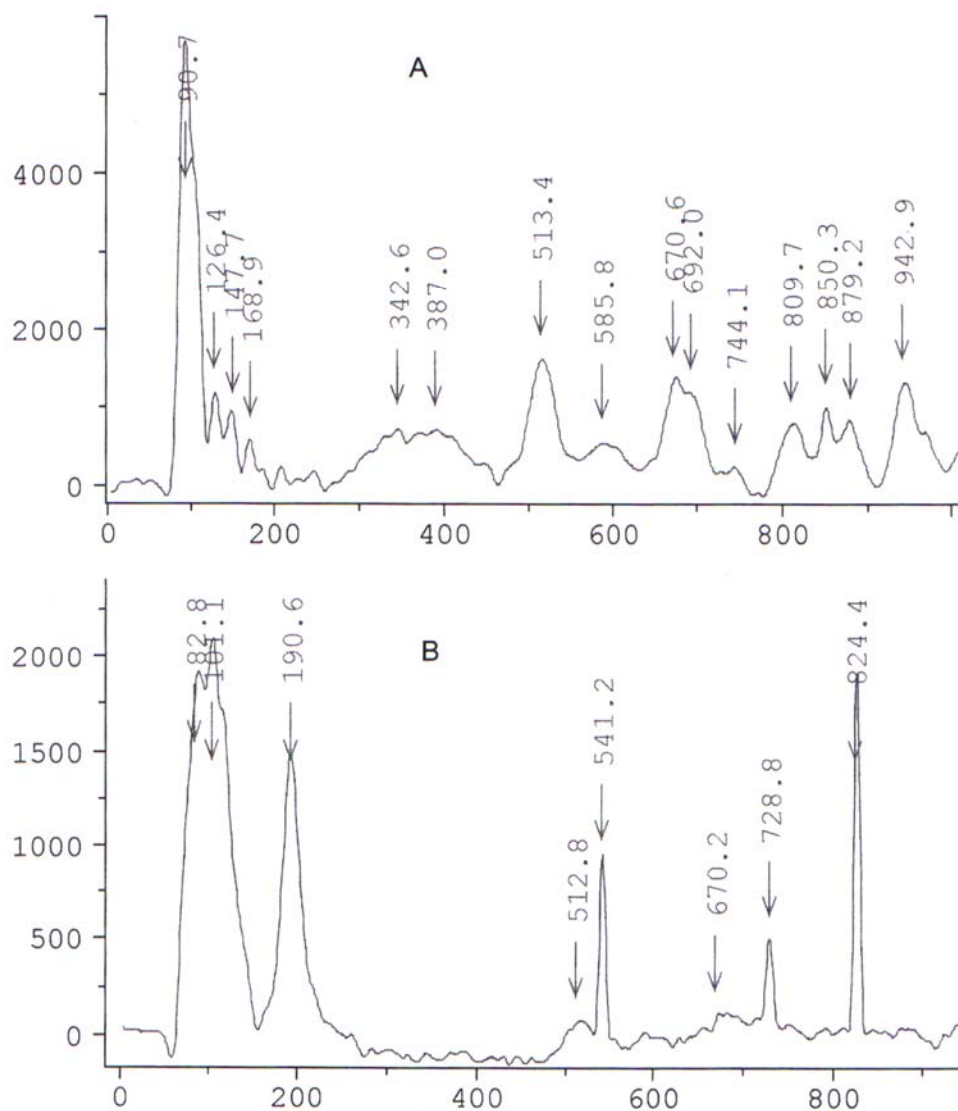
Figure. 4.8.   Raman spectra of MAC monomer and MAC-Fe^{3+} monomer complex.

4.1.6. NMR Studies

^{1}H-NMR was used to determine the synthesis of MAC structure. Figure 4.9 shows the ^{1}H-NMR spectrum of MAC monomer. ^{1}H-NMR spectrum is shown to indicate the characteristic peaks from the groups in MAC monomer. These characteristic peaks are as follows: ^{1}H-NMR (DMSO): 7.67-7.36 ppm belongs to SH and –NH protons. They could not be observed in H_2O because of being mobile protons. Peaks at 5.67 and 5.31 ppm indicate ethylene, 4.16 ppm –CH and 1.88 ppm -CH$_3$.
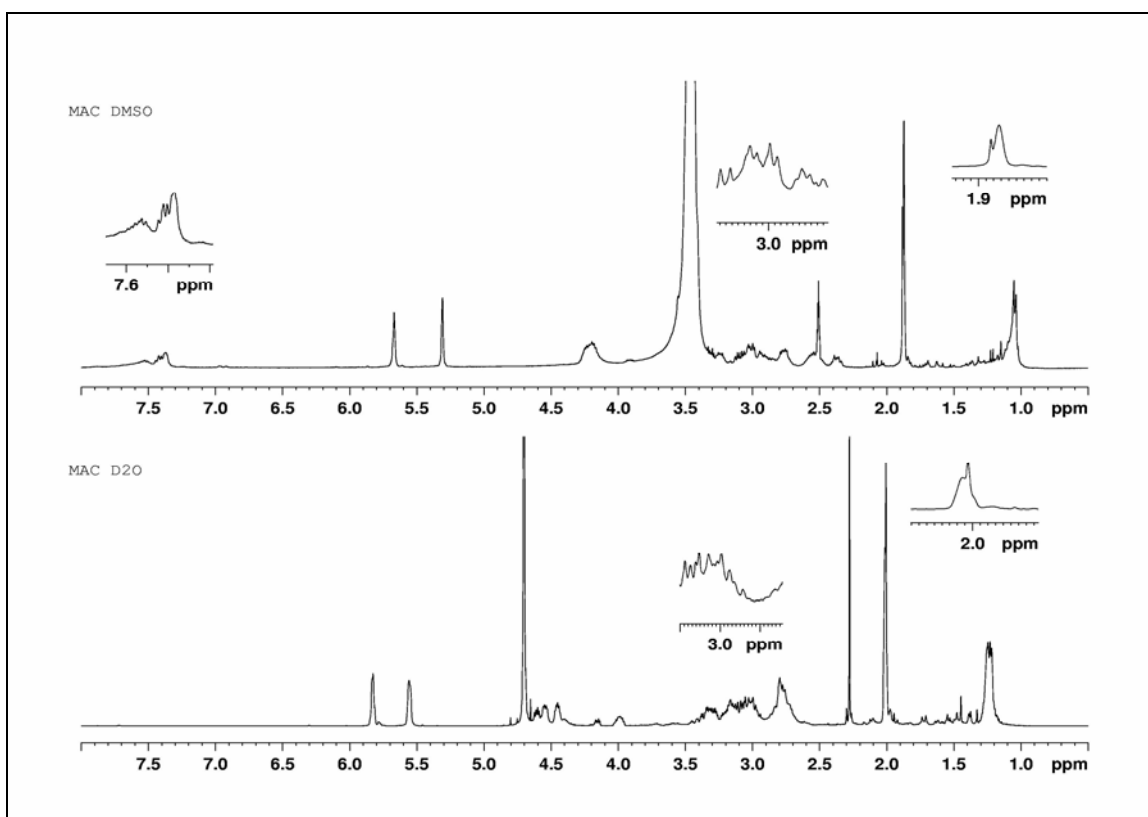
Figure 4.9.   NMR spectra of MAC monomer.

4.2. BLOOD COMPATIBILITY STUDIES

A biomaterial is a substance that is used in medical devices or in prostheses designed for contact with the living body for an intended method of application and for an intended period. Synthetic polymers are the most diverse class of biomaterials. Polymeric biomaterials are widely used in both medical and pharmaceutical applications (Cooper et.al., 1995). These applications include a variety of implants or other supporting materials (e.g. vascular grafts, artificial hearts, intraocular lenses, joints, mammary prostheses and sutures), extracorporeal therapeutic and other supporting devices (e.g. hemodialysis, hemoperfusion, blood oxygenation and bags), controlled release systems and clinical diagnostic assays (mainly as carriers) (Pişkin and Hoffman, 1986). All biomaterials must meet certain criteria and regulatory requirements before they can be qualified for use in medical applications. Depending on the intended end-use, a biomaterial may be subjected to a set of tests, such as blood-

compatibility, tissue-compatibility, carcinogenicity, mutagenicity, biodegradation and mechanical stability (Brash et al., 1991).

When biomaterials in use come into contact with blood, first small molecules (e.g. water and ions) reach to the surface which may or may not be adsorbed. This is followed by plasma protein adsorption. The first protein layer adsorbed on the biomaterial surface determines the subsequent events of the coagulation cascade (via the intrinsic pathway), and the complement activation (via the intrinsic-extrinsic pathways) (Denizli, 1999).

4.2.1. Coagulation Times

In order to estimate the blood-compatibility of the non-imprinted poly(NIPA-MAC) and the Fe^{3+}-imprinted poly(NIPA-MAC) particles, in-vitro coagulation times (CT), activated partial thromboplastin time (APTT) and prothrombin time (PT) tests were carried out. It should be mentioned that APTT tests exhibit the bioactivity of intrinsic blood coagulation factors and PT test relates to extrinsic blood coagulation factors on biomaterial surface. CT test shows in-vitro coagulation time. Table 4.1 summarizes the coagulation data obtained in these tests. As can be seen from Table 4.1, all the clotting times for the non-imprinted poly(NIPA-MAC) and the Fe^{3+}-imprinted poly(NIPA-MAC) particles were lower than control. But these decreases are tolerable by the body. Therefore, we concluded that the blood-compatibility of newly synthesized non-imprinted poly(NIPA-MAC) and Fe^{3+}-imprinted poly(NIPA-MAC) particles were rather good, and all the clotting times were quite reproducible comparing with the values reported in the related literature. Consequently, in this thesis, the incorporation of MAC as a co-monomer may exert beneficial effects in two ways. First, improved blood-compatibility of the particles will reduce adverse body reactions to possible biomedical treatment applications (i.e., extracorporeal therapy), and second, reductions in non-specific adsorption will reduce undesirable losses of beneficial proteins from treated blood (Kim and Jacobs, 1996).

Table 4.1. Coagulation times of human plasma (reported in sec).

Experiments	(APTT)	(PT)	(CT)
Control Plasma	82.4	38.5	289
Non-imprinted poly(NIPA-MAC)	78.9	36.3	276
Imprinted poly(NIPA-MAC)	78.5	36.0	278

4.2.2. Cell Adhesion Studies

Table 4.2, summarizes hematological data obtained from in-vitro blood assay. Loss of platelet with the non-imprinted poly(NIPA-MAC) and the imprinted poly(NIPA-MAC) particles were 1.1% and 1.6%, respectively. Lost of leukocyte with the non-imprinted poly(NIPA-MAC) and the imprinted poly(NIPA-MAC) particles were 3.8% and 5.7%, respectively. As seen here, there is no significant cell adhesion on the particles. These observations showed that surfaces of the particles are resistant to adhesion of platelets and leukocytes. In conclusion, because of the good non-thrombogenic properties, these gels seem to be very promising affinity adsorbents for biomedical applications such as extracorporeal adsorption therapy.

Table 4.2. Platelet and leukocyte adhesion with non-imprinted poly(NIPA-MAC) and the imprinted poly(NIPA-MAC) particles .

Substance	Platelet ($\times 10^{-3}$/mm^3)		Leukocyte ($\times 10^{-3}$/mm^3)	
(%)	Initial/Final	Loss (%)	Initial/Final	Loss
Non-imprinted poly(NIPA-MAC)	430/420	1.1	5.2/5.0	3.8
Imprinted poly(NIPA-MAC)	430/418	1.6	5.2/4.9	5.7

4.3.   ADSORPTION-DESORPTION STUDIES

4.3.1. Effect of Time

Figure 4.10 shows the time dependence of the adsorption values of Fe^{3+} ions on non-imprinted poly (NIPA-MAC) and Fe^{3+} imprinted poly(NIPA-MAC) particles. The adsorption rate to reach saturation was very fast onto the non-imprinted particles compared to the imprinted particles. The equilibrium rates were about 5 min and 60 min for the non-imprinted poly (NIPA-MAC) and the Fe^{3+} imprinted poly(NIPA-MAC) particles, respectively.

Figure 4.10. Time dependent adsorption of Fe^{3+} ions on the non-imprinted and imprinted poly(NIPA-MAC) particles; V: 10 mL; Conc.: 100 mg/L solution, pH: 5.0, 0.01 g polymer and T: 20°C.

The maximum adsorption amounts for Fe^{3+} ions onto the non-imprinted poly (NIPA-MAC) and the Fe^{3+} imprinted poly(NIPA-MAC) particles, were 50.13 mg/g polymer and 13.86 mg/g polymer, respectively. A possible explanation to this phenomenon could be in two ways; (1) According to elemental analysis data, incorporation of MAC into the non-imprinted and the Fe^{3+}-imprinted poly(NIPA-MAC) particles, was found to be 814.70 µmol/g and 276.45 µmol/g polymer, respectively. Higher MAC content in non-imprinted particles resulted

with high adsorption rate and amount when compared to imprinted particles (2) Slow adsorption rate and low adsorption amount of the imprinted particles are considered due to the fact that the shrinkage of the imprinted particles may require long time because of a dense network compared to the non-imprinted particles (Kanazawa et al., 2004).

Several experimental data on the adsorption of various ions by thermosensitive polymers have shown a wide range of adsorption rates. Kanazawa et.al have studied adsorption/desorption properties of heavy metals ions by using poly(*N*-isopropylacrylamide-co-*N*-(4-vinyl)benzyl ethylenediamine) [poly(NIPA-Vb-EDA)] thermosensitive gels and they have found adsorption rate at 100 hours (Kanazawa et al., 2004). Tokuyama et.al, using the same polymer but having different amount of cross-linker, have found the adsorption rate 1100 min. According to these results both the non-imprinted and the imprinted particles have shown fast adsorption rates and amount which are most probably due to high complexation of MAC monomer with Fe^{3+} ions and low diffusion barrier as a result of higher porous polymer network.

4.3.2. Effect of pH

It is well known that metal ion adsorption both nonspecific and spesific sorbents is pH dependent (Kesenci et al., 2002; Denizli et al., 2003; Denizli et al., 1997). In the absence of complexing agents, the hydrolysis and precipitation of the metal ions are affected by the concentration and form of soluble metal species. The effect of pH on the Fe^{3+} adsorption using the non-imprinted and the imprinted thermosensitive particles is given in Figure 4.11. The adsorption amount of Fe^{3+} ions on the non-imprinted poly(NIPA-MAC) and the Fe^{3+} imprinted poly(NIPA-MAC) particles were determined at the pH range between 2.5-6.0 values of buffered solutions. In all of the cases, the adsorption amount increased with increasing pH, reaching a maximum value at around pH 5.0. At low pH values, i.e. pH 2.5, the adsorption amount is lower which can be considered due to fact that in such a low pH, the nitrogen ligands in MAC work as the electron donor. At higher pH values i.e. above the pH 6.25 Fe^{3+} ions precipitate as $Fe(OH)_3$.
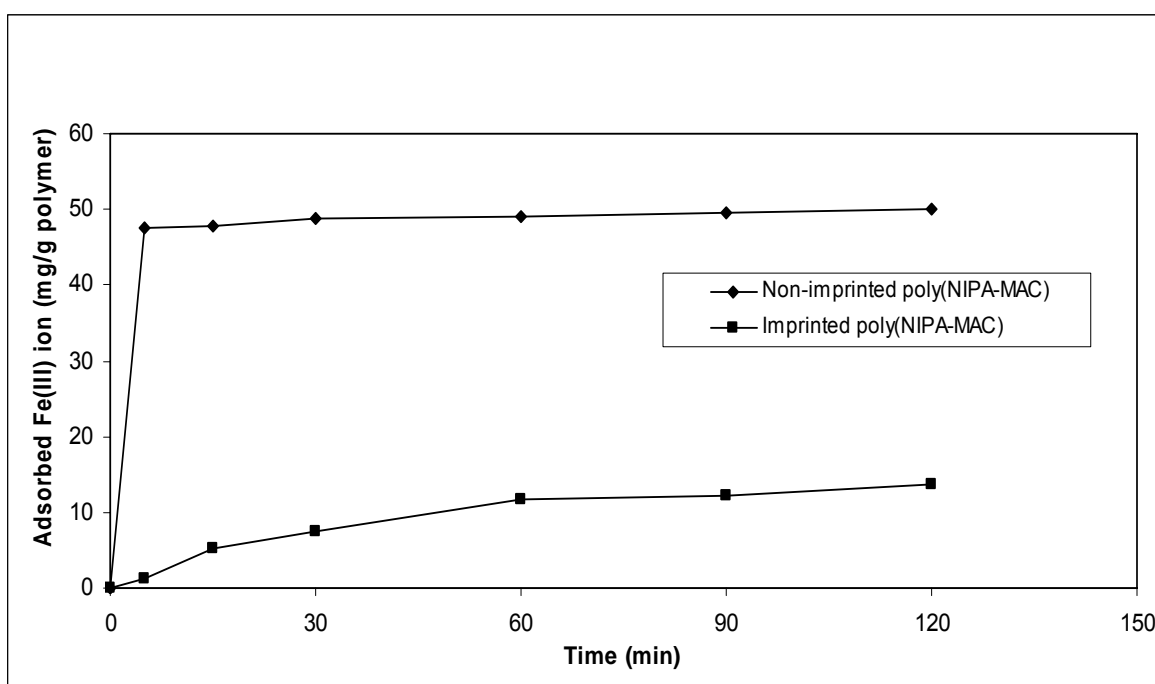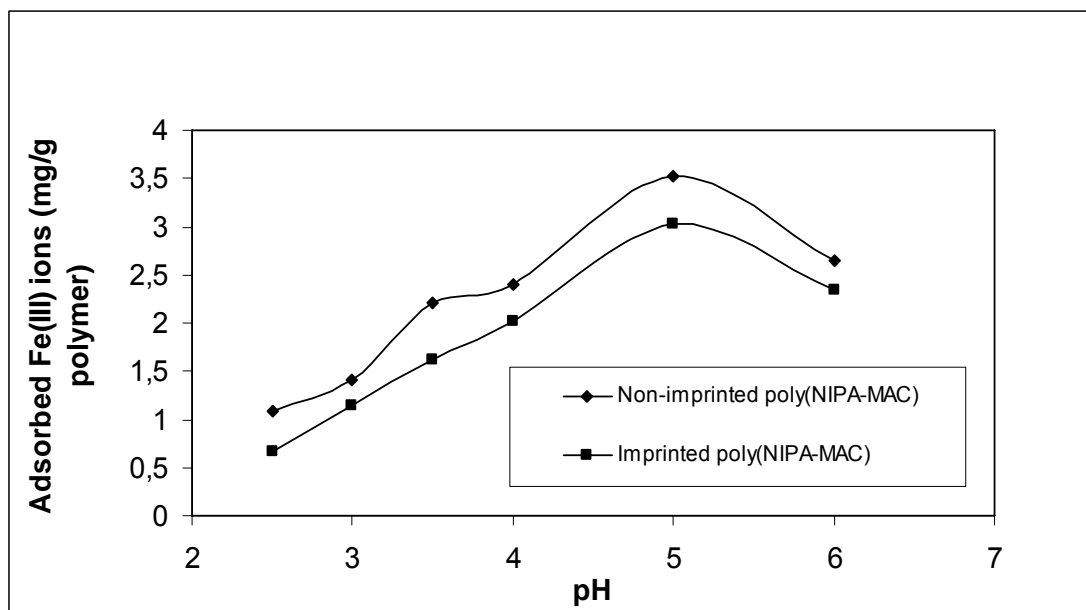
Figure 4.11. Effect of pH on adsorption of Fe^{3+} ions on non-imprinted and imprinted poly(NIPA-MAC) particles; V: 10mL, Conc.: 10 mg/L solutions, 0.01 g polymer, T: 20 °C.

4.3.3. Effect of Initial Concentration of Fe^{3+} ions

Figure 4.12 shows the initial concentration of metal ions dependence of the adsorbed amount of the Fe^{3+} onto the non-imprinted poly(NIPA-MAC) and the Fe^{3+}-imprinted poly(NIPA-MAC) particles. The adsorption amount increased with increasing concentration of Fe^{3+} ions, and a saturation value couldn`t be achieved at ion concentration of 300 mg/L for non-imprinted poly(NIPA-MAC) particles. For the Fe^{3+}-imprinted poly(NIPA-MAC) particles, adsorption amount also increased with increasing concentration of the Fe^{3+} ions, but a saturation value is achieved at ion concentration of 200 mg/L. Maximum adsorption amount of the non-imprinted poly(NIPA-MAC) and the Fe^{3+}-imprinted poly(NIPA-MAC) particles were 128.11 mg/g and 22. 25 mg/g, respectively.

Figure 4.12. Effect of initial Fe^{3+} concentration on the adsorption of Fe^{3+} ions on the non-imprinted and the imprinted poly(NIPA-MAC) particles; pH: 5.0, V: 10 mL, Conc.: 100 mg/L solution, 0.01 polymer, t: 5 min for non-imprinted and 60 min for imprinted gels, T: 20°C.

From the results that we obtained in this study, we resulted that the new polymeric imprinted particles presented in this communication are promising for the adsorption of Fe^{3+} ions from aqueous media.

4.3.4. Effect of Temperature

Figure 4.13 shows the temperature effect to the adsorption capacity on the non-imprinted and the Fe^{3+}-imprinted poly(NIPA-MAC) particles. Adsorption of Fe^{3+} onto the non-imprinted poly(NIPA-MAC) and the Fe^{3+}-imprinted poly(NIPA-MAC) particles were studied from aqueous solutions containing 100 mg/L Fe^{3+} ions in the range of 4-50°C. The amount of adsorbed Fe^{3+} ions increased with increasing temperature and maximum adsorption was observed at 37°C. Maximum adsorption amount was found to be, 55.43 mg/g and 13.98 mg/g for the non-imprinted and the Fe^{3+}-imprinted poly(NIPA-MAC) particles, respectively.
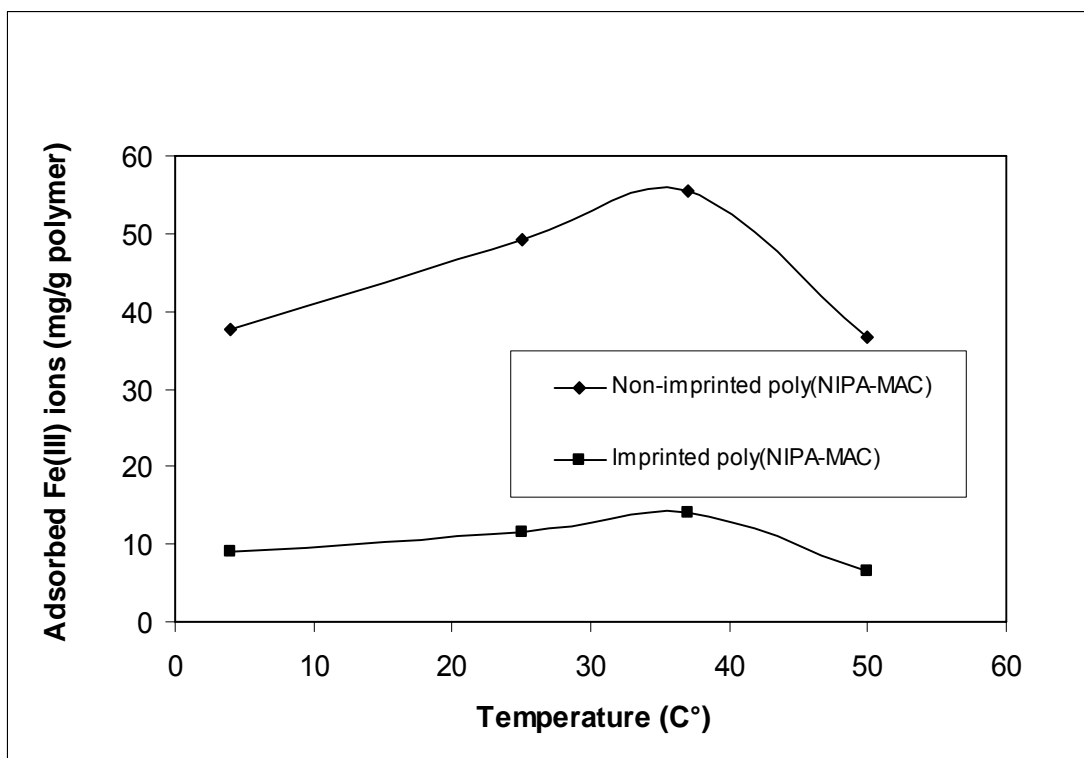
Figure 4.13. Effect of temperature on the adsorption of Fe^{3+} on non-imprinted and the Fe^{3+}-imprinted poly(NIPA-MAC) particles; V:10 mL, Conc.: 100 mg/L solution, pH:5.0, 0.01 g polymer.

4.3.5. Adsorption Isotherms

An adsorption isotherm is used to characterize the interactions of each ion with the adsorbents. This provides a relationship between the concentration of the ions in the solution and the amount of ions adsorbed on the solid phase when the two phases are at equilibrium. The Langmuir adsorption model assumes that the ions are adsorbed at a fixed number of well-defined sites, each of which is capable of holding only one molecule. These sites are also assumed to be energetically equivalent and distant from each other so that there are no interactions between ions adsorbed on adjacent sites.

During the batch experiments, adsorption isotherms were used to evaluate adsorption properties. The Langmuir adsorption isotherm is expressed by Equation 4.1. The corresponding transformations of the equilibrium data for

Results and Discussions

Fe^{3+} ions gave rise to a linear plot, indicating that the Langmuir model could be applied in these systems and described by the equation:

$$Q = Q_{max}. \, b \, . \, C_{eq}/ \, (1+bC_{eq}) \qquad (4.1)$$

where Q is the concentration of bound Fe^{3+} ions in the adsorbent (mg/g), C_{eq} is the equilibrium Fe^{3+} ions concentration in solution (mg/L), b is the Langmuir constant (L/mg) and, Q_{max} is the adsorption capacity (mg/g). This equation can be linearized so that

$$1/Q_{eq} = 1/(Q_{max}. \, b)(1/C_{eq}) + 1/Q_{max} \qquad (4.2)$$

The plot of $1/Q_{eq}$ versus $1/C_{eq}$ was employed to generate the intercept of $1/Q_{max}$ and the slope of $1/Q_{max}.b$ (Figure 4.14).

The maximum adsorption capacity (Q_{max}) data for the adsorption of Fe^{3+} ions was obtained from the experimental data. When the Langmuir adsorption model was applied in the system, the maximum adsorption capacities (Q_{max}) and the Langmuir constants were found to be 27.32 mg/g and 0.0366 g/mg for imprinted and 333.33 mg/g and 0.003 g/mg for non-imprinted particles, respectively.

The maximum adsorption capacity (Q_{max}) data for the adsorption of Fe^{3+} was obtained from the experimental data. The correlation coefficients (R^2) were 0.9972 for imprinted and 0.975 for non-imprinted particles. Due to the results, the Langmuir adsorption model can be applied in this ion imprinted polymers.

The other well-known isotherm, which is frequently used to describe adsorption behavior, is the Freundlich isotherm. This isotherm is another form of the Langmuir approach for adsorption on a heterogeneous surface. The amount of adsorbed molecule is the summation of adsorption on all binding sites. The Freundlich isotherm describes reversible adsorption and is not restricted to the formation of the monolayer. This empirical equation takes the form:

(a)
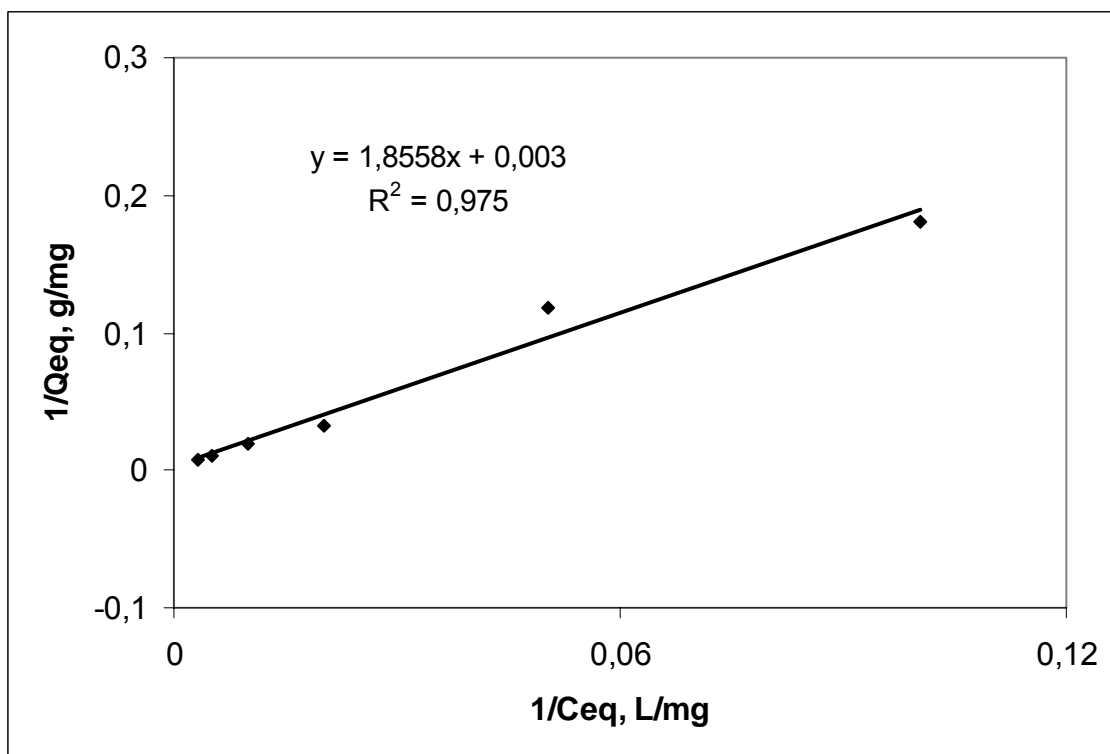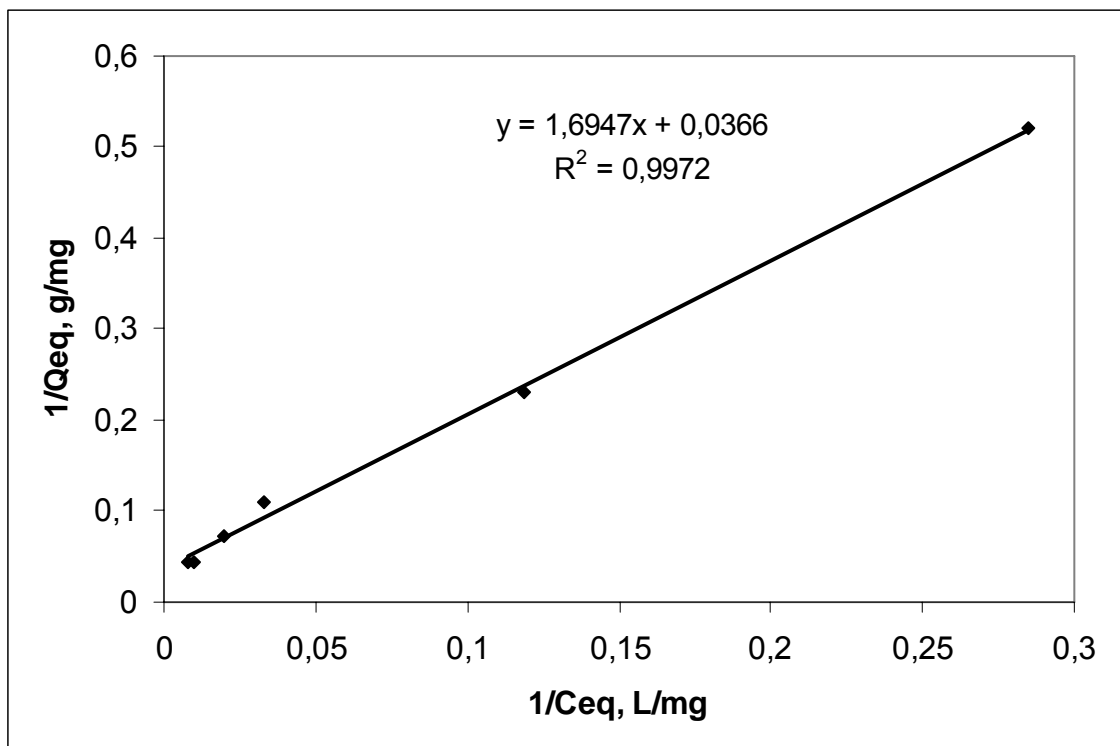
(b)

Figure 4.14. Langmuir adsorption isotherms of the: (a) Imprinted poly(NIPA-MAC); (b) non-imprinted poly(NIPA-MAC).

$$Q_{eq} = K_F (C_{eq})^{1/n} \tag{4.3}$$

where, K_F and n are the Freundlich constants. This equation can be linearized so that

$$\ln Q_{eq} = \ln K_F + (1/n) \times \ln C_{eq} \tag{4.4}$$

The plot of $\ln Q_{eq}$ versus $\ln C_{eq}$ was employed to generate the intercept of $\ln K_F$ and
the slope of '1/n' (Figure 4.15).

The Freundlich isotherm, as mentioned before, shows the surface heterogeneity. It contains two parameters, K_F and 1/n. 1/n, the surface heterogeneity index, is between 0 and 1. If it is closed to 1, the polymer has heterogeneous surface. Then, the 1/n value of MAC is much closed to 1 (0.9923). So, the adsorption process onto the MAC was done via multilayer adsorption.

The adsorption isotherms of imprinted and non-imprinted were found to be linear over the whole concentration range studies and the correlation coefficients were high. According to the correlation coefficients of isotherms, Langmuir adsorption model is favorable for MIP system. In contrast, Freundlich adsorption model is favorable for non-imprinted system. Table 4.3 summarizes the Langmuir and Freundlich adsorption isotherm constants, Kd, n and KF and the correlation coefficients.
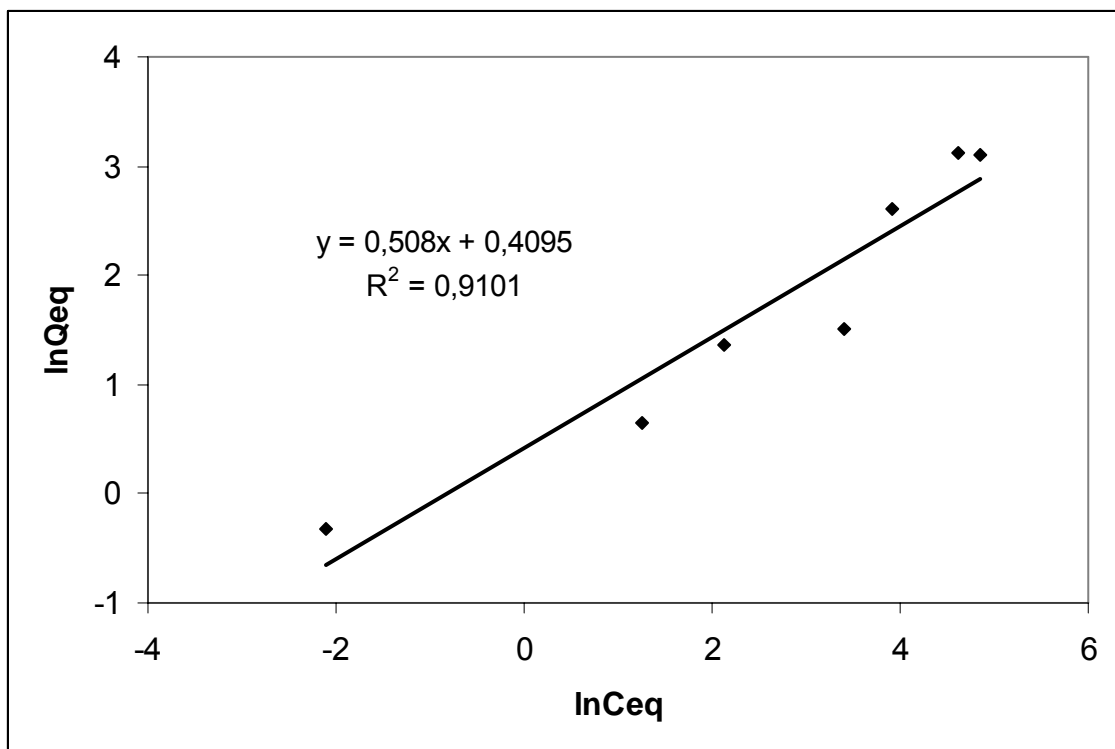
(a)
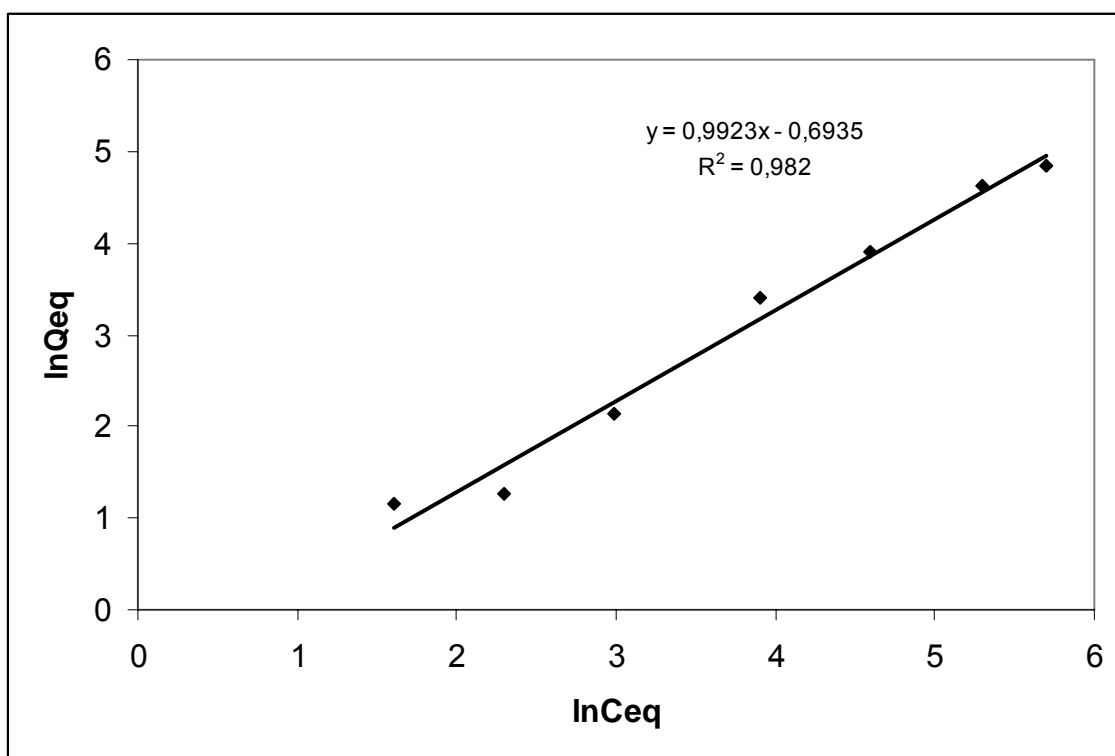
(b)

Figure 4.15.   Freundlich adsorption isotherms of the: (a) Imprinted poly(NIPA-MAC); (b) non-imprinted poly(NIPA-MAC).

Table 4.3.   Langmuir and Freundlich adsorption isotherm constants.

	Experimental	Langmuir Model			Freundlich Model		
	Q_{exp} (mg/g)	Q_{max} (mg/g)	b (L/mg)	R^2	K_F	1/n	R^2
Imprinted	22.25	27.32	0.0366	0.9972	1.506	0.508	0.9101
Non-imprinted	298.72	333.33	0.003	0.972	0.4998	0.9923	0.982

4.3.6. Adsorption Kinetics

In order to examine the controlling mechanism of adsorption process such as mass transfer and chemical reaction, kinetic models were used to test experimental data. The kinetic models (Pseudo-first and second-order equations) can be used in this case assuming that the measured concentrations are equal to adsorbent surface concentrations. The first-order rate equation of Lagergren is one of the most widely used for the adsorption of solute from a liquid solution (Oncel et.al, 2001). It may be represented as follows:

$$\Delta q_t/dt = k_1(q_{eq}-q_t) \tag{4.5}$$

where k_1 is the rate constant of pseudo-first order adsorption (min^{-1}) and q_{eq} and q_t denote the amounts of adsorbed ion at equilibrium and at time t (mg/g), respectively. After integration by applying boundary conditions, q_t=0 at t=0 and q_t=q_t at t=t, gives

$$\log[q_{eq}/(q_{eq}-q_t)] = (k_1 t)/2.303 \tag{4.6}$$

Equation 4.6 can be rearranged to obtain a linear form

$$\log(q_{eq}-q_t) = \log(q_{eq}) - (k_1 t)/2.303 \tag{4.7}$$

a plot of $\log(q_{eq})$ versus t should give a straight line to confirm the applicability of the kinetic model. In a true first-order process $\log(q_{eq})$ should be equal to the interception point of a plot of $\log(q_{eq}-q_t)$ via t.

Results and Discussions

In addition, a pseudo-second order equation based on adsorption equilibrium capacity may be expressed in the form,

$$\Delta q_t/dt = k_2 (q_{eq}-q_t)^2 \qquad (4.8)$$

Where k_2 (g mg^{-1} min^{-1}) is the rate constant of pseudo-second order adsorption process. Integrating Equation 4.8, q and applying the boundary conditions, $q_t=0$ at t=0 and $q_t=q_t$ at t=t, leads to

$$1/(q_{eq}-q_t)] = (1/q_{eq}) + k_2t \qquad (4.9)$$

or equivalently for linear form

$$(t/q_t)= (1/k_2q_{eq}^2) + (1/q_{eq})\, t \qquad (4.10)$$

a plot of t/qt versus t should give a linear relationship for the applicability of the second-order kinetics. The rate constant (k_2) and adsorption at equilibrium (q_{eq}) can be obtained from the intercept and slope, respectively (Figure 4.16 and 4.17).

Table 4.4.   The first and second order kinetic constants for the thermosensitive polymers. (Initial concentration Fe^{3+}: 100 ppm).

Polymer	Experimental	First-order kinetic			Second-order kinetic		
		slope	*intercept*		*intercept*	*slope*	
	Q_{eq} (mg/g)	$k_1 x10^{-2}$ (1/min)	q_{eq} (mg/g)	R^2	k_2 (g/mg.min)	q_{eq} (mg/g)	R^2
Non-imprinted	50.13	3.38	7.45	0.5564	2.71 x10^{-2}	50.25	0.9999
Imprinted	13.60	2.65	13.15	0.97	7.46 x10^{-4}	21.32	0.9014
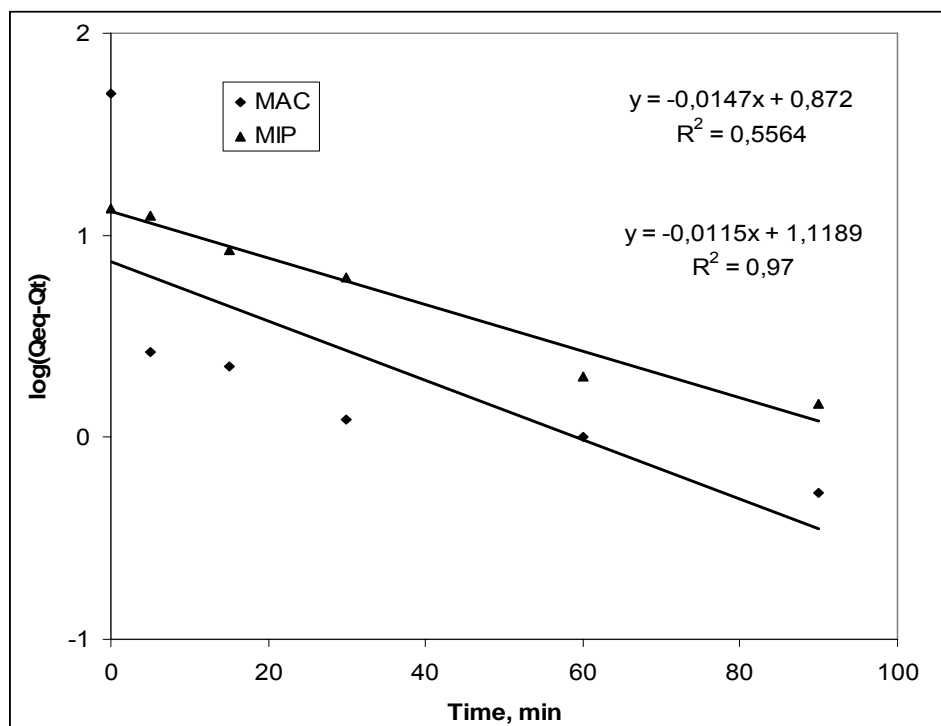
Figure 4.16. Pseudo-first-order kinetic of the experimental data.
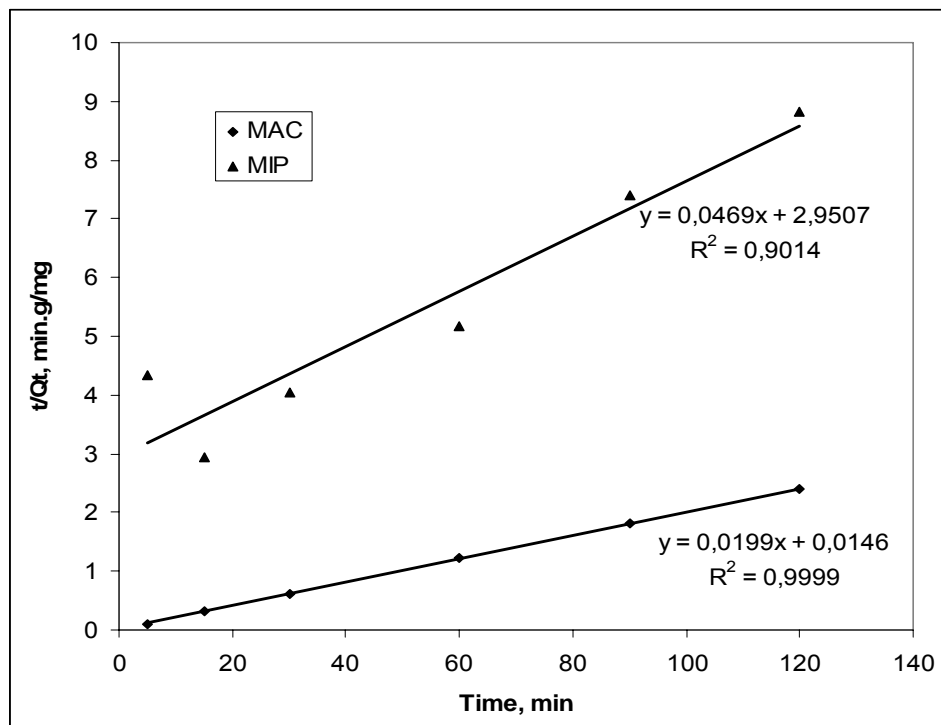
Figure 4.17. Pseudo-second-order kinetic of the experimental data.

Table 4.4 shows the results which are for both first order and the second order kinetic models. The results show that the first order mechanism is applicable for imprinted but the second order mechanism is applicable for non-imprinted (R^2 values are the highest). The rate-limiting step is diffusion in pseudo-first order mechanism. In contrast, chemisorption is the rate-limiting step in pseudo-second order process. So, these results suggest that diffusion is rate-limiting step for imprinted particles, chemisorption for non-imprinted particles. The rate-controlling mechanism may vary during the course of the adsorption process three possible mechanisms may be occurring (Oncel et.al, 2001). There is an external surface mass transfer or film diffusion process that controls the early stages of the adsorption process. This may be followed by a reaction or constant rate stage and finally by a diffusion stage where the adsorption process slows down considerably (Allen et.al, 2005).

4.3.7. Selectivity Experiments

Competitive and selectivity adsorption studies performed in two ways. First, adsorption studies were done by using 100mg/L of Fe^{3+}, Ni^{2+} and Cd^{2+} solutions separately. Second, adsorption studies were done in the mixture of these metals at 100 mg/L. Cd^{2+} and Ni^{2+} were chosen as competitive metal ions because of their similar ionic radius. Figure 4.18 and Figure 4.19 show adsorbed template and Cd^{2+} and Ni^{2+} ions both in imprinted and non-imprinted particles in separate solutions and mixture, respectively.

The Fe^{3+} adsorption capacity of the non-imprinted and the imprinted poly(NIPA-MAC) particles was much more higher than Ni^{2+} and Cd^{2+} ions when adsorption studies were performed in each ion solution. This can be concluded that, of non-imprinted and imprinted poly(NIPA-MAC) particles show the following metal ion affinity in the order of Fe^{3+} > Ni^{2+} > Cd^{2+}. In order to show the competitive adsorption, a mixture of Fe^{3+}, Ni^{2+} , Cd^{2+} ions at 100 mg/L concentration was used. Under competitive conditions, less amount of Fe^{3+}, Ni^{2+}, Cd^{2+} ions adsorbed to the non-imprinted and the imprinted poly(NIPA-MAC) particles because of competitions of these ions. However, less amount of Ni^{2+} and Cd^{2+} ions adsorbed to the particles and selectivity increases.
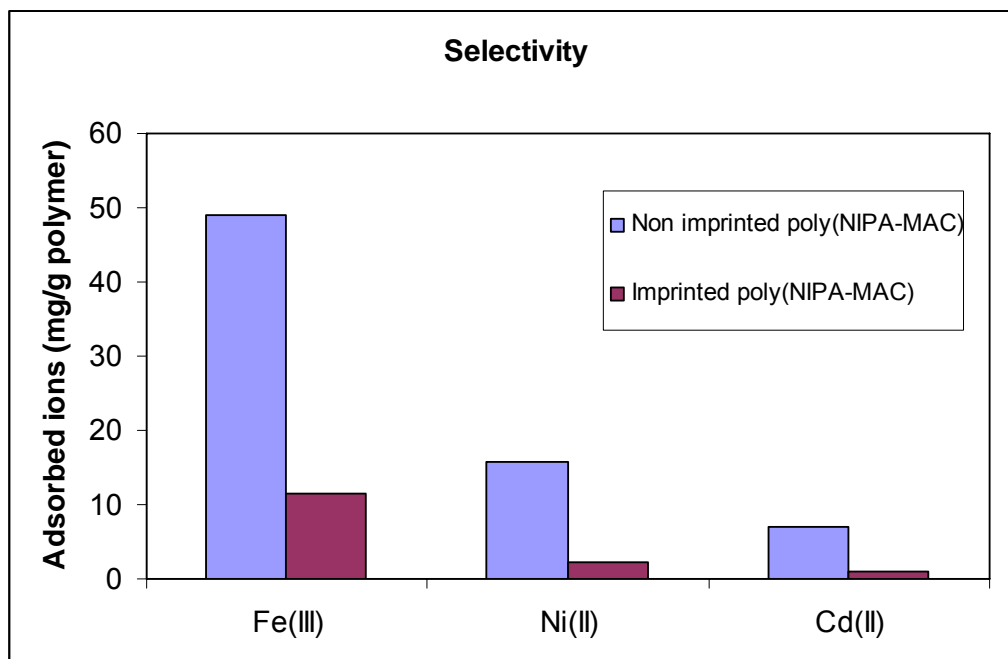
Figure 4.18. Adsorbed Fe^{3+}, Cd^{2+} and Ni^{2+}, ions both in and non and Fe^{3+}-imprinted poly(NIPA-MAC) particles in separate solutions. 10 mL 100 mg/L solution, pH:5.0, 0.01 g polymer, T:20 $^{\circ}$C.
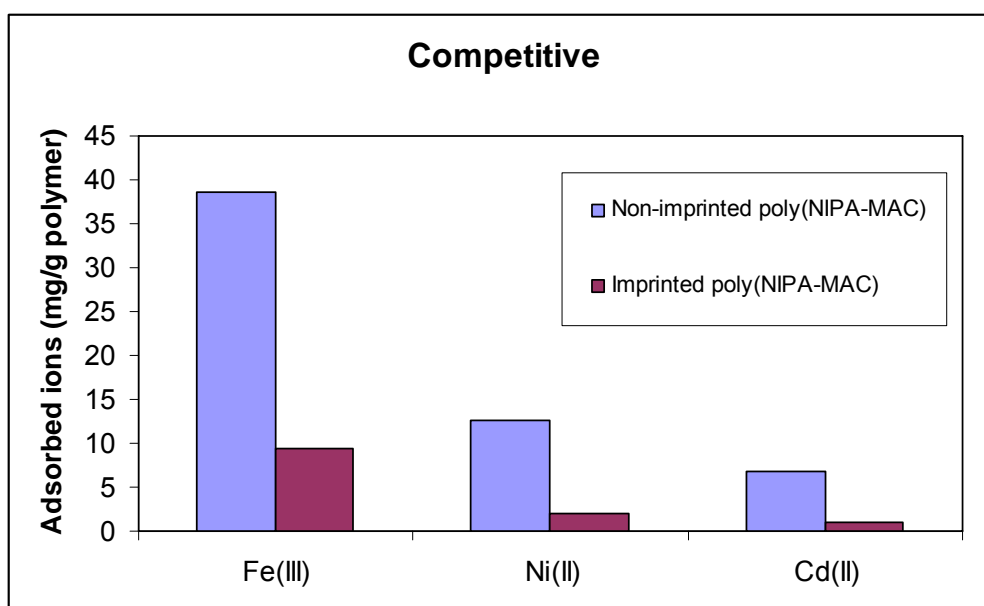
Figure 4.19. Adsorbed Fe^{3+}, Cd^{2+} and Ni^{2+}, ions both in and non and Fe^{3+}-imprinted poly(NIPA-MAC) particles in competitive solutions. 10 mL 100 mg/L solution, pH:5.0, 0.01 g polymer, T:20 $^{\circ}$C.

Results and Discussions

Figure 4.19. shows adsorbed template and Cd^{2+} and Ni^{2+} ions both in imprinted and non-imprinted particles in mixture.

Table 4.5 summarizes K_d, and k, values of Cd^{2+} and Ni^{2+} with respect to Fe^{3+}.

Table 4.5. K_d, k, and *k'* values of the non-imprinted and imprinted particles.

Metal ion	Non-imprinted particles		Imprinted particles		
	Kd	k	Kd	k	k'
Fe^{3+}	0.100		0.180	-	-
Ni^2	0.02	1.05	0.138	4.75	4.52
Cd^{2+}	0.01	1.96	0.071	9.43	4.81

A comparison of the K_d values for the Fe^{3+} the imprinted poly(NIPA-MAC) samples with the control samples show an increase K_d for Fe^{3+} while K_d decrease for Ni^{2+} and Cd^{2+}. The relative selectivity coefficient is an indicator to express metal adsorption affinity of recognition sites to the imprinted Fe^{3+} ions. These results show that relative selectivity coefficients of imprinted beads for $Fe^{3+}/Ni^{2+}/Cd^{2+}$ 4,52 and 4.81 times greater than non-imprinted particles, respectively (Table 4.5).

From these results, it can be said that the particles imprinted with Fe^{3+} ions indicates the selectivity for the Fe^{3+} ion as expected.

4.4. DESORPTION AND REPEATED USE

The regeneration of the adsorbent is likely to be a key factor in improving process economics. Desorption of the Fe^{3+} ions from the non-imprinted and Fe^{3+}-imprinted poly(NIPA-MAC) particles was performed in a batch experimental set-up. Various factors are probably involved in determining rates of Fe^{3+} desorption, such as the extent of hydration of the metal ions and polymer microstructure. However, an important factor appears to be binding strength. In this study, the desorption time was found to be 60 min. Desorption ratios are high (up to 73% and 69% for the non-imprinted and the Fe^{3+}-

imprinted poly(NIPA-MAC) particles respectively). In order to obtain the reusability of the non-imprinted and the Fe^{3+}-imprinted poly(NIPA-MAC) particles, adsorption-desorption cycles were repeated 5 times by using the same imprinted beads. The adsorption capacity of the recycled non-imprinted and Fe^{3+}-imprinted poly(NIPA-MAC) particles can still be maintained at level 73% and 69% at the 5th cycle (Figure 4.20). It can be seen concluded that the non-imprinted and Fe^{3+}-imprinted poly(NIPA-MAC) particles can be used many times without decreasing their adsorption capacities significantly.
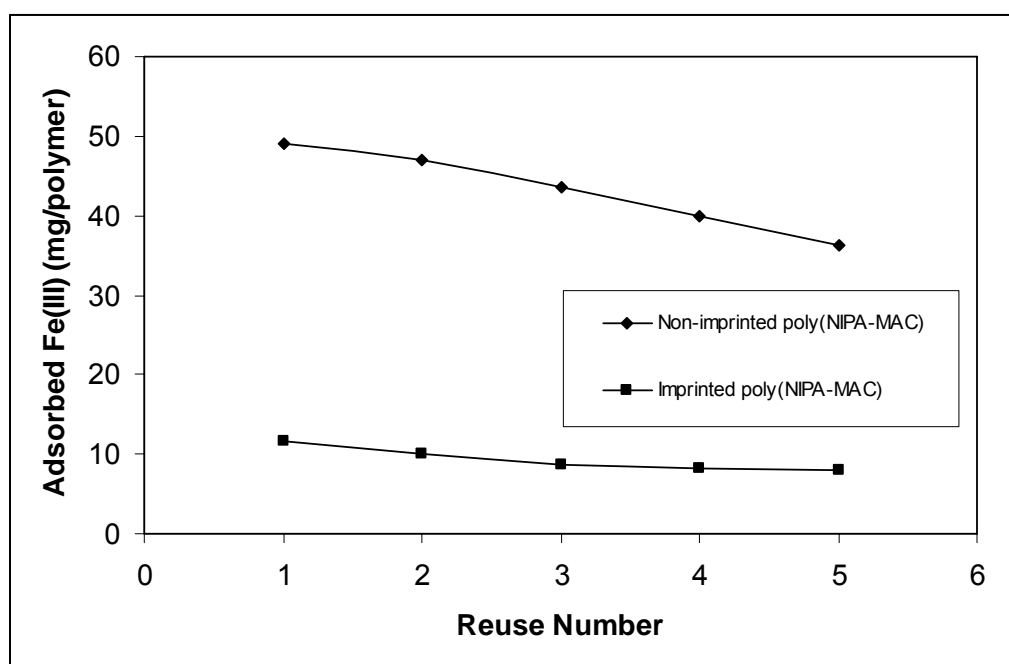
Figure 4.20.   Adsorption-desorption cycle of non-imprinted and Fe^{3+}-imprinted poly(NIPA-MAC) particles.

4.5.   Adsorption of Fe^{3+} ions from thalassemia patient plasma

4.5.5. Effect of Fe^{3+} ions concentration

The results obtained from the adsorption experiments of Fe^{3+} ions at different equilibrium concentrations are summarized in Figure 4.21. The adsorption values increased with increasing Fe^{3+} ions, and a saturation value is achieved at Fe^{3+} ion concentration of 1000 µg/Dl, which represents saturation of active binding cavities on the Fe^{3+}-imprinted poly(NIPA-MAC) particles. As postulated in previous works, the increase in the adsorption amount of Fe^{3+}-imprinted

poly(NIPA-MAC) particles may be indicative of the formation of new binging sites that are not present in the poly(NIPA-MAC) particles. The maximum adsorbed amount of Fe^{3+} ions on the Fe^{3+}-imprinted poly(NIPA-MAC) particles was found to be 2.2. mg/g.

Figure 4.21. Adsorption isotherm of Fe^{3+}-imprinted poly(NIPA-MAC) particles.

5. CONCLUSION

The poly(NIPA-MAC) has about 11.81 swelling ratio within 240 min, whereas the poly(NIPA) has about 12.56 within the same time frames. Template removed Fe^{3+}-imprinted poly(NIPA-MAC) has about 10.87 swelling ratio within 240 min, whereas non-imprinted poly(NIPA-MAC) has about 11.81 within the same time frames.

Poly(NIPA) particles showed a LCST temperature about 32°C. Introducing MAC residue into the polymer structure, the LCST temperature increased from 32°C to 34°C and 36°C, at non-imprinted poly(NIPA-MAC) and template removed Fe^{3+}-imprinted poly(NIPA-MAC) particles, respectively.

The incorporation of the MAC was found to be 814.70 μmol/g and 276.45 μmol/g polymer in non-imprinted and Fe^{3+}-imprinted poly(NIPA-MAC) particles by using sulfur stoichiometry.

FTIR spectrum of MAC has the characteristic stretching vibration carboxyl–carbonyl, amide I and amide II absorption bands at 1607 cm^{-1}, 1533 cm^{-1} and 1453 cm^{-1}, respectively The S–H bending peak appears at 2625 cm^{-1} of MAC. For the characteristic determination of complex, due to linear coordinate covalent complex formation, the S-H bending peak at 2625 cm^{-1} slips to the down field at 2514 cm^{-1}, as a result of decreasing the electron density of sulfhydryl of MAC monomer.

The FTIR spectrum of non-imprinted poly(NIPA-MAC) and Fe^{3+}-imprinted poly(NIPA-MAC) particles showed a broad band in the range of 3600–3200 cm^{-1}, which belongs to N–H stretching vibration of the poly(NIPA). The typical amide I band (1648 cm^{-1}), consisting of C=O stretch of poly(NIPA) and

amide II band (1541 cm^{-1}), including N–H vibration were evident in both spectrum.

The C-S peak of MAC monomer in the structure of poly(NIPA-MAC) around 620 cm^{-1} was disappeared in the case where NIPA monomer was polymerized with MAC-Fe^{3+} complex because of decreasing the electron density in C-S interaction.

Raman spectra in the range of 50-1000 cm^{-1} were performed to confirm the formation of the complex. The band observed at 692 cm^{-1} can be assigned to the n (C-S) stretching vibration (shifts to 670.2 cm^{-1} in complex monomer). The band at 513.4 cm^{-1} is from the bending mode of d (C-C-C) (shifts to 512.8 cm^{-1} in complex monomer). The formation of bands at 190.6 cm^{-1}, 541.2 cm^{-1}, 824.4 cm^{-1} are assigned to the complex formation with MAC-Fe^{3+}. The appearance of the n (C-S) stretching vibration bands at 630-750 cm^{-1} confirms the formation of MAC- Fe^{3+}complex.

MAC monomer`s characteristic peaks are as follows: ^{1}H-NMR (DMSO): 7.67-7.36 ppm belongs to SH and –NH protons. They could not be observed in H$_2$0 because of being mobile protons. Peaks at 5.67 and 5.31 ppm indicate ethylene, 4.16 ppm –CH and 1.88 ppm -CH$_3$.

In order to estimate the blood-compatibility of non-imprinted poly(NIPA-MAC) and Fe^{3+}-imprinted poly(NIPA-MAC) particles, in-vitro coagulation times (CT), activated partial thromboplastin time (APTT) and prothrombin time (PT) tests were carried out.

All the clotting times for non-imprinted poly(NIPA-MAC) and Fe^{3+}-imprinted poly(NIPA-MAC) particles were lower than control. But these decreases are tolerable by the body.

Conclusion

Loss of platelet with the non-imprinted poly(NIPA-MAC) and the imprinted poly(NIPA-MAC) particles were 1.1% and 1.6%, respectively. Lost of leukocyte with the non-imprinted poly(NIPA-MAC) and the imprinted poly(NIPA-MAC) particles were 3.8% and 5.7%, respectively.

The adsorption rate to reach saturation was very fast onto the non-imprinted particles compared to the imprinted particles. The equilibrium rates were about 5 min and 60 min for the non-imprinted poly (NIPA-MAC) and the Fe^{3+} imprinted poly(NIPA-MAC) particles, respectively. The maximum adsorption amounts for Fe^{3+} ions onto the non-imprinted poly (NIPA-MAC) and the Fe^{3+} imprinted poly(NIPA-MAC) particles, were 50.13 mg/g polymer and 13.86 mg/g polymer, respectively.

The adsorption amount of Fe^{3+} ions on the non-imprinted poly(NIPA-MAC) and the Fe^{3+} imprinted poly(NIPA-MAC) particles were determined at the pH range between 2.5-6.0 values of buffered solutions. In all of the cases, the adsorption amount increased with increasing pH, reaching a maximum value at around pH 5.0.

The adsorption amount increased with increasing concentration of Fe^{3+} ions, and a saturation value couldn`t be achieved at ion concentration of 300 mg/L for non-imprinted poly(NIPA-MAC) particles. For the Fe^{3+}-imprinted poly(NIPA-MAC) particles, adsorption amount also increased with increasing concentration of the Fe^{3+} ions, but a saturation value is achieved at ion concentration of 200 mg/L. Maximum adsorption amount of the non-imprinted poly(NIPA-MAC) and the Fe^{3+}-imprinted poly(NIPA-MAC) particles were 128.11 mg/g and 22. 25 mg/g, respectively.

Adsorption of Fe^{3+} onto the non-imprinted poly(NIPA-MAC) and the Fe^{3+}-imprinted poly(NIPA-MAC) particles were studied from aqueous solutions

containing 100 mg/L Fe^{3+} ions in the range of 4-50°C. The amount of adsorbed Fe^{3+} ions increased with increasing temperature and maximum adsorption was observed at 37°C. Maximum adsorption amount was found to be, 55.43 mg/g and 13.98 mg/g for the non-imprinted and the Fe^{3+}-imprinted poly(NIPA-MAC) particles, respectively.

The maximum adsorption capacity (Q_{max}) data for the adsorption of Fe^{3+} ions was obtained from the experimental data. When the Langmuir adsorption model was applied in the system, the maximum adsorption capacities (Q_{max}) and the Langmuir constants were found to be 27.32 mg/g and 0.062 g/mg for imprinted and 333.33 mg/g and 0.0056 g/mg for non-imprinted particles, respectively. The correlation coefficients (R^2) were 0.9972 for imprinted and 0.975 for non-imprinted particles. Due to the results, the Langmuir adsorption model can be applied in this ion imprinted polymers.

The Freundlich isotherm, as mentioned before, shows the surface heterogeneity. It contains two parameters, K_F and $1/n$. $1/n$, the surface heterogeneity index, is between 0 and 1. If it is closed to 1, the polymer has heterogeneous surface. Then, the $1/n$ value of MAC is much closed to 1 (0.9923). So, the adsorption process onto the MAC was done via multilayer adsorption.

The adsorption isotherms of imprinted and non-imprinted were found to be linear over the whole concentration range studies and the correlation coefficients were high. According to the correlation coefficients of isotherms, Langmuir adsorption model is favorable for MIP system. In contrast, Freundlich adsorption model is favorable for non-imprinted system.

According to the first order and the second order kinetic models, the results show that the first order mechanism is applicable for imprinted but the second order mechanism is applicable for non-imprinted (R^2 values are the highest).

Conclusion

A comparison of the K_d values for the Fe^{3+} the imprinted poly(NIPA-MAC) samples with the control samples show an increase K_d for Fe^{3+} while K_d decrease for Ni^{2+} and Cd^{2+}. The relative selectivity coefficient is an indicator to express metal adsorption affinity of recognition sites to the imprinted Fe^{3+} ions. These results show that relative selectivity coefficients of imprinted beads for $Fe^{3+}/Ni^{2+}/Cd^{2+}$ 4,52 and 4.81 times greater than non-imprinted particles, respectively.

Desorption ratios are high (up to 73% and 69% for the non-imprinted and the Fe^{3+}-imprinted poly(NIPA-MAC) particles respectively). In order to obtain the reusability of the non-imprinted and the Fe^{3+}-imprinted poly(NIPA-MAC) particles, adsorption-desorption cycles were repeated 5 times by using the same imprinted beads. The adsorption capacity of the recycled non-imprinted and Fe^{3+}-imprinted poly(NIPA-MAC) particles can still be maintained at level 73% and 69% at the 5th cycle.

The adsorption values increased with increasing Fe^{3+} ions, and a saturation value is achieved at Fe^{3+} ion concentration of 1000 µg/Dl, which represents saturation of active binding cavities on the Fe^{3+}-imprinted poly(NIPA-MAC) particles. As postulated in previous works, the increase in the adsorption amount of Fe^{3+}-imprinted poly(NIPA-MAC) particles may be indicative of the formation of new binging sites that are not present in the poly(NIPA-MAC) particles. The maximum adsorbed amount of Fe^{3+} ions on the Fe^{3+}-imprinted poly(NIPA-MAC) particles was found to be 2.2. mg/g.

REFERENCES

Agarwal M.B., SGupte.S., Viswanathan C. *et al.*, Long-term assessment of efficacy and toxicity of L1 (1,2-dimethyl-3-hydroxypyrid-4-one) in transfusion dependent thalassemia: Indian trial. *Drugs. Today.* 28 **(1992),** p. 107.

Ahn Y.H., *et al.* Reversible gelling culture media for *in-vitro* cell culture in three-dimensional matrices. US patent, US6103528. **(2001)**

Allen, S.J., Koumanova, B., Kircheva, Z., Nenkova, S., Ind. Eng. Chem. Res., 44 **(2005)** 2281.

Al-Rafaie F.N., Wonke B., Hoffbrand A.V. *et al.*, Efficacy and possible adverse effects of the oral iron chelator 1,2-dimethyl-3-hydroxypyrid-4-one (L1) in thalassaemia major. *Blood* 80 **(1992),** pp. 593–599.

Al-Refaie F.N., Wonke B. and Hoffbrand A.V., Deferiprone-associated myelotoxicity. *Eur. J. Haematol.* 53 **(1994),** pp. 298–301.

Al-Refaie F.N., Hershko C., Hoffbrand A.V., Kosaryan M., Olivieri N.F., Tondury P. and Wonke B., Results of long-term deferiprone (L1) therapy: a report by the international study group on oral iron chelators. *Br. J. Haematol.* 91 **(1995)**, pp. 224–229.

Anastase-Ravion S., Ding Z., Pelle A., Hoffman A.S. and Letourneur D., New antibody purification procedure using a thermally responsive poly(*N*-isopropylacrylamide)–dextran derivative conjugate, *J Chromatogr B* 761 **(2001),** pp. 247–254.

Andac¸ M., Say, R., Denizli, A., Molecular recognition based cadmium removal from human plasma, *J. of Chrom. B*, 811, 2, 25 **(2004)**, 119–126.

Andac¸ M., Mirel, S., Senel, S., Say, R., Ersoz, A., Denizli, A., Ion-imprinted beads for molecular recognition based mercury removal from human serum, *Int. J. of Biol. Mac.* 40 **(2007)** 159–166

References

Aoki T., Kawashima M., Katono H., Sanui K., Ogata N., Okano T. and Sakurai Y., Temperature-responsive interpenetrating polymer networks constructed with poly(acrylic acid) and poly(*N,N*-dimethylacrylamide), *Macromolecules* 27 **(1994),** pp. 947–952.

Aoyagi T. *et al.*, Novel bifunctional polymer with reactivity and temperature sensitivity. *J. Biomater. Sci. Polym. Edn.* 11 **(2000),** pp. 101–110

Avnir D., Braun S., Lev O. and Ottolenghi M. In: L.C. Klein, Editor, *Sol–Gel Optics—Processing and Applications*, Kluwer, Boston **(1992a)** (Chapter 23).

Avnir D., Braun S., Lev O., Ottolenghi M., Encapsulation of organic molecules and enzymes in sol–gel glasses, in: T. Bein (Ed.), ACS Symposium Ser., Washington, D.C., **(1992b)**.

Avnir D., Braun S., Lev O. and Ottolenghi M., *Chem. Mater.* 6 **(1994),** p. 1605.

Avnir D., *Acc. Chem. Res.* 28 **(1995),** p. 3328.

Benito-Pena E., Moreno-Bondi M.C., Aparicio S., Orellana G., Cederfur J. and Kempe M., *Anal. Chem.* 78 **(2006),** p. 2019.

Bergeron R.J., Wiegand J. and Brittenham G.M., HBED: a potential alternative to deferoxamine for iron-chelating therapy. *Blood* 91 **(1998),** pp. 1446–1452.

Bergeron R.J., Wiegand J. and Brittenham G.M., HBED: the continuing development of a potential alternative to deferoxamine for iron-chelating therapy. *Blood* 93 **(1999),** pp. 370–375

Bignotti F., Penco M., Sartore L., Peroni I., Mendichi R. and Casolaro M. *et al.*, Synthesis, characterisation and solution behaviour of thermo- and pH-responsive polymers bearing l-leucine residues in the side chains, *Polymer* 41 **(2000),** pp. 8247–8256

Blum J., Avnir D. and Schumann H., *CHEMTECH* 29 **(1999),** p. 32.

References

Borgna-Pignatti C., Rugolotto S., De Stefano P., Piga A., Di Gregorio F., Gamberini MR., Sabato V., Melevendi C., Cappellini MD. and Verlato G., Survival and disease complications in thalassemia major. *Ann. N.Y. Acad. Sci.* 850 **(1998),** pp. 227–231.

Brash, J.L., 1991, Modern Aspects of Protein Adsorption on Biomaterials, Missirlis, Y.F., Lemm, W.Eds., Kluwer Academic Publishers, 39-47.

Brennan J.D., *Appl. Spectrosc.* 53 **(1999),** p. 106A.

Brinker C.J. and Scherer G.W., Sol–Gel Science, Academic Press, New York **(1989).**

Brown W. *et al.*, Triblock copolymers in aqueous solution studies by static and dynamic light scattering and oscillatory shear measurements. Influence of relative block sizes, *J Phys Chem* 96 **(1992),** pp. 6038–6044.

Bulmus V. *et al.*, Site-specific polymer–streptavidin bioconjugate for pH-controlled binding and triggered release of biotin. *Bioconjugate. Chem.* 11 **(2000),** pp. 78–83

Carturan G., Toso R.D., Boninsegna S. and Monte R.D., *J. Mater. Chem.* 14 **(2004),** p. 2087.

Cass T. and Ligler F.S., Editors, *Immobilized biomolecules in analysis*, Oxford University Press, Oxford **(1998),** pp. 135–147.

Cazzola M., De Stefano P., Poncho F., Locatelli Y. and Beguin Y., Relationship between transfusion regimen and suppression of erythropoiesis in beta-thalassemia major. *Br. J. Haematol.* 89 **(1995),** pp. 473–478.

Chilkoti A., Dreher M.R., Meyer D.E. and Raucher D., Targeted drug delivery by thermally responsive polymers, *Adv Drug Deliv Rev* 54 **(2002a),** pp. 613–630.

Chodavarapu V.P., Bukowski R.M., Kim S.J., Titus A.H., Cartwright A.N. and Bright F.V., *Electron. Lett.* 41 **(2005),** p. 1031.

References

Cooper, S.L., Bamford, C.H., Tsutura, T., (Ed) 1995, Polymer biomaterials in solution as interfaces and as Solids, VSP, Ultrecht, The Nederlands.

Dagani R., Intelligent gels. *Chem. Eng. News* 9 **(1997),** pp. 26–37.

Dai S., Burleig M.C., Shin Y., Morrow C.C., Barnes C.E., Xue Z., Imprint coating: a novel synthesis of selective functionalized ordered mesoporous sorbents., Angew. Chem. Int. Ed., 38 (9), **1999**, 1235–1239.

Dai S., Burleig M.C., Ju Y.H., Gao H.J., Lin J.S., Pennycook S.J., Barnes C.E., Xue Z.L., Hierarchically imprinted sorbents for the separation of metal ions., J. Am. Chem. Soc., 122 (5), **2000**, 992–993.

Dautzenberg H., Gao Y. and Hahn M., Formation, structure, and temperature behavior of polyelectrolyte complexes between ionically modified thermosensitive polymers, *Langmuir* 16 **(2000),** pp. 9070–9081

Dave B.C., Dunn B., Valentine J.S. and Zink J.I., *Anal. Chem.* 66 **(1994),** p. 1120A.

De Montalembert M., Girot R., Mattlinger B. and Lefrere J-J., Transfusion-dependent thalassemia: viral complications (epidemiology and follow-up). *Sem. Hematol.* 32 **(1995),** pp. 280–287.

Deborah R. and Eliezer R., Critical Reviews in Oncology/Hematology Volume 33, Issue 2, **2000,** pp 105-118

Denizli, A., J.Chrom. B, 668 (1), **(1995)** pp 13-19

Denizli, A., Tanyolac, D., Salih, B., Aydinlar, E., Özdural, A., Pişkin, E., Adsorption of heavy-metal ions on Cibacron Blue F3GA-immobilized microporous polyvinylbutyral-based affinity membranes, *J of Memb Sci.*, 137,1-2, **(1997)** pp 1-8.

Denizli, A., Garipcan, B., Karabakan, K., Say, R., Emir, S., Patır, S., Metal-complexing ligand methacryloylamidocysteine containing polymer beads for Cd(II) removal, *Sep. and Pur. Tech.*, 30, 1**, (2003)** pp 3-10.

References

Doumas B. R., Watson W., Biggs H., Clin. Chim. Acta, 31, **1971**, 87.

Dzgoev A. and Haupt K., *Chirality* 11 **(1999),** p. 465.

Ebara M., Yamato M., Hirose M., Aoyagi T., Kikuchi A., Sakai K. and Okano T., Copolymerization of 2-carboxyisopropylacrylamide with *N*-isopropylacrylamide accelerates cell detachment from grafted surfaces by reducing temperature, *Biomacromolecules* 4 **(2003),** pp. 344–349.

Ekberg B. and Mosbach K., *Trends Biotechnol.* 16 **(1989),** p. 321.

Ersöz, E., Denizli, A., Özcan, A., R., Say, Molecularly imprinted ligand-exchange recognition assay of glucose by quartz crystal microbalance, *Biosens. and Bioelect.*, 20, 11 **(2005)** 2197-2202.

Filipcsei G., Feher J. and Zrinyi M., Electric field sensitive neutral polymer gels, *J Mol Struct* 554 **(2000),** pp. 109–117.

Fong R.B., Ding Z., Long C.J., Hoffman A.S. and Stayton P.S., Thermoprecipitation of streptavidin via oligonucleotide-mediated self-assembly with poly(NIPAAm), *Bioconjugate Chem* 10 **(1999),** pp. 720–725

Fujishige S. and Ando K.K.I., Phase transition of aqueous solutions of poly(*N*-isopropylacrylamide) and poly(*N*-isopropylmethacrylamide), *J Phys Chem* 93 **(1989),** pp. 3311–3313.

Garay M.T., Llamas M.C. and Iglesias E., Study of polymer–polymer complexes and blends of poly(*N*-isopropylacrylamide) with poly(carboxylic acid). 1. Poly(acrylic acid) and poly(methacrylic acid), *Polymer* 38 **(1997),** pp. 5091–5096

Galaev I.and Mattiasson B., Editors, *Smart polymers for bioseparation and bioengineering*, Taylor & Francis, London **(2002).**

Galaev Y. I. and Mattiasson B., 'Smart' polymers and what they could do in biotechnology and medicine, *Trends Biotechnol* 17 **(2000)**, pp. 335–340.

References

Galaev, Yu I.. Gupta M.N. and Mattiasson B., Use smart polymers for bioseparations, *CHEMTECH* 26 **(1996),** pp. 19–25.

Garcia R., Pinel C., Madic C., Lemaire M., Ionic imprinting effect in gadolinium/lanthanum separation, Tetrahedron Lett., 39, **1998**, 8651–8654.

Gil E.S. and Hudson S.M., Stimuli-responsive polymers and their bioconjugates, *Prog Polym Sci* 29 **(2004),** pp. 1173–1222

Grady R.W. and Giardina P.J., Oral iron chelation: HBED may yet prove to be a very useful agent. *Blood* 92 **2 (1998a),** p. 17b.

Grady R.W., Berdoukas V.A. and Giardina P., Iron Chelation: Combined therapy could be a better approach. *Blood* 92 **2 (1998b),** p. 16b.

Graham A.L., Carlson C.A. and Edmiston P.L., *Anal. Chem.* 74 **(2002),** p. 458.

Guenet J.M., Editors, *Thermoreversible gelation of polymers and biopolymers*, Academic Press, London **(1992).**

Gupta R. and Chaudhury N.K., *Biosens. Bioelectron.* 22 **(2007),** p. 2387.

Hall A.J., Quaglia M., Manesiotis P., De Lorenzi E. and Sellergren B., *Anal. Chem.* 78 **(2006),** p. 8362

Haupt, K., Mosbach, K., Trends Biotechnol, 16, (**1998**), 468– 475.

Herrero-Vanrella R., Rincon A.C., Alonso M., Reboto V., Molina-Martineza I.T. and Rodríguez-Cabelloc J.C., Self-assembled particles of an elastin-like polymer as vehicles for controlled drug release, *J Control Release* 102 **(2005),** pp. 113–122.

Hershko C., Konijn A.M. and Link G., Iron chelators for thalassemia. *Br. J. Haematol.* 101 **(1998),** pp. 399–406.

Heskins M. and Guillet J.E., Solution properties of poly (*N*-isopropylacrylamide), *J Macromol Sci Chem* A2 **(1968)**, pp. 1441–1455.

References

Hirokawa Y. *et al.*, Direct observation of internal structures in poly(*N*-isopropylacrylamide) chemical gels. *Macromolecules* 32 **(1999),** pp. 7093–7099.

Hirotsu S., Hirokawa Y. and Tanaka T., *J. Chem. Phys.* 87 **(1987),** p. 1392.

Hoffbrand A.V.,. Bartlett A.N, Veys P.A. *et al.*, Agranulocytosis and thrombocytopenia in patient with Blackfan-Diamond anaemia during oral chelator trial. *Lancet* 2 **(1989),** p. 457.

Hoffman A.S., Intelligent polymers in medicine and biotechnology. *Macromol Symp* 98 **(1995),** pp. 645–664.

Hoffman A.S., Stayton P.S., Bulmus V., Chen G., Jinping C.and Chueng C.*et al.*, Really smart bioconjugates of smart polymers and receptor proteins, *J Biomed Mater Res* 52 **(2000)**, pp. 577–586.

Homer M.L., Yen S.P.S., Ryan M.A. and Ksendzov A., *Proc. Electrochem. Soc.* 2004-08 **(2004),** p. 394.

Hong J.M., Andreson P.E., Qian J. and Martin C.E., *Chem. Mater.* 10 **(1998),** p. 1029

Huang Y.C., Lin C.C. and Liu C.Y., *Electrophoresis* 25 **(2004),** p. 554

Inoue T. *et al.*, Temperature sensitivity of a hydrogel network containing different LCST oligomers grafted to the hydrogel backbone. *Polym. Gels Networks* 5 **(1997),** pp. 561–575.

Ito S., *Kobunshi Ronbunshu* 46 **(1989),** p. 437.

Jeong B. *et al.*, New biodegradable polymers for injectable drug delivery systems. *J. Control. Release* 62 **(1999a),** pp. 109–114.

Jeong B. *et al.*, Thermoreversible gelation of PEG–PLGA–PEG triblock copolymer aqueous solutions. *Macromolecules* 32 **(1999b),** pp. 7064–7069.

Jeong B. *et al.*, Thermogelling biodegradable polymers with hydrophilic backbones: PEG-g-PLGA. *Macromolecules* 33 **(2000),** pp. 8317–8322.

References

Jeong B. and Gutowska A., Lessons from nature: stimuli-responsive polymers and their biomedical applications, *Trends Biotechnol* 20 **(2002a)**, pp. 305–311.

Jeong B., Lee K.M., Gutowska A. and An Y.H., Thermogelling biodegradable copolymer aqueous solutions for injectable protein delivery and tissue engineering, *Biomacromolecules* 3 **(2002b),** pp. 865–868.

Jin W. and Brennan J.D., *Anal. Chim. Acta* 461 **(2002),** p. 1.

Juodkazis S., Mukai N., Wakaki R., Yamaguchi A., Matsuo S. and Misawa H., Reversible phase transitions in polymer gels induced by radiation forces, ***Nature*** 408 **(2000),** pp. 178–181.

Kabanov, V.A.; Efendiev, A.A.; Orujev, D.D., Complex-forming polymeric sorbents with macromolecular arrangement favorable for ion sorption, J. Appl. Polym. Sci., 24, **(1979)**, 259–267.

Kabanov V.A., Physicochemical basis and the prospects of using soluble interpolyelectrolyte complex, *Polym Sci* 36 **(1994),** pp. 143–156.

Kanazawa R., Mori K., Tokuyama H. and Sakohara S., *J. Chem. Eng. Jpn.* 37 **(2004),** p. 804.

Kandimalla V.B. and Hunagxian J., *Anal. Bioanal. Chem.* 380 **(2004),** p. 587

Kaneko Y. *et al.*, Rapid deswelling response of poly(*N*-isopropylacrylamide) hydrogels by the formation of water release channels using poly(ethylene oxide) graft chains. *Macromolecules* 31 **(1998),** pp. 6099–6105.

Kang S. and Bae Y.H., A sulfonamide based glucose-responsive hydrogel with covalently immobilized glucose oxidase and catalase, *J Control Release* 86 **(2003),** pp. 115–121.

Kesenci, K., Say, R., Denizli, A., Removal of heavy metal ions from water by using poly(ethyleneglycol dimethacrylate-co-acrylamide) beads, *Eur Poly Jour.,* 38, I7, **(2002),** pp 1443-1448.

References

Kikuchi A. and Okano T., Intelligent thermoresponsive polymeric stationary phases for aqueous chromatography of biological compounds, *Prog Polym Sci* 27 **(2002)**, pp. 1165–1193.

Kim, S.W., Jacops, H.,1996, Blood Purification, 14, 357-372.

Kim H.K. and Park T.G., Synthesis and characterization of thermally reversible bioconjugates composed of a-chymotrypsin and poly(*N*-isopropylacrylamide-co-acrylamido-2-deoxy- -glucose). *Enzyme Microb. Technol.* 25 **(1999),** pp. 31–37.

Kirsch N., Alexander C., Davies S. and Whitcombe M.J., *Anal. Chim. Acta* 504 **(2004),** p. 63.

Kobayashi J., Kikuchi A., Sakai K. and Okano T., Aqueous chromatography utilizing hydrophobicity-modified anionic temperature-responsive hydrogel for stationary phases, *J Chromatogr A* 958 **(2002),** pp. 109–119

Kontoghiorghes G.J., New orally active iron chelators (letter). *Lancet* 1 **(1985),** pp. 817.

Kontoghiorghes G.J., Aldouri M.A., Sheppard L. and Hoffbrand A.V., 1,2-Dimethyl-3-hydroxypyrid-4-one, an orally active chelator for treatment of iron overload. *Lancet* 1 **(1987),** pp. 1294–1295

Kontoghiorghes G.J., Bartlett A.N., Hoffbrand A.V. *et al.*, Long-term trial with the oral iron chelator 1,2-dimethyl-3-hydroxypyid-4-one (L1). *Br. J. Haematol.* 76 **(1990),** p. 295.

Kriz, D., Ramstrom, O., Mosbach, K., Anal. Chem., 69, (**1997**), A 345–A 349.

Kujawa P. and Winnik F.M., Volumetric studies of aqueous polymer solutions using pressure perturbation calorimetry: a new look at the temperature-induced phase transition of poly(*N*-isopropylacrylamide) in water and D_2O. *Macromolecules* 43 **(2001),** pp. 4130–4135.

References

Kurisawa M. and Yui N., Dual-stimuli-responsive drug release from interpenetrating polymer network-structured hydrogels of gelatin and dextran, *J Control Release* 54 **(1998),** pp. 191–200.

Kushida A., Yamato M., Isoi Y., Kikuchi A. and Okano T., A noninvasive transfer system for polarized renal tubule epithelial cell sheets using temperature-responsive culture dishes, *Eur Cells Mater* 10 **(2005)**, pp. 23–30.

Lackey C.A., Murthy N., Press O.W., Tirrell D.A., Hoffman A.S. and Stayton P.S., Hemolytic activity of pH-responsive polymer–streptavidin bioconjugates, *Bioconjugate Chem* 10 **(1999),** pp. 401–405

Lagergren M., Ollsson P., Sweedenborg J., Surgery, **1974**, 643.

Lan, E.H. Dave B.C., Fukuto J.M., Dunn B., Zink J.I. and Valentine J.S., *J. Mater. Chem.* 9 **(1999),** p. 45.

Leclercq L., Boustta M. and Vert M., A physico-chemical approach of polyanion-polycation interactions aimed at better understanding the *in vivo* behaviour of polyelectrolyte-based drug delivery and gene transfection, *J Drug Target* 11 **(2003),** pp. 129–138.

Lee H. and Park T.G., Conjugation of trypsin by temperature-sensitive polymers containing a carbohydrate moiety: thermal modulation of enzyme activity. *Biotechnol. Prog.* 14 **(1998),** pp. 508–516

Lee S.B. *et al.*, A new class of biodegradable thermosensitive polymers. 2. Hydrolytic properties and salt effect on the lower critical solution temperature of poly(organophosphazenes) with methoxy poly(ethylene glycol) and amino acid ester side groups. *Macromolecules* 32 **(1999),** pp. 7820–7827.

Lev O., Tsionsky M., Rabinovich L., Glezer V., Sampath S., Pankratov I. and Gun J., *Anal. Chem.* 67 **(1995),** p. 22A.

Lomadze N. and Schneider H.-J., Ternary complex formation inducing large expansions of chemomechanical polymers by metal chelators, aminoacids and peptides as effectors, *Tetrahedron Lett* 46 **(2005),** pp. 751–754.

References

Maier N.M., Buttinger G., Welhartizki S., Gavioli E. and Lindner W., *J. Chromatogr. B* 804 **(2004),** p. 103.

Mathew-Krotz J. and Shea K.J., *J. Am. Chem. Soc.* 118 **(1996),** p. 8154.

Matsui J., Higashi M. and Takeuchi T., *J. Am. Chem. Soc.* 122 **(2000),** p. 5218.

Matsunaga T. and Takeuchi T., *Chem. Lett.* 35 **(2006),** p. 1030.

Meyer, D.E., Kong, G.A., Dewhirst, M.W., Zalutsky M.R., Chilkoti, A., Targeting a genetically engineered elastin-like polypeptide to solid tumors by local hyperthermia, *Cancer Res* 61 **(2001),** pp. 1548–1554.

Miyata T., Asami N. and Uragami T., A reversibly antigen-responsive hydrogel, *Nature* 399 **(1999),** pp. 766–769.

Monji N. and Hoffman A.S., A novel immunoassay system and bioseparation process based on thermal phase separating polymers, *Appl Biochem Biotechnol* 14 **(1987),** pp. 107–120.

Mosbach K., *Trends Biochem. Sci.* 19 **(1994),** p. 9

Mosbach, K., Cormack, P., Molecular imprinting: recent developments and the road ahead, Reactive & Functional Polymers, (**1999**), 41,115–124. 645–647.
Mosbach, K., Haupt, K., Liu, X.-C., Cormack, P.A.G., Ramstrom, O., in: Bartsch, R.A., Maeda, M. (Eds.), Molecular and Ionic Recognition with Imprinted Polymers, ACS Symposium Series, Vol. 703, **(1998)**

Na K., Lee K.H., Lee D.H. and Bae Y.H., Biodegradable thermo-sensitive nanoparticles from poly(l-lactic acid)/poly(ethylene glycol) alternating multi-block copolymer for potential anti-cancer drug carrier, *Eur J Pharm Sci* 27 **(2006),** pp. 115–122

Nakajima K., Honda S., Nakamura Y., Redondo F.L.H., Kohsaka S., Yamato M., Kikuchi A. and Okano T., Intact microglia are cultured and non-invasively harvested without pathological activation using a novel cultured cell recovery method, *Biomaterials* 22 **(2001),** pp. 1213–1223.

References

Nandkumar M.A., Yamato M., Kushida A., Konno C., Hirose M., Kikuchi A. and Okano T., Two-dimensional cell sheet manipulation of heterotypically co-cultured lung cells utilizing temperature-responsive culture dishes results in long-term maintenance of di differentiated epithelial cell functions, *Biomaterials* 23 **(2002),** pp. 1121–1130

Nishide, H., Tsuchida, E., Makromol. Chem. **1976,** 177, 2295.

Odabasi, M., Say, R., Denizli, A. Molecular imprinted particles for lysozyme purification, *Mat. Sci. and Eng: C, 27, 1, (2007), 90-99.*

Okano T. and Yoshida R., Intelligent polymeric materials for drug delivery. In: T. Tsuruta, T. Hayashi, K. Kataoka, K. Ishihara and Y. Kimura, Editors, *Biomedical applications of polymeric materials*, CRC Press, Boca Raton, FL **(1993a),** pp. 407–428.

Okano T., Molecular design of temperature-responsive polymers as intelligent materials. In: K. Dusek, Editor, *Responsive gels: volume transitions* vol. II, Springer, Berlin **(1993b),** pp. 180–197.

Okano T., Molecular design of temperature-responsive polymers as intelligent materials. In: K. Dusek, Editor, *Advances in polymer science, responsive gels; volume transition II*, Springer, Berlin **(1993c),** pp. 179–197.

Okano T., Yui N., Yokoyama M. and Yoshida R. *Advances in polymeric systems for drug delivery*, Gordon & Breach, Yverdon, Switzerland **(1994).**

Okano T., Editor, *Biorelated polymers and gels: controlled release and applications in biomedical engineering*, Academic Press, Chestnut Hill, MA **(1998).**

Olivieri N.F., Brittenham G.M., Matsui D., Berkovitch M., Blendis L.M., Cameron R.G., McClelland R.A., Liu P.P., Templeton D.M. and Koren G., Iron-chelation therapy with oral deferiprone in patients with thalassemia major. *New. Engl. J. Med.* 332 **(1995),** pp. 918–922.

References

Olivieri N.F., Long term therapy with deferiprone. *Acta Hematol.* 95 **(1996),** pp. 37–48.

Olivieri N.F. and Brittenham G.M., Iron-chelating therapy and the treatment of thalassemia. *Blood* 89 **(1997),** pp. 739–761.

Olivieri N.F., Gary M.D., Brittenham G.M., McLaren E., Templeton D.M., Cameron R.G., McClelland R.A., Burt A.D. and Fleming K.A., Long-term safety and effectiveness of iron-chelation therapy with deferiprone for thalassemia major. *New. Engl. J. Med.* 339 **(1998),** pp. 417–423.

Oncel, S, Uzun, L., Garipcan, B., Denizli, A., Synthesis of Phenylalanine-Containing Hydrophobic Beads for Lysozyme Adsorption, *Ind. Eng. Chem. Res.;* 44 , 18, **(2005)** pp 7049-7056.

Oya T. *et al.,* Reversible molecular adsorption based on multipoint interaction by shrinkable gels. *Science* 286 **(1999),** pp. 1543–1545.

Ozcan, A. A., Say, R., Denizli, A., Ersoz, A., L-Histidine Imprinted Synthetic Receptor for Biochromatography Applications, *Anal. Chem.*; 78, 20, **(2006)** pp 7253-7258.

Peng T. and Cheng, Y.L. PNIPAAm and PMAA co-grafted porous PE membranes: living radical co-grafting mechanism and multi-stimuli responsive permeability, *Polymer* 41 **(2001),** pp. 2091–2100.

Philippova O.E., Hourdet D., Audebert R. and Khokhlov A.R., pH-responsive gels of hydrophobically modified poly(acrylic acid), *Macromolecules* 30 **(1997),** pp. 8278–8285.

Piga A., Facello S., Gaglioti C., Pucci A., Pietribiasi F. and Zimmerman A., No progression of liver fibrosis in thalassemia major during deferiprone or desferrioxamine iron chelation. *Blood* 92 **2 (1998),** p. 21b.

Piletskaya E.V., Romero-Guerra M., Chianella I., Karim K., Turner A.P.F. and Piletsky S.A., *Anal. Chim. Acta* 542 **(2005),** p. 111.

References

Piletsky S.A., Piletskaya E.V., Elgersma A.V., Yano K., Karube I. and Parhometz Y.P., *Biosens. Bioelectron.* 10 **(1995),** p. 959.

Pinkrah V.T., Snowden M.J., Mitchell J.C., Seidel J., Chowdhry B.Z. and Fern G.R., Physicochemical properties of poly(*N*-isopropylacrylamide-*co*-4-vinylpyridine) cationic polyelectrolyte colloidal microgels, *Langmuir* 19 **(2003a),** pp. 585–590.

Pinkrah V.T., Snowden M.J., Mitchell J.C., Seidel J.,. Chowdhry B.Z and. Fern G.R, Physicochemical properties of poly (*N*-isopropylacrylamide-co-4-vinylpyridine) cationic polyelectrolyte colloidal microgels, *Langmuir* 19 **(2003b),** pp. 585–590.

Piomelli S., The management of patients with Cooley's anemia: transfusions and splenectomy. *Sem. Hematol.* 32 **(1995),** pp. 262–268.

Pişkin, E., Hoffman, A., 1986, Polymeric Biomaterials, Dordrecht, The Netherlands, Martinus Nijhoff Pupl. Co.

Qiu Y. and Park K., Environment-sensitive hydrogels for drug delivery, *Adv Drug Deliv Rev* 53 **(2001)**, pp. 321–339

Schild H.G., Poly(*N*-isopropylacrylamide): experiment, theory and application, *Prog Polym Sci* 17 **(1992),** pp. 163–249.

Sellergren B., *J. Chromatogr. A* 673 **(1994),** p. 133.

Shalev O., Repka T., Goldfarb A., Grinberg L., Abrahamov A., Olivieri N.F., Rachmilewitz E.A. and Hebbel R.P., Deferiprone (L-1) chelates pathologic iron deposits from membranes of intact thalassemic and sickle RBC both in vitro and in vivo. *Blood* 86 **(1995),** pp. 2008–2013.

Shimizu T. *et al.,* Two-dimensional manipulation of cardiac myocyte sheets utilizing temperature-responsive culture dishes augments the pulsatile amplitude. *Tissue Eng.* 7 **(2001),** pp. 141–151.

References

Song S.C. *et al.*, A new class of biodegradable thermosensitive polymers. 1. Synthesis and characterization of poly(organophosphazenes) with methoxy poly(ethylene glycol) and amino acid ester side groups. *Macromolecules* 32 **(1999),** pp. 2188–2193

Soutar I., Swanson L., Thorpe F.G. and Zhu C., Fluorescence studies of the dynamic behavior of poly(dimethylacrylamide) and its complex with poly(methacrylic acid) in dilute solution, *Macromolecules* 29 **(1996),** pp. 918–924.

Sun R., Huimin Y., Hui L. and Zhongyao S., *J. Chromatogr. A* 1055 **(2004),** p. 1.

Suwa K., Morishita K., Kishida A. and Akashi M., Synthesis and functionalities of poly(*N*-vinylalkylamide). V. Control of a lower critical solution temperature of poly (*N*-vinylalkylamide), *J Polym Sci Part A: Polym Chem* 35 **(1997),** pp. 3087–3094.

Tao Z., Tehan E.C., Bukowski R.M., Tang Y., Shughart E.L., Holthoff W.G., Cartwright A.N., Titus A.H. and Bright F.V., *Anal. Chim. Acta* 564 **(2006),** p. 59.

Taylor L.D. and Gerankowski L.D., Preparation of films exhibiting balanced temperature dependence to permeation by aqueous solutions—a study of lower consolute behavior, *J Polymer Sci Polymer Chem Ed* 13 **(1975),** pp. 2551–2570.

Tokuyama H., Fujioka M. and Sakohara S., *J. Chem. Eng. Jpn.* 38 **(2005a),** p. 633

Tokuyama H., Kanazawa R. and Sakohara S., *Sep. Purif. Technol.* 44 **(2005b),** p. 152.

Tondury P., Kontoghiorghes G.J., Ridolfi-Luthy A. *et al.*, L1 (1,2-dimethyl-3-hydroxpyrid-4-one) for oral iron chelation in patients with beta-thalassaemia major. *Br. J. Haematol.* 76 **(1990),** p. 550.

Tonge S.R. and Tighe B.J., Responsive hydrophobically associating polymers: a review of structure and properties, *Adv Drug Deliv Rev* 53 **(2001),** pp. 109–122.

Topp M.D.C. *et al.*, Thermosensitive micelle forming block copolymers of poly(ethylene glycol) and poly(*N*-isopropylacrylamide). *Macromolecules* 30 **(1997),** pp. 8518–8520.

References

Tsukagoshi, K., Kai, Y.Y., Maeda, M., Takagi, M., *Bull. Chem. Soc. Jpn.*, **(1993)**, 66, 114.

Twaites B.R., Alarcon C.H., Cunliffe D., Lavigne M., Pennadam S. and Smith J.R. *et al.*, Thermo and pH responsive polymers as gene delivery vectors: effect of polymer architecture on DNA complexation *in vitro*, *J Control Release* 97 **(2004),** pp. 551–566.

Uchida K., Sakai K., Ito E., Kwon O.H., Kikuchi A., Yamato M. and Okano T., Temperature-dependent modulation of blood platelet movement and morphology on poly(*N*-isopropylacrylamide)-grafted surfaces, *Biomaterials* 21 **(2000),** pp. 923–929.

Ulijn R.V., Enzyme-responsive materials: a new class of smart biomaterials, *J Mater Chem* 16 **(2006),** pp. 2217–2225

Urraca J.L., Marazuela M.D. and Moreno-Bondi M.C., *Anal. Bioanal. Chem.* 385 **(2006a),** p. 1155.

Urraca J.L., Marazuela M.D., Merino E.R., Orellana G. and Moreno-Bondi M.C., *J. Chromatogr. A* 1116 **(2006b),** p. 127.

Vernon B. *et al.*, Insulin release from islets of Langerhans entrapped in a poly(*N*-isopropylacrylamide-co-acrylic acid) polymer gel. *J. Biomater. Sci. Polym. Ed.* 10 **(1999),** pp. 183–198.

Vlatakis, G., Andersson, L.I., Muller, R., Mosbach, K., Nature (London), 361, **(1993)**

Wang H.Y., Kobayashi T. and Fujii N., *Langmuir* 12 **(1996),** p. 4850.

Wanka G., Hoffmann H. and Ulbricht W., Phase diagrams and aggregation behavior of poly (oxyethylene)-poly (oxypropylene)–poly(oxyethylene) triblock copolymers in aqueous solutions, *Macromolecules* 27 **(1994),** pp. 4145–4159.

Weatherall D.J. and Clegg J.B., Thalassemia-a global public health problem. *Nature. Med.* 2 **(1996),** pp. 847–849.

References

Weidner J., Drug targeting using thermally responsive polymers and local hyperthermia, *Drug Discov Today* 6 **(2001),** pp. 1239–1248.

Whitcombe M.J., Rodriguez M.E., Villar P. and Vulfson E.N., *J. Am. Chem. Soc.* 117 **(1995),** p. 7105.

Whitcombe M.J. and Vulfson E.N., *Tech. Instrumn. Anal. Chem.* 23 **(2001),** p. 203.

Wonke B., Wright C. and Hoffbrand A.V., Combined therapy with deferiprone and desferrioxamine. *Br. J. Haematol.* 103 **(1998),** pp. 361–364.

Wulff G., Vesper W., Grobe-Einsler R. and Sarhan A., *Makromol. Chem.* 178 **(1977),** p. 2799

Wulff G., Molecular imprinting in cross-linked materials with the aid of molecular templates-a way towards artificial antibodies, Angew. Chem. Int. Ed. Engl., 34, **1995**, 1812–1832.

Wulff G., *Chem. Tech.* 28 **(1998),** p. 19.

Yamato M., Konno C., Kushida A., Hirose M., Utsumi M., Kikuchi A. and Okano T., Release of adsorbed fibronectin from temperature-responsive culture surfaces requires cellular activity, *Biomaterials* 21 **(2000),** pp. 981–986.

Yan L., Zhu Q. and Kenkare P.U., Lower critical solution temperature of linear PNIPA obtained from a Yukawa potential of polymer chains, *J Appl Polym Sci* 78 **(2000),** pp. 1971–1976.

Yan M. and Ramstrom O., Editors, *Molecularly Imprinted Materials: Science and Technology*, Marcel Dekker, New York, NY **(2005).**

Ye L., Cormack P.A.G. and Mosbach K., *Anal. Comm.* 36 **(1999),** p. 35.

Yoshida R. *et al.,* Comb-type grafted hydrogels with rapid deswelling response to temperature changes. *Nature* 374 **(1995),** pp. 240–242.

Yusa S., Sakakibara A., Yamamoto T. and Morishima Y., Fluorescence studies of pH-responsive unimolecular micelles formed from amphiphilic polysulfonates

References

possessing long-chain alkyl carboxyl pendants, *Macromolecules* 35 **(2002),** pp. 10182–10188.

Zareie H.M. *et al.,* Investigation of stimuli-responsive copolymer by atomic force microscopy. *Polymer* 41 **(2000),** pp. 6723–6727.

Zhang Z., Haiping L., Li H., Nie L. and Yao S., *Anal. Biochem.* 336 **(2005),** p. 108.

Zhu X., Su Q., Cai J., Yang J. and Gao Y., *J. Appl. Polym. Sci.* 101 **(2006),** p. 4468

Zrinyi M., Intelligent polymer gels controlled by magnetic fields, *Colloid Polym Sci* 278 **(2000),** pp. 98–103.

Curriculum Vitea

SEÇİL UTKU

Date of Birth	:	21.12.1979
Place of Birth	:	Eskişehir
Gender	:	Female
Nationality	:	Turkish
Marital Status	:	Single
Foreign Language	:	English
e-mail	:	secilutku@gmail.com

EDUCATION

High School	Anıttepe High School, Ankara, 1993-1995.
BSc	Chemistry Department, Hacettepe University, Ankara, 1999-2004
MSc	Chemistry Department, Biochemistry Div., Hacettepe University, Ankara, 2004-2007

WORK EXPERINCE

Chemical, Petroleum, Rubber and Plastic Industries Employers' Association of Turkey (KİPLAS), (Research and Development Specialist)

Work Telephone	: (+90 216) 651 49 00
Fax	: (+90 216) 474 91 92